

JAERI - M

86-182

FUSION BLANKET BENCHMARK EXPERIMENTS
ON A 60 CM-THICK LITHIUM-OXIDE
CYLINDRICAL ASSEMBLY

December 1986

Hiroshi MAEKAWA, Yujiro IKEDA, Yukio OYAMA
Seiya YAMAGUCHI, Koichi TSUDA, Tooru FUKUMOTO*
Kazuaki KOSAKO*, Michio YOSHIZAWA** and
Tomoo NAKAMURA

日本原子力研究所
Japan Atomic Energy Research Institute

JAERI-M レポートは、日本原子力研究所が不定期に公刊している研究報告書です。
入手の問合せは、日本原子力研究所技術情報部情報資料課（〒319-11 茨城県那珂郡東海村）
あて、お申しこしください。なお、このほかに財団法人原子力弘済会資料センター（〒319-11 茨城
県那珂郡東海村日本原子力研究所内）で複写による実費領布をおこなっております。

JAERI-M reports are issued irregularly.

Inquiries about availability of the reports should be addressed to Information Division, Department
of Technical Information, Japan Atomic Energy Research Institute, Tokai-mura, Naka-gun,
Ibaraki-ken 319-11, Japan.

© Japan Atomic Energy Research Institute, 1986

編集兼発行 日本原子力研究所
印 刷 山田軽印刷所

Fusion Blanket Benchmark Experiments
on a 60 cm-thick Lithium-Oxide Cylindrical Assembly

Hiroshi MAEKAWA, Yujiro IKEDA, Yukio OYAMA, Seiya YAMAGUCHI
Koichi TSUDA, Tooru FUKUMOTO*, Kazuaki KOSAKO*
Michio YOSHIZAWA** and Tomoo NAKAMURA

Department of Reactor Engineering,
Tokai Research Establishment
Japan Atomic Energy Research Institute
Tokai-mura, Naka-gun, Ibaraki-ken

(Received December 1, 1986)

Integral experiments on a Li₂O cylindrical assembly have been carried out, using the FNS facility to provide benchmark data for verification of methods and data used in fusion neutronics research. The size of assembly was 63 cm (diameter) by 61 cm (length). Measurements included ⁶Li and ⁷Li tritium production rates ; ²³⁵U, ²³⁸U, ²³⁷Np and ²³²Th fission rates ; ²⁷Al(n,α)²⁴Na, ⁵⁸Ni(n,2n)⁵⁷Ni, ¹¹⁵In(n,n')^{115m}In and ¹¹⁵In(n,γ)¹¹⁶In reaction rates. Neutron energy spectra in the assembly, as well as response rates of TLDs and PIN diodes, were also measured. Measured data are presented in tabular form together with estimated errors. A sample calculation using the DOT3.5 code is provided to facilitate the reader understanding of the experiments. Although several different measuring techniques are used in the experiment, the data are mutually consistent. This fact supports that present experimental data can be applied to the benchmark verification of methods and data.

KEYWORDS: Fusion Neutronics, Benchmark Experiment, Lithium-oxide, FNS, Tritium, Neutron Spectrum, Foil Activation, TLD, PIN Diode, DOT3.5, JENDL-3

* Present address, Century Research Center Corporation Ltd.

** Faculty of Engineering, Hokkaido University,
Present address, Department of Health Physics, JAERI

酸化リチウム 60 cm厚円筒体系による核融合炉
プランケットベンチマーク実験

日本原子力研究所東海研究所原子炉工学部

前川 洋・池田裕二郎・大山 幸夫

山口 誠哉・津田 孝一・福本 亨*

小迫 和明*・吉沢 道夫**・中村 知夫

(1986年12月1日受理)

核融合炉の研究で用いられている計算手法およびデータベースを検証するベンチマークデータを提供する目的で、酸化リチウム (Li_2O) 円筒体系での積分実験をFNSを用いて行った。体系は直径 63 cm, 長さ 61 cm である。 ^6Li と ^7Li のトリチウム生成率分布, ^{235}U , ^{238}U , ^{237}Np と ^{232}Th の核分裂率分布, $^{27}\text{Al}(\text{n}, \alpha)^{24}\text{Na}$, $^{58}\text{Ni}(\text{n}, 2\text{n})^{57}\text{Ni}$, $^{115}\text{In}(\text{n}, \text{n}')$, ^{115m}In と $^{115}\text{In}(\text{n}, \gamma)^{116}\text{In}$ の反応率分布を測定した。また、体系内の中性子エネルギースペクトルやTLDとPINダイオードのレスポンス分布も測定した。測定データは誤差と共に、表で示されている。読者が実験を良く理解できるように、DOT 3.5による計算例を示した。種々の測定法を用いたにもかかわらず、実験値同志の整合性は良かった。この事実は今回測定した実験データが、核融合炉プランケットの設計や解析に用いられている計算手法やデータベースの評価のためのベンチマークデータとして使用できることを示している。

東海研究所：〒319-11 茨城県那珂郡東海村白方字白根2-4

* 現センチュリー・リサーチ・センタ㈱

** 北海道大学工学部、現原研保健物理部

Contents

1.	Introduction	1
2.	Experimental Assembly and Neutron Source	4
3.	Tritium Production-Rate Distributions	12
3.1	Tritium Production Rates Measured by Liquid Scintillation Method with Li ₂ O Pellets	12
3.2	Tritium Production Rates Measured by a Pair of Lithium-Glass Scintillators	14
3.3	Tritium Production Rates of ⁷ Li Measured by an Small Sphere NE213 Spectrometer	16
4.	Fission Rate Distributions Measured by Micro-Fission Chambers	25
5.	Reaction-Rate Distributions Measured by Activation Foils	30
6.	Spectra measured by a small spherical NE213 spectrometer	35
7.	Discussions and Concluding Remarks	56
	Acknowledgement	58
	References	61
A.1	Fission Rate distributions Measured by Fission Track Recorders (FTD)	63
A.2	Response Distribution of PIN Diode	67
A.3	Response Distributions of TLDs	69
A.4	Sample Calculation	72

目 次

1. 緒 言	1
2. 実験体系および中性子源	4
3. トリチウム生成率分布	12
3.1 Li_2O ベレットを用いた液体シンチレーション法で測定したトリチウム生成率	12
3.2 Li ガラスシンチレータで測定した ${}^6\text{Li}$ によるトリチウム生成率	14
3.3 小型球形NE 213で測定した ${}^7\text{Li}$ によるトリチウム生成率	16
4. 小型核分裂計数管で測定した核分裂率分布	25
5. 放射化箔で測定した反応率分布	30
6. 体系内中性子スペクトル	35
7. 検討および結語	56
謝 辞	58
参考文献	61
A. 1 核分裂片検出器(FTD)で測定した核分裂率分布	63
A. 2 PINダイオードのレスポンス分布	67
A. 3 TLDのレスポンス分布	69
A. 4 計 算 例	72

1. Introduction

The design of an effective blanket for a controlled thermonuclear reactor calls for an exact knowledge of the behavior of neutrons within the blanket medium. The methods and data used in the design and analysis of fusion blanket should be examined by comparing the calculated results with experiments. At the JAERI a number of such integral experiments on simulated blanket assemblies had been carried out using the PNS-A neutron source.⁽¹⁾⁻⁽⁷⁾ The installation of a more powerful D-T neutron generator, the Fusion Neutronics Source facility (FNS),⁽⁸⁾⁽⁹⁾ provided the opportunity for additional benchmark experiments on simulated blanket assemblies. In particular, the tritium production-rate distributions were measured in two such blanket assemblies.⁽¹⁰⁾

Lithium oxide (Li_2O) had been proposed by JAERI's designers as a ceramic solid tritium breeding material.⁽¹¹⁾ This in turn led to urgent requests for benchmark experiments on fusion blankets of Li_2O using the FNS facility.

In blanket design calculations as well as in the interpretation of experimental data, it is necessary to describe the angular distributions of secondary neutrons with some accuracy. Two transport codes, BERMUDA-2DN⁽¹²⁾ and MORSE-DD⁽¹³⁾ were developed at the JAERI for this task, both employ a double differential cross section (DDX) format. A new nuclear data file based on DDX is in process of evaluation by the Japanese Nuclear Data Committee, to be issued as JENDL-3 in March 1987. Meanwhile, some important nuclides of interest blanket work, i.e., ^6Li , ^7Li , Be, C, O, Cr, Fe and Ni have been made available as JENDL-3PR1 (JENDL-3 preliminarily version one). These methods and data should be examined by the benchmark experiments.

Experimental assemblies to be obtained the benchmark data must have simple geometry with simple composition. In the case of the spherical assemblies used in the previous experiments,⁽¹⁾⁻⁽⁷⁾ one-dimensional calculation was applied to the analysis because of the limit of computer resource at that time. There are two problems in this case. First, the energy and angular distributions of D-T source neutrons are not uniform due to the kinematics of D-T reaction and scattering effect by the structural material of target assembly. Second, there is some ambiguity in the boundaries of experimental

assembly to make a one-dimensional calculation model, since the actual experimental assembly was composed by rectangular blocks. Recent innovation of computer resource makes us the two-dimensional calculation within reasonable time.

As a series of clean benchmark experiments, an integral experiment on a lithium-oxide (Li_2O) cylindrical assembly was planned and carried out. The assembly was placed in front of the target. In this case, it is easy to make the calculational model of two-dimensional geometry in the condition of reasonable accuracy. Moreover, source neutrons entered almost isotropically into the assembly.

It is also very important to know the characteristics of source neutrons accurately in the benchmark problem. They were measured by time-of-flight technique, foil activation method and an NE213 spectrometer.(14) These measured values were confirmed by an analysis based on Monte Carlo calculation.(15)

Benchmark data suitable for comparison with calculation must, on one hand, furnish absolute values ; on the other hand, it is highly desirable to obtain as many measurements as possible to afford internal cross-checks among the data and provide a large amount of information. This cross-check should support the reliability of measured values.

Measured quantities and methods of measurement in this work are summarized as follows:

- (a) Tritium production-rate distributions
 - * liquid scintillation counting of tritium extracted from irradiated ${}^6\text{Li}_2\text{O}$ and ${}^7\text{Li}_2\text{O}$ pellets
 - * online pulse height spectroscopy with a pair of ${}^6\text{Li}$ - and ${}^7\text{Li}$ -glass scintillators
 - * online neutron spectroscopy with an NE213 scintillator and evaluated nuclear data of ${}^7\text{Li}(\text{n},\text{n}'\text{t}){}^4\text{He}$
- (b) Fission-rate distributions
 - * online micro-fission chambers containing ${}^{235}\text{U}$, ${}^{238}\text{U}$, ${}^{237}\text{Np}$ and ${}^{232}\text{Th}$
- (c) Reaction-rate distributions, for ${}^{27}\text{Al}(\text{n},\alpha){}^{24}\text{Na}$, ${}^{58}\text{Ni}(\text{n},2\text{n})$ ${}^{57}\text{Ni}$, ${}^{115}\text{In}(\text{n},\text{n}'){}^{115}\text{mIn}$ and ${}^{115}\text{In}(\text{n},\gamma){}^{116}\text{In}$
 - * offline gamma-ray spectroscopy of irradiated Al, Ni and In foils

- (d) Neutron spectra within the assembly
 - * online pulse-height spectrum recording and unfolding of a small sphere NE213 spectrometer
 - * offline evaluation of threshold reactions induced in foils (MFA)[†]

In addition to these measurements, the response distributions of PIN diodes and thermoluminescence dosimeters (TLD) were measured as well as fission-rate distributions by offline scanning of solid-state track recorders packaged with ^{238}U and ^{232}Th foils, in an effort to develop new techniques. They are presented in Appendix. To give the reader a better understanding of the use of the experimental data for purposes of comparison with theoretical predictions, a calculation based on DOT3.5⁽¹⁶⁾ is provided in Appendix A.4.

[†] The result of the MFA measurements is omitted from this report and will be published elsewhere.

2. Experimental Assembly and Neutron Source

Three types of Li_2O blocks were made to construct a experimental assembly. The outside dimensions of these blocks had an area of 5.06 cm \times 5.06 cm and lengths of 5.06, 10.12 and 20.24 cm. The bricks, which were almost cubic, were made from Li_2O powder by cold pressing. Density of Li_2O bricks was 75.5 % of theoretical density. One, two and four Li_2O bricks were encapsulated, respectively, in a 0.2 mm-thick stainless steel box, edge-welded with a 2.5 mm deep rim. A photograph of these blocks is shown in Fig. 2.1.

These blocks were supported by a framework consisting of thin-walled, aluminum square tubes. Sectional views of the cylindrical slab assembly and Li_2O blocks are shown in Fig. 2.2. The size of the assembly was 63.0 cm in average diameter and 61.0 cm in length. Appendix A.4 describes a two-dimensional model for the experimental analysis. Homoginized nuclide densities in each region are presented in Table 2.1.

An experimental channel — a set of square tube and drawer made of 0.2 mm-thick stainless steel (SS304) — was prepared for saving the time to change the detector location and thus minimizing the personnel exposure. A photograph of the square tube and drawer is shown in Fig. 2.3. This experimental channel was set at the central axis of the assembly. Three types of special-sized Li_2O blocks were manufactured for loading in the drawer. The cross section of special-sized blocks is a little smaller than that of the standard ones, i.e., 4.98 cm \times 4.98 cm. While the length of them equals that of the standard blocks. Lithium-oxide blocks with an experimental hole were also made to allow insertion of a detector. This outer size was 4.98 cm cube and the hole size was 2.0 cm \times 2.0 cm. Four small blocks were stacked and fixed by stainless steel solder to form the experimental hole. A drawing and photograph are shown in Figs. 2.4 and 2.5. An additional experimental channel was placed at off-central axis located three units above the center ($r = 15.2$ cm).

The 80° beam line in the first target room of the FNS facility was used for the present experiment. An experimental layout is shown in Fig. 2.6. A high speed water-cooled target assembly⁽¹⁷⁾ was set at the end of the beam line. A 20 Ci Ti-T target was mounted on the target assembly. Neutrons were generated at the distance of 20 cm from the assembly surface on its central axis. The setting accuracy is

estimated to be within ± 0.1 cm. A view of the experimental arrangement is shown in Fig. 2.7. The layout of the first $15\text{ m} \times 15\text{ m}$ target room is shown in Fig. 2.8. The distances from the target to the west and south walls are 5.5 m, and those to the ceiling, the grating floor and the basement floor are 7.9, 1.8 and 3.8 m, respectively.

Neutron yields were determined by means of the associated α -particle detection method.⁽¹⁸⁾ A small silicon surface-barrier detector was mounted in the target assembly to detect the α -particle of $^3\text{T(d,n)}^4\text{He}$ reaction. Source characteristics⁽¹⁴⁾ --- neutron yield, angular distribution and spectra --- of the target assembly were measured by the time-of-flight technique,⁽¹⁹⁾ foil activation and an NE213 spectrometer.⁽²⁰⁾

The agreement between neutron yields measured by different methods was well within the experimental error. An analysis by Monte Carlo computation⁽¹⁵⁾ also showed fairly good agreement with measured neutron energy spectra as well as angular distributions, the latter obtained by foil activation. Thus, the calculated source spectrum and other characteristics were essentially confirmed and can be used as input information in the benchmark calculations.

Table 2.1 Homogenized nuclide density for each region of Li_2O assembly.

Region	Inner Li_2O	Stainless steel	Outer Li_2O
Outer Radius	2.71_9 cm	2.86_6 cm	31.5 cm
^6Li	4.221_{1-3}^*	----	4.191_{4-3}^{-3}
^7Li	5.277_{4-2}	----	5.240_{4-2}
O	2.849_{8-2}	----	2.829_{8-2}
Fe	5.204_{9-4}	2.324_{4-2}	1.111_{9-3}
Ni	6.296_{3-5}	2.812_{1-3}	1.351_{6-4}
Cr	1.433_{3-4}	6.397_{5-3}	3.067_{5-4}
Mn	7.244_{9-6}	3.294_{8-4}	1.880_{1-5}

* Read as $4.221_1 \times 10^{-3}$ [10^{24} atoms / cm^3]

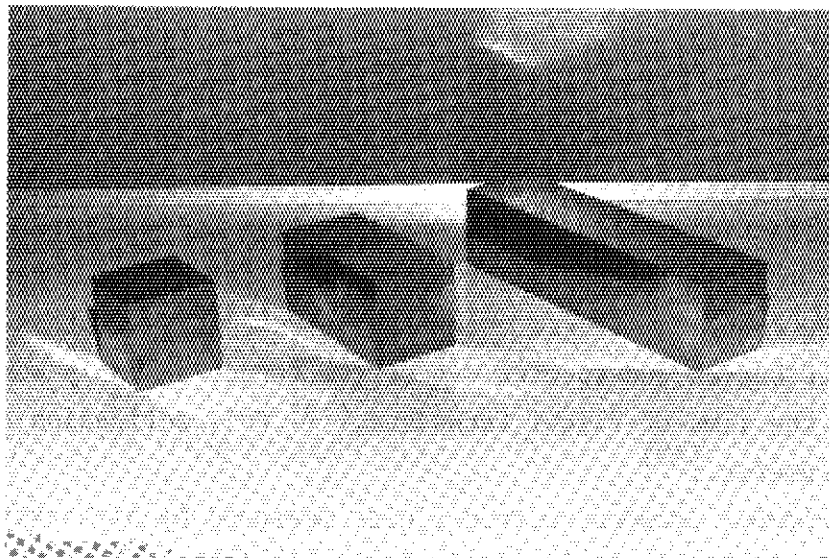


Fig. 2.1 Lithium-oxide blocks.

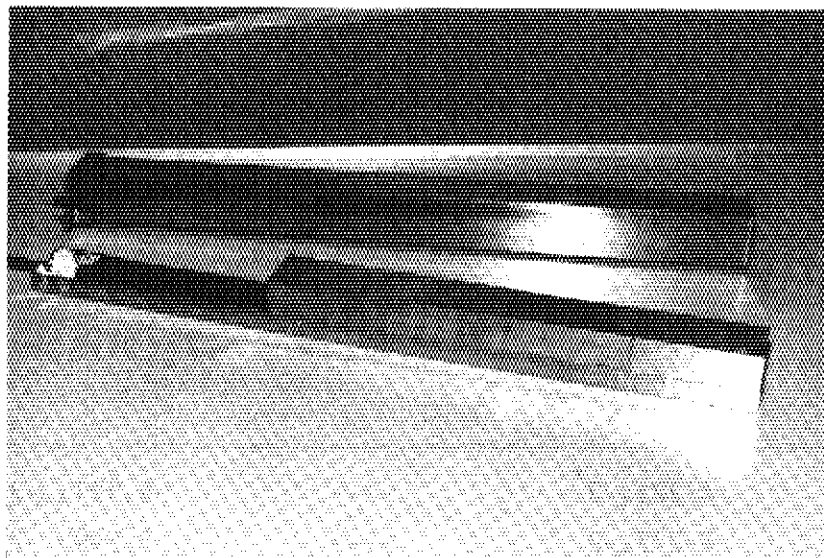


Fig. 2.3 Thin-walled square tube and drawer made of SS304 for the experimental channel.

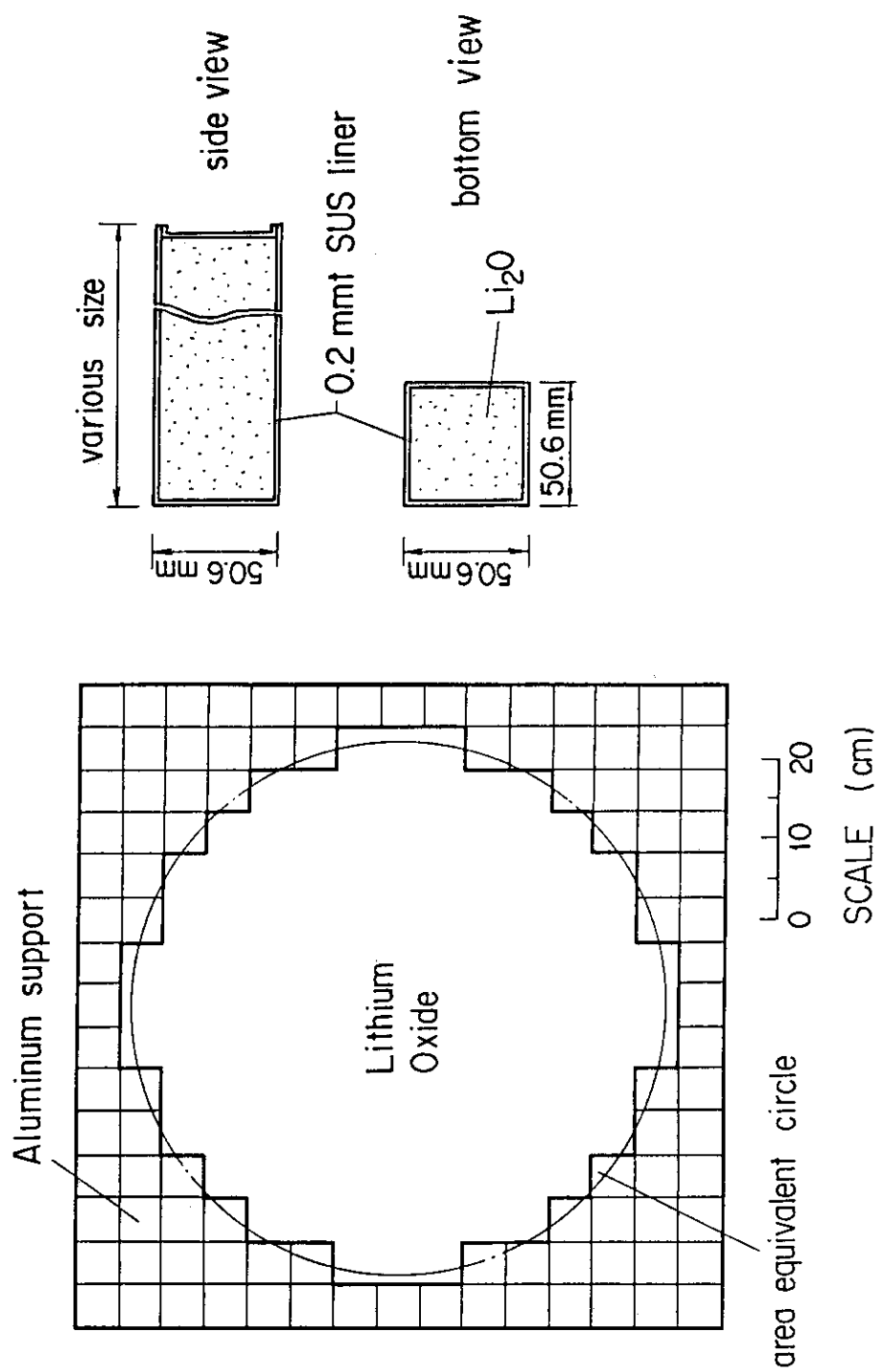


Fig. 2.2 Sectional views of the cylindrical assembly and Li_2O blocks.

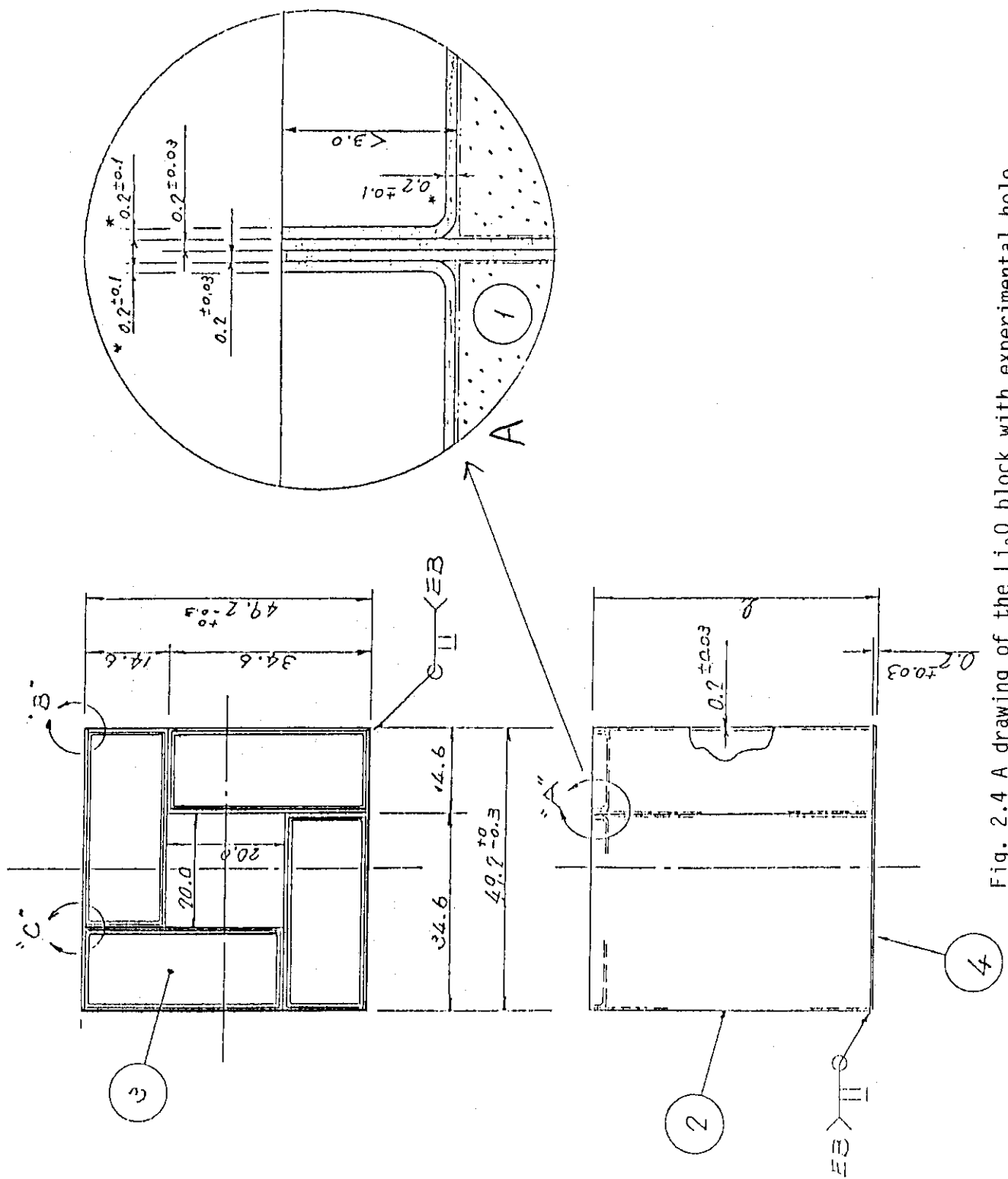


Fig. 2.4 A drawing of the Li_2O block with experimental hole.

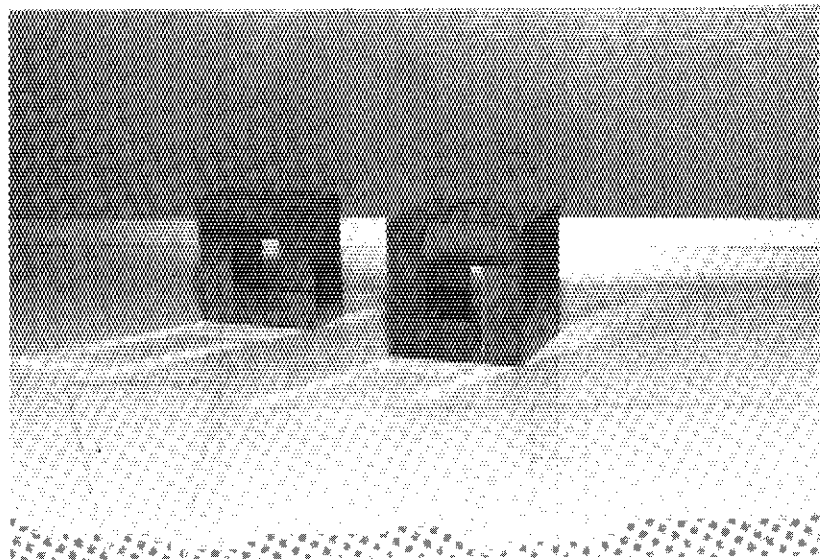


Fig. 2.5 Lithium-oxide blocks with experimental hole.

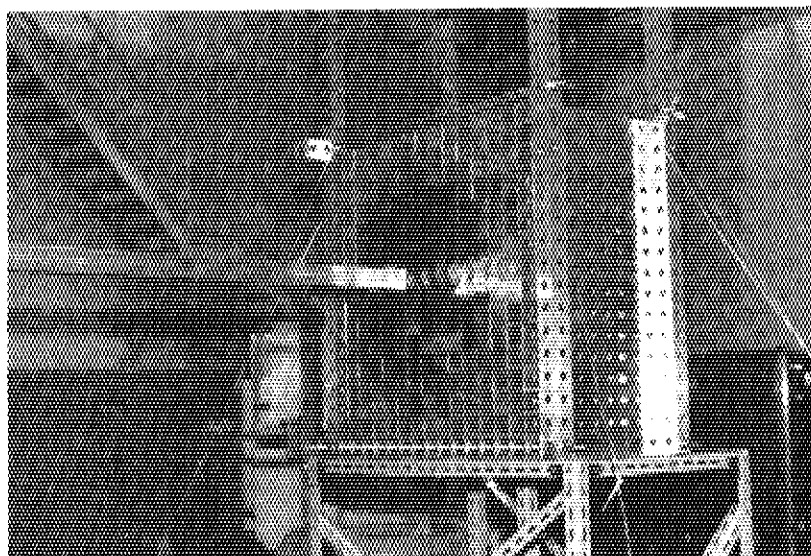


Fig. 2.7 A view of the experimental arrangement.

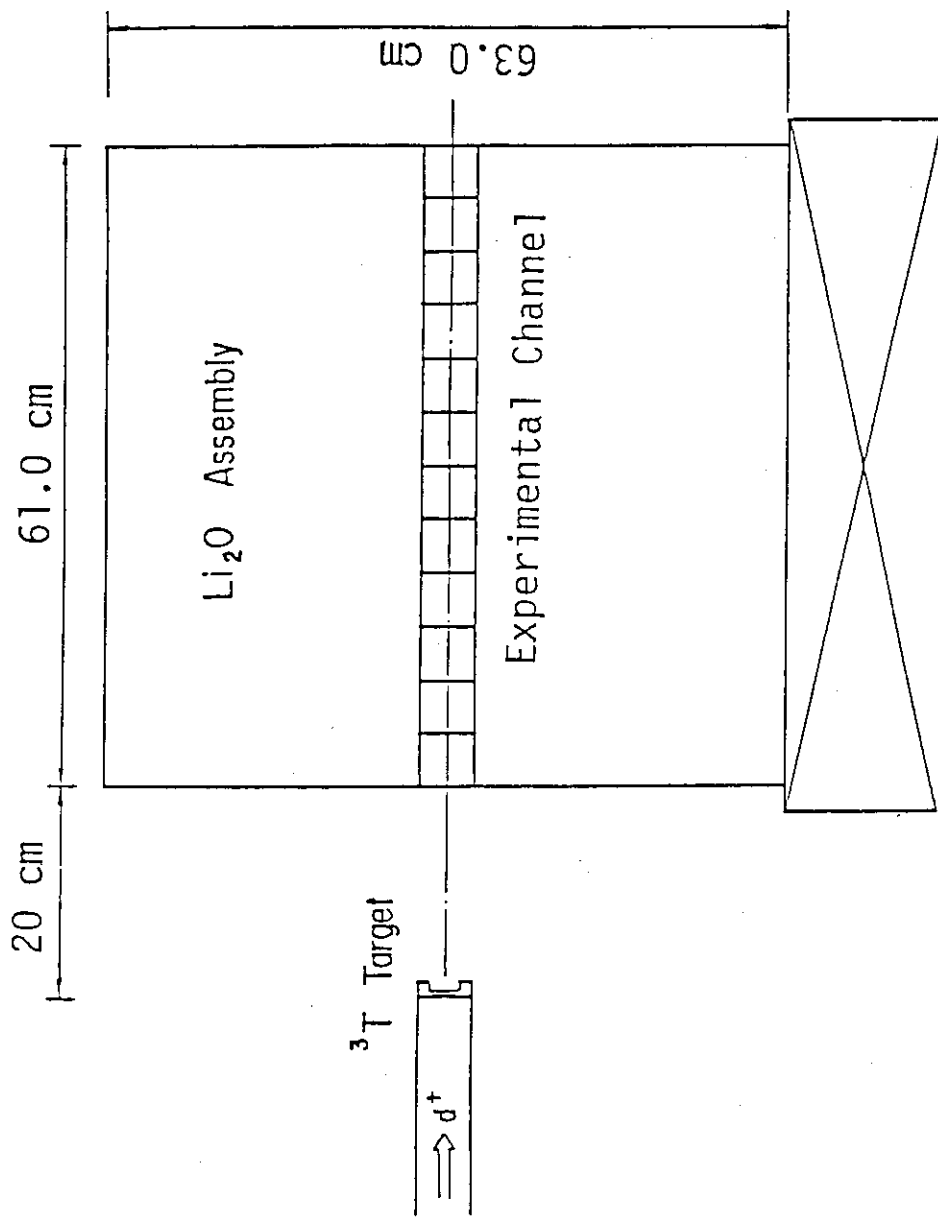
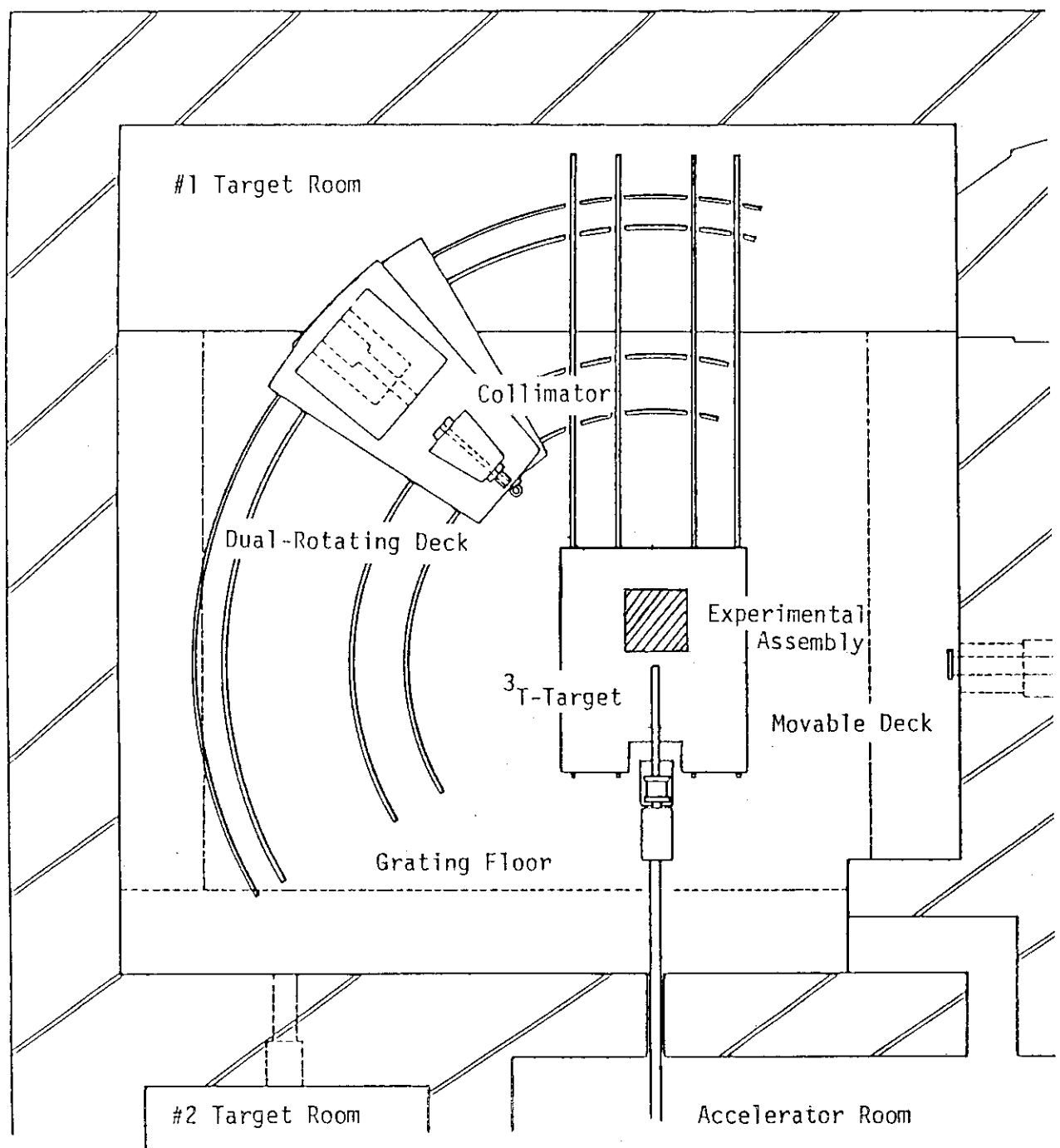


Fig. 2.6 Experimental layout.



Experimental layout

Fig. 2.8 Layout of the FNS first target room.

3. Tritium Production-Rate Distributions

3.1 Tritium Production Rates Measured by Liquid Scintillation Method with Li₂O Pellets

Tritium production-rate (TPR) distributions were measured by the liquid scintillation counting method, using sintered Li₂O pellets. The size and density of pellets were 12 mm dia. x 2 mm and about 83 % of theoretical density, respectively. Enriched ⁶Li(95.446 atom %) and ⁷Li(99.952 atom %) pellets were placed in the 2.5 mm deep cavities between welding rims of the special-sized Li₂O blocks arranged along the central axis. They are shown in Figs. 3.1 and 3.2. Deuteron beam energy, average beam current and total irradiation time were 310 keV, 2 mA and 17 hours. Total neutron yield at the target was estimated to be 9.39×10^{15} .

Irradiated pellets were dissolved in 6.5 ml of water ; complete solution required about 2 days. The solution was distilled with an apparatus shown in Fig. 3.3. As the first step, the solution was poured into a "boiling flask" and frozen in a liquid nitrogen dewar. The apparatus was then evacuated by a rotary pump ; upon complete evacuation, the flask was warmed up in a water bath of 80°C while a "condensing flask" was, in turn, cooled down with a liquid nitrogen dewar. This resulted in the transfer of almost all of the water to the condensing flask. Six ml of the collected water was pipetted into a 20 ml vial; then, 4 ml of ethylalcohol and 10 ml liquid scintillation cocktail were added. The addition of ethylalcohol made liquid (single phase) samples clear and stable. The tritium activity in the sample was measured by a calibrated low background liquid scintillation counting system (Aloka LSC-LB1).

To estimate tritium escape during the irradiation and chemical treatment, some pellets, covered with aluminum foil of 210 μm thickness were placed near the rotating target of the FNS. The foil, in which recoil tritons were trapped during the irradiation, were treated chemically and the tritium was measured by a radio gas chromatograph. The HT gas undissolved in the solution was extracted by the D₂ gas bubbling method and measured in a similar way. Measured values are summarized in Table 3.1. The total escaped tritium rates were (6.1 ± 1.3) % and (7.1 ± 0.9) % for ⁶Li₂O and ⁷Li₂O pellets,

respectively. An additional experiment for estimating the escaped tritium is being carried out using the same method and a different method from the method mentioned above. Preliminary data support the above data within the experimental errors. After the correction for escaped tritium, the TPRs of ${}^6\text{Li}$ and ${}^7\text{Li}$ were obtained by making use of the atomic ratios of pellets.

The experimental data are presented in Table 3.2 together with experimental error. Three values for ${}^6\text{Li}$ TPR are listed in the table. First, the observed tritium production rate in the pellet, i.e., the data including corrections for tritium decay and escape ; Secondly the data corrected for the self-shielding. This correction was based on a simple model of the group-wise self-shielding factor G_i ,

$$G_i = \frac{1 - e^{-\tau}}{\tau}$$

where $\tau = \sigma_i N t_m$
 σ_i : absorption cross section of *i*-th group
 N : atom density
 t_m : mean chord length = $4V / S$
 V : volume of pellet
 S : surface area of pellet.

For the ${}^6\text{Li}_2\text{O}$ pellet, the diameter is 12 mm, thickness 2 mm and atom density 6.934×10^{22} of ${}^6\text{Li}$.

The third value in the table includes both corrections for self-shielding and for room-return effects ; the room-return effect was evaluated by the MORSE-DD code.⁽²¹⁾

The experimental error analysis is summarized in Table 3.3. The major error source was the statistical error in the tritium count. A comparison with the sample calculation is given in Appendix A.4.

3.2 Tritium Production Rates Measured by a Pair of Lithium-Glass Scintillators

The tritium production rates(TPR) of ^6Li along the central axis and the off-central axis were measured by a pair of ^6Li - and ^7Li -glass scintillators. This method, newly-developed at the JAERI for TPR measurement,⁽²²⁾ offers the following specific advantages :

- 1) no heavy irradiation is required, because of its high sensitivity,
- 2) on line measurement is provided,
- 3) the size of the scintillator is small (10 mm dia. \times 3.0 mm), hence the positional resolution is high.

The γ -ray background is removed by subtracting the pulse height spectrum of ^7Li -glass scintillator from that of the ^6Li -glass scintillator, after the adjustment of pulse height spectrum by the use of the ratio of γ -ray detection efficiencies of the two scintillators. This ratio was determined experimentally.

3.2.1 Measurement

The measurements were carried out at 11 points along the central axis ($r = 0$ cm) and 5 points along the off-central axis ($r = 15.2$ cm). The positions of the scintillator center and schematic configuration of Li_2O block are shown in Fig. 3.4, respectively. The Li-glass detector was inserted in the special Li_2O blocks equipped with a square central hole of 20 mm \times 20 mm. Solid blocks were used to fill space forward of the detector. These blocks holding the detector were loaded in the drawer, then this drawer was inserted into the experimental Li_2O assembly. The traverses of the two detectors were performed separately. During the traverses, the accelerated deuteron energy was 330 keV. Beam currents were 0.8 to 33 μA and 0.8 to 75 μA for ^6Li and ^7Li detectors, respectively, adjusted to the detector location so as to keep the anode current of the photo-multiplier tube almost constant. In order to achieve this condition, the product of channel number I and count C(I) in a MCA (multi-channel pulse height analyzer) was computed for every measurement ; and the current

adjusted proportionately :

$$S = \sum_I I \times C(I) = \text{const.}$$

The object of adjustment of the beam current was to prevent the gain drift.

The ${}^6\text{Li}$ atom number in the ${}^6\text{Li}$ -glass scintillator was 4.426×10^{21} [atom/cm³], calculated by using the values of a chemical analysis.*

3.2.2 Experimental results and experimental errors

Experimental results are shown in Table 3.4 and in Fig. 3.5. Experimental errors are summarized in Table 3.5. Self-shielding corrections were not included. The error in the ${}^6\text{Li}$ atom number was estimated to be $\pm 0.5\%$. Triton and α -particle escape was estimated by calculating the probability of total kinetic energy deposition in the scintillator.⁽²²⁾ To estimate the void effect on the TPR due to the channel (See Fig. 3.4), the calculated TPR for the case with the channel was compared with that without the channel. The TPRs for both cases agreed well within 1 %. Random errors of counts ($\Delta s/s$) resulting from the ${}^6\text{Li}(n,\alpha){}^3\text{T}$ reaction are larger in the frontal region of the assembly because the signal-to-noise ratio is small there. The fitting error is 10 ~ 40 % for the data of $Z \leq 30.1$ cm and 5 ~ 10 % for the data of $Z \geq 40.2$ cm.

* The chemical analysis was performed by Mr. & Mrs. Tamura of Analytical Chemistry Laboratory of JAERI by means of the isotope dilution method.

3.3 Tritium Production Rates of ^7Li Measured by an Small Sphere NE213 Spectrometer

The threshold energy of $^7\text{Li}(n,n't)^4\text{He}$ reaction is about 3 MeV. If we can measure the in-system spectra above this energy, the TPR of ^7Li (T_7) is obtained using an evaluated nuclear data of $^7\text{Li}(n,n't)^4\text{He}$. That is,

$$T_7 = \int \phi(E) \cdot \sigma_7(E) dE,$$

where

$\phi(E)$: measured neutron spectrum,
 $\sigma_7(E)$: evaluated cross section of $^7\text{Li}(n,n't)^4\text{He}$.

Newly developed small sphere NE213 spectrometer (20) is enough for this purpose. Therefore, the T_7 data were obtained automatically from the in-system spectra measurement (See Section 6).

Experimental results are shown in Table 3.6. The data of JENDL-3PR1 are used as the evaluated cross section of $^7\text{Li}(n,n't)^4\text{He}$. Experimental error due to the unfolding is estimated from the confidence interval (See section 6).

Table 3.1 Evaluation of escaped tritium rates during the irradiation and chemical treatment of Li_2O pellet.

Pellet	Escaped tritium rate (%) [*]		
	Recoil	Gas	Total escape
$^6\text{Li}_2\text{O}$	3.93 ± 0.18	2.14 ± 1.07	6.07 ± 1.25
$^7\text{Li}_2\text{O}$	1.81 ± 0.14	5.29 ± 0.76	7.10 ± 0.90

* The ratio divided by total produced tritium.

Table 3.2 Measured tritium production rates (TPR) in the 60 cm-thick Li₂O cylindrical slab assembly by liquid scintillation method with sintered Li₂O pellets.

(a) ${}^6\text{Li}(n,t){}^4\text{He}$

Position ^{*1} [cm]	Measured TPR		Corrected TPR for self-shielding	Corrected TPR ^{*4} for both effects
	[³ T / source neutron / atom]			
19.8 ₉	7.58	-29 ^{*2} (4.8%) ^{*3}	7.71 -29	7.66 -29
22.4 ₀	8.81	-29 (4.5%)	8.98 -29	8.93 -29
24.9 ₄	9.30	-29 (4.5%)	9.48 -29	9.44 -29
27.4 ₈	9.17	-29 (4.5%)	9.28 -29	9.23 -29
30.0 ₂	9.01	-29 (4.5%)	9.19 -29	9.15 -29
35.1 ₀	8.05	-29 (4.7%)	8.23 -29	8.18 -29
40.1 ₈	6.89	-29 (4.9%)	7.06 -29	7.01 -29
45.2 ₆	5.61	-29 (5.3%)	5.75 -29	5.71 -29
50.3 ₃	4.48	-29 (5.8%)	4.60 -29	4.55 -29
55.4 ₁	3.42	-29 (6.5%)	3.52 -29	3.48 -29
60.4 ₉	2.73	-29 (7.3%)	2.81 -29	2.76 -29
65.5 ₇	2.01	-29 (8.7%)	2.08 -29	2.03 -29
70.6 ₅	1.47 ₀	-29 (10.5%)	1.51 ₈ -29	1.46 ₂ -29
75.7 ₃	8.65	-30 (15.7%)	8.94 -30	8.36 -30
80.8 ₁	7.11	-30 (18.3%)	7.34 -30	----

^{*1} Distance from the target^{*2} Read as 7.58×10^{-29} ^{*3} Experimental error^{*4} Self-shielding and room-return effects^{*5} Room-return effect was very large and estimated to be over 200 %

Table 3.2 (continued)

(b) $^7\text{Li}(n,n't)^4\text{He}$

Position ^{*1} [cm]	Measured TPR	
[^3T / source neutron / atom]		
19.8 ₉	6.32 -29 ^{*2}	(4.2%) ^{*3}
22.4 ₀	4.60 -29	(4.9%)
24.9 ₄	3.85 -29	(5.6%)
27.4 ₈	2.67 -29	(6.4%)
30.0 ₂	2.08 -29	(7.6%)
35.1 ₀	1.26 ₁ -29	(10.7%)
45.2 ₆	4.57 -30	(23.8%)
50.3 ₃	3.92 -30	(28.1%)

Table 3.3 Error analysis for the TPR measurement by liquid scintillation method with sintered Li_2O pellet.
The measured data are presented in Table 3.2.

Item	Systematic error	Random error
Neutron yield	$\pm 1.5\%$	negligible
Efficiency curve	$\pm 1\%$	$\pm 2\%$
Tritium count	----	$\pm 2.8 \sim 24\%$
Li atom number	$\pm 0.1\%$	negligible
Tritium decay	negligible	----
Tritium escape	----	$\pm 0.9 \sim 1.3\%$

Table 3.4 Measured tritium production rates (TPR) in the Li₂O assembly by a pair of Li-glass scintillators.

Location [cm]		TPR1/ ⁶ Li atom/source neutron (error [%]) ^{*1}	Systematic error ^{*1}	Random error	
z	R			Δs/s	ΔCα/Cα
<u>Central axis</u>					
20.2 ₅	0	5.44 -29 (± 11.0)	± 5.4 * ²	± 3.6	± 2.0
22.5 ₃	0	7.05 -29 (± 9.9)		± 2.6	± 1.9
25.0 ₆	0	8.49 -29 (± 9.1)		± 1.7	± 2.0
27.6 ₁	0	7.63 -29 (± 10.5)		± 3.1	± 2.0
30.1 ₂	0	7.32 -29 (± 8.3)		± 1.3	± 1.6
40.2 ₄	0	6.21 -29 (± 7.9)		± 0.90	± 1.6
50.3 ₈	0	4.23 -29 (± 7.1)		± 0.60	± 1.1
60.5 ₀	0	2.52 -29 (± 7.3)		± 0.76	± 1.1
70.6 ₄	0	1.33 ₀ -29 (± 6.9)		± 0.72	± 0.80
75.7 ₂	0	8.28 -30 (± 6.8)		± 0.75	± 0.65
80.7 ₀	0	8.13 -29 (± 6.6)		± 0.63	± 0.56
<u>Off-central axis</u>					
20.2 ₅	15.2	6.10 -29 (± 9.5)		± 2.4	± 1.7
25.0 ₆	15.2	6.56 -29 (± 8.3)		± 1.3	± 1.6
30.1 ₂	15.2	6.04 -29 (± 8.6)		± 1.3	± 1.9
50.3 ₈	15.2	3.57 -29 (± 7.7)		± 0.88	± 1.4
70.6 ₄	15.2	1.11 ₂ -29 (± 6.8)		± 0.70	± 0.70

*1 Fitting and self-shielding errors are excluded.

*2 Systematic error is same for all data.

Table 3.5 Error Analysis for the TPR measurement by Li-glass scintillators.

items	systematic	random
count ($\Delta s/s$) ^{*1}	-----	$\pm (0.6 \sim 3.6) \%$
${}^6\text{Li}$ Atom Number	$\pm 0.5 \%$	-----
Edge Effect	< 2.0 %	-----
Void Effect	< 1.0 %	-----
Neutron Yield	$\pm 1.9 \%$	$\pm (0.6 \sim 2.0) \%$
Self-Shielding	$3.0 \sim 25 \%$	-----
Fitting ^{*2}	$5 \sim 40 \%$	-----

*1 Statistical error for subtracted count.

*2 This error is originated from the ambiguity of fitting region.(22)

Table 3.6 Measured tritium production rates (TPR) of ${}^7\text{Li}(n,n't){}^4\text{He}$ in the Li_2O assembly by a small spherical NE213 spectrometer.

Position ^{*1} [cm]	Measured TPR of ${}^7\text{Li}$		
	[${}^3\text{T}$ / atom / source neutron]		
21.6	4.61 -29 ^{*2}	(2.1%) ^{*3}	(3.3%) ^{*4}
31.5	1.65 ₆ -29	(1.0%)	(2.7%)
41.6	6.23 -30	(1.0%)	(2.7%)
51.7	2.40 -30	(2.4%)	(2.5%)
61.8	9.04 -31	(3.2%)	(2.4%)
72.0	3.46 -31	(4.1%)	(2.4%)
82.1	1.25 ₃ -31	(3.6%)	(2.3%)

*1 Distance from the target.

*2 Read as 4.61×10^{-29} .

*3 Experimental error due to the unfolding process.

*4 Experimental error for source intensity.

(See Tables 6.1 and 6.2)

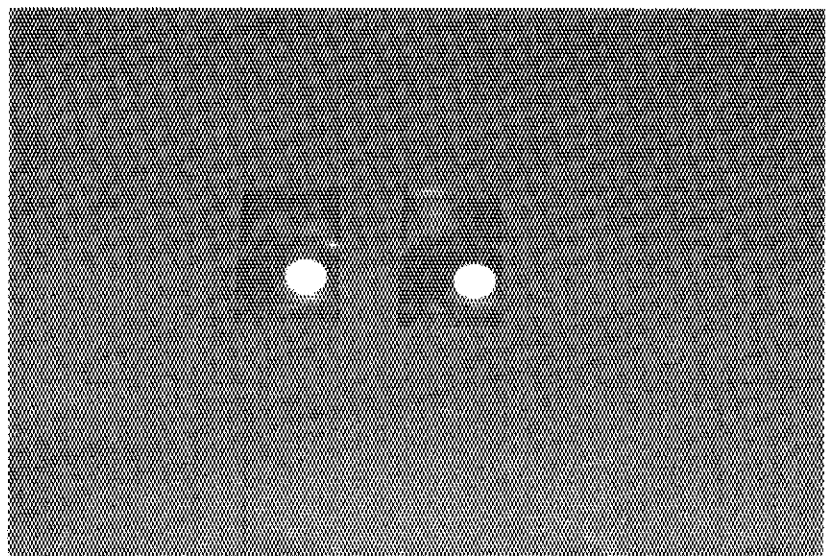


Fig. 3.1 Sintered Li_2O pellets.

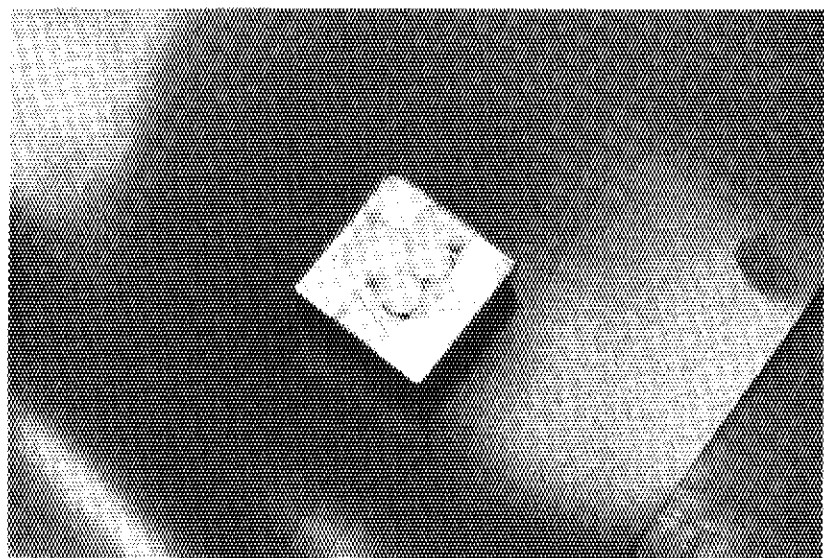


Fig. 3.2 Arrangement of sintered pellets in the space within the welding rim of a Li_2O block.

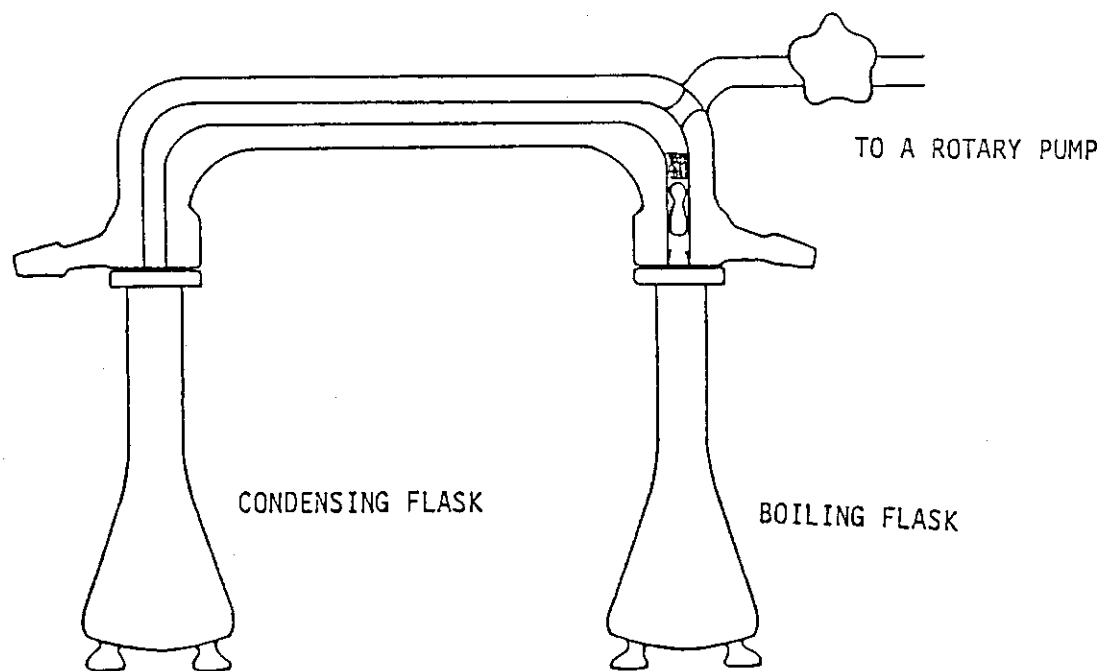
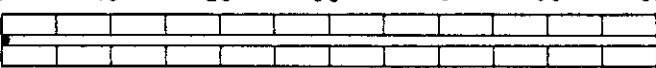
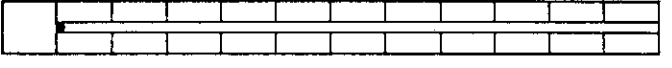
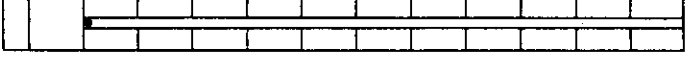
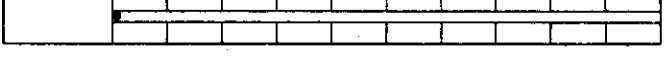
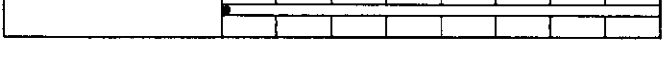
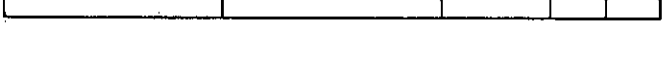
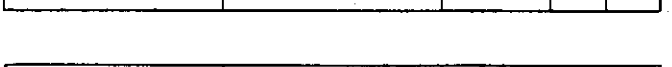


Fig. 3.3 Apparatus used for tritium extraction.

	Location ⁺ (cm)
	0.25 ± 0.05*
	2.53 ± 0.05
	5.06 ± 0.05*
	7.61 ± 0.05
	10.12 ± 0.05*
	20.24 ± 0.05
	30.38 ± 0.05*
	40.50 ± 0.10
	50.64 ± 0.10*
	55.72 ± 0.10
	60.70 ± 0.10

+ distance from the surface

• Measuring points ┌─┐ Li₂O block with experimental hole

* TPRs are measured along both central and off-central axis,
otherwise only central axis

Fig. 3.4 Detector locations and block configuration in the drawer
for TPR measurement using Li-glass scintillators.

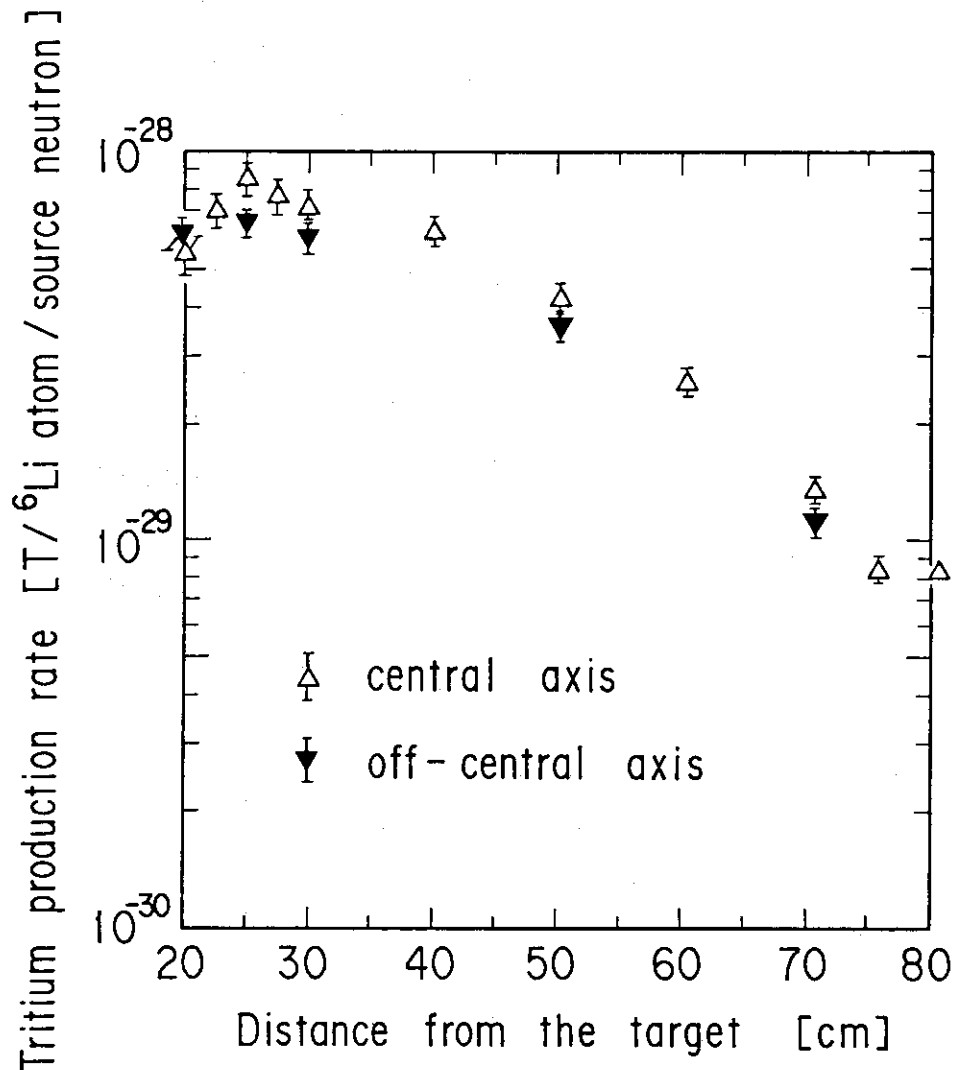


Fig. 3.5 Tritium production-rate distribution measured by a pair of Li-glass scintillators.

4. Fission-Rate Distributions Measured by Micro-Fission Chambers

Fission-rate distributions were measured with three micro-fission chambers coated respectively with about 4 mg of the oxides of ^{235}U , ^{238}U and ^{232}Th ; a fourth chamber was coated with about 1.6 mg of the oxide of ^{237}Np . The chamber were Type FC4A manufactured by T.C. Centronic Ltd, had 6.25 mm O.D. and 25.4 mm active length.

All the counter traverse experiments were made in the central experimental hole of 2 cm \times 2 cm. Fission rates in the ^{235}U and ^{238}U chambers were measured simultaneously, side by side, in the same hole. Similar measurements were carried out with the ^{237}Np and ^{232}Th chambers. As the detector was successively withdrawn along the axis, the channeled Li_2O blocks were replaced by solid blocks of the same material, to minimize neutron streaming. The remaining channel toward the rear of the assembly served to pass the signal cable.

The deuteron beam energy during the counter traverse was 330 keV and the beam current was varied from 100 μA to 2 mA with the count rate.

The four fission chambers were calibrated by a scheme very similar to that used in a previous experiment.⁽⁴⁾ A chamber was placed in front of the water-cooled target at distances of 20, 30 and 40 cm to count the neutrons emitted in the forward direction. The chamber was positioned with its axis at 0°, 45° and 90° to the incident d^+ beam. To correct for the effect of room-return neutrons, the fission chamber was placed in front of the target at a distance of 2 m. The background effect was found to be 9.3 and 1.6 % for the ^{235}U and ^{237}Np chambers respectively, and effect was negligible for the other chambers. The room background was subtracted from the data.

The number of effective atoms present in the chamber coating is calculated by the equation

$$N = \frac{C_0}{P \bar{\sigma}_f Y}, \quad [\text{fissile atoms/chamber}] \quad (4.1)$$

where N is the effective number of atoms in the micro-fission chamber, Y the neutron yield at the target obtained by α -monitoring, C_0 the

total count of fissions during the measuring time, P a geometrical factor determined by the configuration of target and chamber, $\bar{\sigma}_f$ the fission cross section averaged over the source spectrum and the atomic composition ;

$$\bar{\sigma}_f = \sum_i \sigma_f^i N_i , \quad (4.2)$$

where σ_f^i the average fission cross section, is given by,

$$\sigma_f^i = \int \sigma(E) \phi_f(E) dE , \quad (4.3)$$

where

N_i : isotopic abundance of i -th fissile material,

$\sigma(E)$: fission cross section,

$\phi_f(E)$: forward source neutron spectrum.

The fission cross-section data were taken from the ENDF/B-IV data file and the result of a Monte Carlo calculation⁽¹⁵⁾ was used as the source spectrum. It may be noted that the integral of the forward source neutron spectrum is not unity. The value of P was calculated by numerical integration.⁽⁴⁾

The effect of the structural material of the chamber was included in the effective atom number. The effective numbers of fissile atoms present in the chambers were calculated by Eq. (4.1) and are summarized in Table 4.1. The data at 45° were very close to those of 90 degree, while the data of 0 degree were a little differed from those of the others. Therefore the data for 0° to the axis (parallel) were calculated by averaging over three positions and the data of non-parallel over the other positions. The calibration errors were estimated to be 2.8 % for ^{235}U , ^{238}U and ^{232}Th , and 3.8 % for ^{237}Np chambers. Major sources of error were uncertainties in the neutron yield (Y) and positioning (P) ; the latter error was 1 %.

The absolute fission rate $R(z)$, for each chamber at the position z is given by the equation

$$R(z) = \frac{F_0(z)}{N(z) Y_t} , \quad [\text{fissions/source neutron/atom}] \quad (4.4)$$

where $F_0(z)$ is the total fission count at z , $N(z)$ the number of effective fissile atoms present in the chamber, and Y_t the total neutron yield at the target during the measurement. The $N(z)$ was estimated by assist of a pre-experimental analysis. An energy integrated angular flux within 6.72 degree was assumed as the forward (parallel) component. The $N(z)$ was obtained by averaging over the calculated fluxes of parallel and non-parallel components.

The uranium in the ^{235}U micro-fission chamber contained 7 % ^{238}U , and inversely that in the ^{238}U chamber 0.044 % ^{235}U , for which appropriate corrections were made in the observed fission rates. In the ^{237}Np chamber, the neptunium contained 0.1 % plutonium, mostly ^{239}Pu . Fissions contributed by this plutonium fraction were accounted for estimating its fission rate from that of ^{235}U , assuming an average ratio of 1.26 between the fission cross sections of ^{239}Pu and ^{235}U . The error due to this assumption should be small. The corresponding amount of impurity for ^{232}Th chamber was unknown, hence, the results obtained with ^{232}Th were not corrected.

The absolute fission rates thus determined are summarized in Table 4.2. The error estimates given in the table were determined in the following manner. The error was mainly caused by the errors of total neutron yield (2.1 %) and effective fissile atom numbers (3.2 ~ 4.6 %). The latter error included the angular-dependency of chambers. The absolute fission-rate distributions are shown in Fig. 4.1.

Room-return effect for the fission-rate of ^{235}U was evaluated by the MORSE-DD code.⁽²¹⁾ The corrections were 7.4, 3.8, 2.2, 1.4 and 1.0 % for 77.2, 72.1, 67.1, 62.0 and 56.9 cm from the target, respectively.

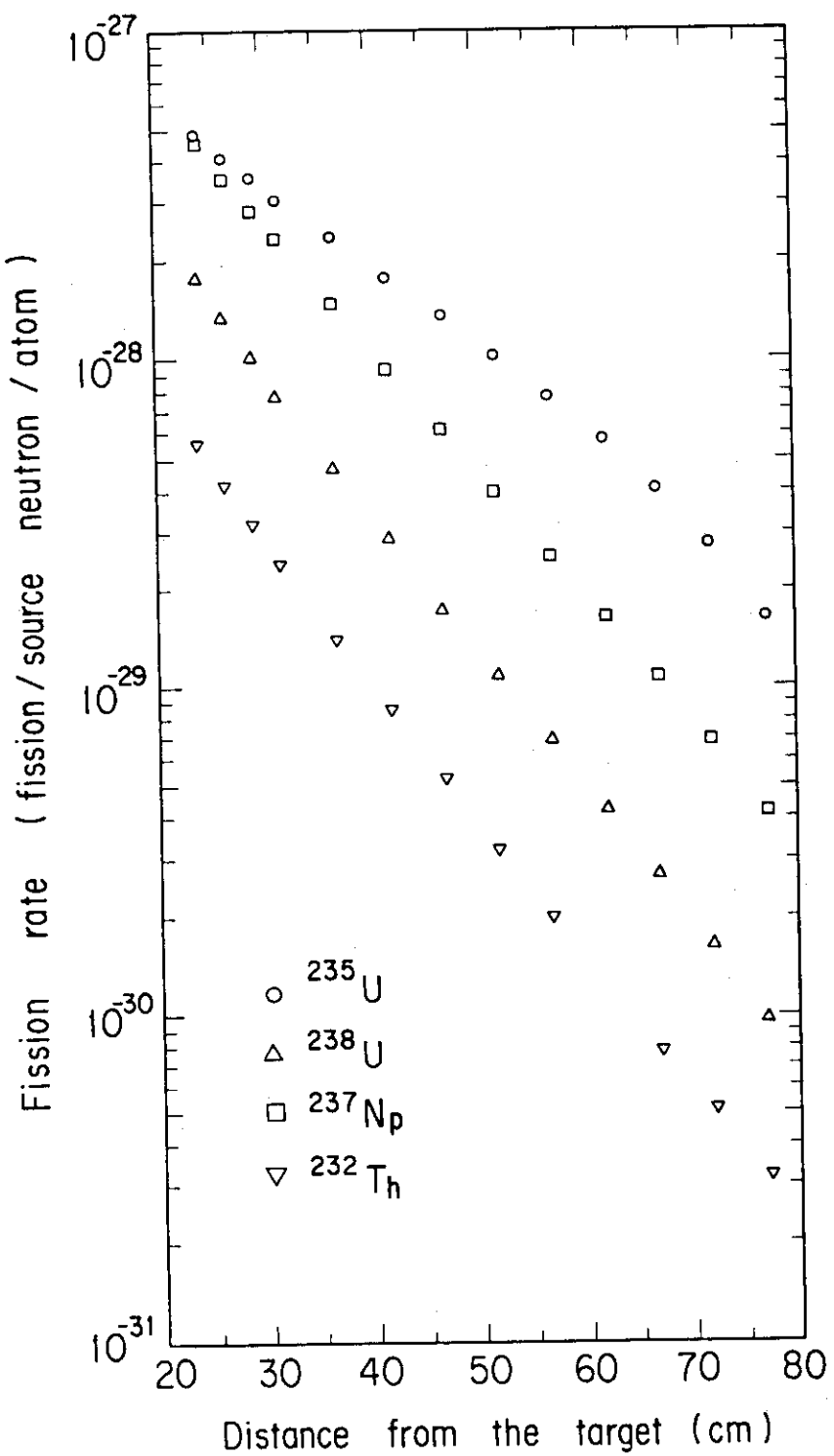
Table 4.1 Measured effective fissile atom numbers in micro-fission chambers.

Chamber	Effective fissile atom number [$\times 10^{18}$ atoms/chamber]			
	^{238}U	^{235}U	^{237}Np	^{232}Th
Parallel	7.32 ₈	6.73 ₄	2.20 ₅	6.78 ₆
Non-parallel	7.77 ₈	7.33 ₂	2.43 ₂	7.61 ₃

Table 4.2 Fission-rate distribution in the Li_2O cylindrical slab assembly.

Position ^{*1} [cm]	Fission rate [fission / source neutron / atom]			
	U-235	U-238	Np-237	Th-232
23.9	5.00 -28 (4.1%)	1.84 ₅ -28 (3.9%)	4.71 -28 (5.1%)	5.74 -29 (4.7%)
26.4	4.24 ₅ -28 (4.2%)	1.40 ₆ -28 (3.9%)	3.67 -28 (5.1%)	4.29 -29 (4.7%)
29.0	3.67 -28 (4.1%)	1.04 ₈ -28 (3.9%)	2.93 -28 (5.1%)	3.29 -29 (4.7%)
31.5	3.14 ₆ -28 (4.1%)	8.04 -29 (3.9%)	2.38 -28 (5.1%)	2.45 -29 (4.7%)
36.6	2.40 -28 (4.1%)	4.87 -29 (3.9%)	1.50 ₉ -28 (5.1%)	1.44 ₄ -29 (4.7%)
41.7	1.83 ₄ -28 (4.1%)	2.97 -29 (3.9%)	9.57 -29 (5.1%)	8.73 -30 (4.7%)
46.7	1.39 ₆ -28 (4.1%)	1.80 ₈ -29 (3.9%)	6.33 -29 (5.1%)	5.40 -30 (4.7%)
51.8	1.06 ₀ -28 (4.1%)	1.13 ₆ -29 (3.9%)	4.04 ₆ -29 (5.1%)	3.29 -30 (4.8%)
56.9	7.96 -29 (4.1%)	7.05 -30 (3.9%)	2.62 -29 (5.2%)	2.05 -30 (5.2%)
62.0	5.90 -29 (4.1%)	4.42 -30 (4.0%)	1.68 ₄ -29 (5.2%)	—
67.1	4.18 -29 (4.1%)	2.80 -30 (4.0%)	1.10 ₀ -29 (5.2%)	7.87 -31 (6.4%)
72.1	2.81 -29 (4.1%)	1.72 ₀ -30 (4.0%)	7.13 -30 (5.3%)	5.22 -31 (5.6%)
77.2	1.67 ₉ -29 (4.2%)	9.97 -31 (4.2%)	4.31 -30 (5.2%)	3.30 -31 (5.7%)

^{*1} Distance from the target.^{*2} Read as 5.00×10^{-28} .^{*3} Estimated error

Fig. 4.1 Absolute fission-rate distributions in the Li_2O assembly.

5. Reaction-Rate Distributions Measured by Activation Foils

Reaction-rate distributions of $^{27}\text{Al}(n,\alpha)^{24}\text{Na}$, $^{58}\text{Ni}(n,2n)^{57}\text{Ni}$, $^{115}\text{In}(n,n')^{115\text{m}}\text{In}$ and $^{115}\text{In}(n,\gamma)^{116\text{m}}\text{In}$ were measured along the central axis of the assembly by the foil activation technique. The four reactions were selected for their different energy responses, covering the whole energy region from thermal to 15 MeV. The reaction-rate of $^{58}\text{Ni}(n,2n)^{57}\text{Ni}$, with a threshold energy of 12.5 MeV, senses the direct D-T neutron flux. Since the $^{27}\text{Al}(n,\alpha)^{24}\text{Na}$ cross section is well known, the reaction-rate is expected to provide accurate information on the flux above 5 MeV neutron energy. The $^{115}\text{In}(n,n')^{115\text{m}}\text{In}$ reaction senses the intermediate flux because of its low threshold energy (about 0.5 MeV). The $^{115}\text{In}(n,\gamma)^{116\text{m}}\text{In}$ reaction, sensitive to slow neutrons, is appropriate to estimate the low energy neutron flux distribution.

5.1 Irradiation of foils and measurement of induced activities

Stacked foils of Al, Ni and In were inserted into the small spaces between Li_2O blocks, in the same manner as the Li_2O pellet measurement. The Al and Ni foils were 10 mm in diameter and 0.5 mm in thickness ; the In foils were 10 mm square and 0.1 mm in thickness. Foils were irradiated for 12 hours by D-T neutrons at an average intensity of $2.797 \times 10^{11} \text{ n/sec}$ at the target. After irradiation, spectra of gamma-rays emitted by the foils were measured with a 60 cm^3 Ge(Li) detector. The spectra were analyzed by the code BOB75,⁽²³⁾ to compute peak areas. Reaction rates were deduced from the measured gamma-ray peak counts, detector efficiency and decay data, with corrections for self-absorption, sum peak and saturation factor during the irradiation. The reaction-rate, R, is given by

$$R = \frac{\lambda \cdot C}{N \cdot X \cdot Y \cdot Y_n},$$

$$N = \frac{W \cdot N_0 \cdot a}{A},$$

$$X = e_f \cdot b \cdot s ,$$

$$Y = (1 - e^{-\lambda \cdot t_b}) \cdot e^{-\lambda t_c} \cdot (1 - e^{-\lambda \cdot t_m}) ,$$

where,

λ : decay constant,

C : measured gamma-ray counts,

W : weight of foil,

N_0 : Avogadro constant,

Y_n : source neutron yield,

a : abundance,

A : atomic number,

e_f : detector efficiency,

b : gamma-ray branching ratio,

P : gamma-ray self-absorption coefficient for each foil,

s : saturation correction coefficient,

t_b : irradiation time,

t_c : cooling time,

t_m : measuring time.

The neutron yield was monitored by the associated α -particle counting method.⁽¹⁸⁾ Decay data of the reaction products, taken from Ref.(24), are summarized in Table 5.1.

5.2 Observed reaction rates and their errors

The reaction rates at various positions are listed in Table 5.2. Counting statistics errors were in the range of ± 0.5 to 9 % ; the uncertainty of detector efficiency was about 2.5 %. Other error sources were in the decay data, the source neutron yield and corrections for self-absorption, sum peak and saturation factors. The error assessment is given in Table 5.3.

Table 5.1 Decay data needed for reaction-rate calculation.

Reaction	Half life	Detected γ -ray energy [keV]	γ -ray branching ratio [%]
$^{27}\text{Al}(\text{n},\alpha)^{24}\text{Na}$	15.02 h	1368.6	100
$^{57}\text{Ni}(\text{n},2\text{n})^{57}\text{Ni}$	36.0 h	1377.6	77.6
$^{115}\text{In}(\text{n},\text{n}')^{115m}\text{In}$	4.49 h	336.2	45.9
$^{115}\text{In}(\text{n},\gamma)^{116}\text{In}$	54.1 m	1293.5	85.0

Table 5.2 Reaction rate distribution in the Li₂O assembly.(a) $^{115}\text{In}(n,n')$ ^{115m}In and $^{115}\text{In}(n,\gamma)$ ^{116}In

Position *1 [cm]	$^{115}\text{In}(n,n')$ ^{115m}In	$^{115}\text{In}(n,\gamma)$ ^{116}In
[reaction rate / atom / source neutron]		
29.9 ₆	2.01 -29*2 (3.8%)*3	3.38 -29 (5.6%)*3
40.1 ₂	9.12 -30 (4.1%)	2.65 -29 (4.9%)
50.2 ₉	3.77 -30 (4.6%)	1.79 ₁ -29 (4.3%)
60.4 ₅	1.62 ₀ -30 (7.2%)	1.12 ₅ -29 (4.7%)
70.6 ₁	6.58 -31 (9.5%)	4.92 -30 (4.5%)

(b) $^{27}\text{Al}(n,\alpha)$ ^{24}Na

Position (cm)	[reaction rate/atom/source]
19.9 ₅	2.12 -29 (3.2 %)*3
22.4 ₄	1.57 ₂ -29 (3.1 %)
24.9 ₈	1.17 ₆ -29 (3.1 %)
27.5 ₂	8.61 -30 (3.3 %)
30.0 ₆	6.31 -30 (3.3 %)
35.1 ₄	3.60 -30 (3.3 %)
40.2 ₂	2.12 -30 (3.5 %)
45.3 ₀	1.27 ₅ -30 (3.5 %)
50.2 ₉	7.62 -31 (3.5 %)
55.4 ₇	4.49 -31 (3.1 %)
60.5 ₅	2.84 -31 (3.8 %)
65.6 ₃	1.66 ₇ -31 (3.8 %)
70.7 ₁	9.87 -32 (3.7 %)
75.7 ₉	6.11 -32 (3.6 %)

Table 5.2 (continued)

(c) $^{58}\text{Ni}(n,2n)^{57}\text{Ni}$

Position [cm]	[reaction rate/atom/source]
19.8 ₅	8.00 -30 (3.1%)*3
22.3 ₄	5.19 -30 (2.8%)
24.8 ₈	3.61 -30 (3.2%)
27.4 ₂	2.34 -30 (4.5%)
29.9 ₆	1.61 ₉ -30 (5.3%)
35.0 ₄	8.84 -31 (5.3%)
40.1 ₂	4.10 -31 (6.6%)
45.2 ₀	2.35 -31 (6.7%)
50.2 ₉	1.23 ₃ -31 (7.1%)
55.3 ₇	6.13 -32 (2.8%)
60.4 ₅	3.22 -32 (9.5%)
65.5 ₃	2.01 -32 (9.6%)
70.6 ₁	1.15 ₈ -32 (10.3%)
75.6 ₉	6.12 -33 (8.9%)

*1 Distance from the target.

*2 Read as 2.01×10^{-29} .

*3 Experimental error.

This error excludes the error of neutron yield.

Table 5.3 Error analysis for the reaction-rate measurements.

The measured data are presented in Table 5.2.

Item	Error [\pm %]
Counting statistics	0.5 ~ 9
Detector efficiency	2.5
Natural abundance	< 0.2
Foil weight	< 0.1
Sum peak	0.5 (only for ^{24}Na)
Saturation factor	0.3 for ^{57}Ni 0.5 for ^{24}Na 1.0 for ^{115m}In 2.0 for ^{116m}In
Source neutron yield	3.0
Times for irradiation,	\sim negligible
Cooling and measuring	
Decay data	< 0.5

6. Spectra measured by a small spherical NE213 spectrometer

A 14 mm-diameter spherical NE213 neutron spectrometer was used to make in-system neutron spectrum measurements. This spectrometer, newly developed for this purpose,⁽²⁰⁾ is shown in Fig. 6.1. The spectrometer measures pulse height spectra produced by hydrogen recoils in an NE213 liquid scintillator. The observed spectra are unfolded to yield neutron energy spectra by using previously prepared response matrices. The energy resolution of the detector is folded into the final spectra. The uncertainty of this technique depends mainly on response matrices and unfolding techniques.

6.1 Measurement and Data Processing

The detector was inserted into the experimental Li₂O assembly described in Section 3.2 for the Li-glass scintillator experiment. Positions of the detector center are summarized in Table 6.1. The table also shows the α -particle counts detected by the source neutron monitor. The deuteron energy was 310 keV ; the conversion factor from alpha counts to the total neutron yield is 5.517×10^7 [neutrons/alpha count] for that energy. The measuring time was 2000 sec each position at an average count rate of about 1 kcps for the sum of neutrons and gamma-rays. The signal from the photomultiplier anode was split into two signal lines after the pre-amplifier and analyzed by two independent pulse height analyzers, with separate amplifier gain and pulse shape discrimination systems (JAERI model 154A).⁽²⁵⁾ This scheme provided a linear overall response over the wide dynamic range that must be covered.

The two pulse height spectra thus obtained were joined at an appropriate energy point. This combined recoil-proton spectrum was unfolded by the FORIST code⁽²⁶⁾ and normalized to the total neutron yield. Data were stored on a floppy disk and later processed by means of a VAX-11/780 computer system.

The FORIST code determines the appropriate resolution function by internal iteration, hence, the computed resolution function differs somewhat from the actual detector resolution. The resolution function (window function $W(E)$) is thus given, together with the unfolded spectrum, for each case. A Gaussian function is used in smearing the

calculational spectrum :

$$\Phi_{\text{obs}}(E) = \int_0^{\infty} \frac{1}{\sqrt{2\pi}\sigma} \exp \left[-\frac{(E-E')^2}{2\sigma^2(E')} \right] \cdot \Phi_{\text{cal}}(E') dE' \quad (6.1.1)$$

where

$$\sigma(E') = \frac{W(E') \cdot E'}{235} .$$

and the denominator 235 is the conversion factor⁽²⁶⁾.

6.2 Results and Errors

The unfolded results obtained by this measurement are summarized in Tables 6.3 - 6.9. These tables indicate the upper and lower limits of the confidence interval given by the FORIST code, which means the true spectrum exists in this range with 67 % probability. The tables also include the window functions related to the detector resolution mentioned above. All spectra presented in the tables have been smeared by these resolution functions and have been normalized to scalar fluxes per unit 4π source neutron produced at the target. Figures 6.2 - 6.8 show midpoints of the upper and lower fluxes with uncertainty band (confidence interval).

The probable errors of the results include two contributions. One of these, the statistical error, is included in the results as the confidence interval. The other is error related to the response matrices which are used in the unfolding procedure. This is included in the systematic errors summarized in Table 6.2. The systematic errors also include the error in the alpha-monitor, as described in Ref. (18). The response matrix error is difficult to evaluate because there is no good way to determine the covariance matrix of response matrix terms. Thus we just give the efficiency error as the error of the integrated spectrum for mono-energetic neutrons which is calibrated through comparison with a time-of-fli to the detector area, which is used in conversion to scalar fluxes, is given by the actual volume of scintillation liquid.

Table 6.1 Detector location and alpha count of
in-system neutron spectral measurement.

Data No.	Position*1 [cm]	alpha counts : C_α [counts]
1	21.6 ± 0.1	1,962 (3.3%)*2
2	31.5 ± 0.1	5,474 (2.7%)
3	41.6 ± 0.1	5,389 (2.7%)
4	51.7 ± 0.1	10,319 (2.5%)
5	61.8 ± 0.1	35,654 (2.4%)
6	72.0 ± 0.1	88,963 (2.4%)
7	82.1 ± 0.1	318,777 (2.3%)

*1 Distance from the target.

*2 Experimental error for source intensity.
(See Table 6.2)

Table 6.2 Systematic errors in the unfolded spectra*1.

Item	Error [%]	Comment
Source intensity	$\pm \sqrt{(2.34)^2 + (10^4/C_\alpha)}$	Alpha monitor
Efficiency	(+ 0.4 ~ - 1.6) %	Calibration error*2

*1 Except the error related to the unfolding process.

*2 The calibration was performed by using the same D-T neutron source and α -monitor.

Therefore, the systematic error (2.34 %) is excluded in the value.

Table 6.3 In-system neutron spectrum in the Li₂O assembly ($z = 21.6$ cm).

(a) scalar spectrum									
60 CM Li ₂ O ASSEMBLY -- 14 PHI NE213 -- [Z=21.6 CM]									
** UNFOLDED SPECTRUM ***									
J	ENERGY(EV)	PMID	ERR	WIND	J	ENERGY(EV)	PMID	ERR	WIND
1	2.1020E+05	-2.9059E-04	1.0000E+00	3.1680E+01	4.6	1.9950E+06	2.1055E-05	1.2425E-01	3.6000E+01
2	2.2100E+05	-3.5789E-04	1.0000E+00	8.0510E+01	4.7	2.0970E+06	2.1100E-05	1.2777E-01	3.5140E+01
3	2.3230E+05	-4.3124E-04	1.0000E+00	7.9340E+01	4.8	2.2040E+06	2.4157E-05	1.0559E-01	3.4310E+01
4	2.4420E+05	-5.2568E-04	1.0000E+00	7.8160E+01	4.9	2.3170E+06	2.8622E-05	8.2654E-02	3.3550E+01
5	2.5680E+05	-6.2889E-04	1.0000E+00	7.7000E+01	5.0	2.4360E+06	3.2442E-05	6.9533E-02	3.2800E+01
6	2.6990E+05	-7.3690E-04	1.0000E+00	7.5820E+01	5.1	2.5610E+06	3.4043E-05	6.5221E-02	3.2040E+01
7	2.8380E+05	-9.0237E-04	1.0000E+00	7.4660E+01	5.2	2.6920E+06	3.2856E-05	6.8285E-02	3.1250E+01
8	2.9830E+05	-1.0545E-03	1.0000E+00	7.3480E+01	5.3	2.8300E+06	2.9409E-05	8.3618E-02	3.0490E+01
9	3.1360E+05	-1.2201E-03	1.0000E+00	7.2320E+01	5.4	2.9750E+06	2.4899E-05	2.9740E+01	2.9740E+01
10	3.2970E+05	-1.3934E-03	1.0000E+00	7.1140E+01	5.5	3.1280E+06	2.0620E-05	2.9020E+01	2.9020E+01
11	3.4660E+05	-1.5606E-03	1.0000E+00	6.9980E+01	5.6	3.2880E+06	1.7695E-05	2.2349E-01	2.8300E+01
12	3.6440E+05	-1.7128E-03	1.0000E+00	6.8800E+01	5.7	3.4570E+06	1.6938E-05	2.1725E-01	2.7580E+01
13	3.8300E+05	-1.8229E-03	1.0000E+00	6.7680E+01	5.8	3.6340E+06	1.8638E-05	1.5518E-01	2.6820E+01
14	4.0270E+05	-1.8848E-03	1.0000E+00	6.6600E+01	5.9	3.8210E+06	2.2228E-05	2.6060E+01	2.6060E+01
15	4.2330E+05	-1.9530E-03	1.0000E+00	6.5630E+01	6.0	4.0160E+06	2.6577E-05	1.0599E-01	2.5270E+01
16	4.4500E+05	-1.8104E-03	1.0000E+00	6.4690E+01	6.1	4.2220E+06	2.9958E-05	1.1495E-01	2.4550E+01
17	4.6780E+05	-1.6537E-03	1.0000E+00	6.3830E+01	6.2	4.4390E+06	3.1192E-05	1.0961E-01	2.3940E+01
18	4.9180E+05	-1.4472E-03	1.0000E+00	6.2960E+01	6.3	4.6660E+06	2.9718E-05	1.0326E-01	2.3330E+01
19	5.1700E+05	-1.1844E-03	1.0000E+00	6.2100E+01	6.4	4.9060E+06	2.5753E-05	1.1738E-01	2.2720E+01
20	5.4360E+05	-8.8930E-03	1.0000E+00	6.1200E+01	6.5	5.1570E+06	2.0160E-05	1.0833E-01	2.2130E+01
21	5.7140E+05	-6.3193E-04	1.0000E+00	6.0300E+01	6.6	5.4220E+06	1.4830E-05	2.4751E-01	2.1670E+01
22	6.0700E+05	-4.0335E-04	1.0000E+00	5.9360E+01	6.7	5.7000E+06	1.2274E-05	3.0759E-01	2.1100E+01
23	6.3150E+05	-2.3446E-04	1.0000E+00	5.8430E+01	6.8	5.9920E+06	1.3226E-05	2.8639E-01	2.0560E+01
24	6.6390E+05	-1.1931E-04	1.0000E+00	5.7490E+01	6.9	6.2990E+06	1.5555E-05	2.6915E-01	2.0020E+01
25	6.9790E+05	-4.2617E-05	1.0000E+00	5.6560E+01	7.0	6.6220E+06	2.0148E-05	1.6767E-01	2.1300E+01
26	7.3370E+05	-1.4780E-05	1.0000E+00	5.5620E+01	7.1	6.9610E+06	1.4830E-05	2.4751E-01	2.0970E+01
27	7.7130E+05	-6.0929E-07	5.7950E+02	5.4720E+01	7.2	7.3180E+06	1.6107E-05	3.4655E-01	1.8490E+01
28	8.1090E+05	-6.0854E-06	1.4337E+01	5.3866E+01	7.3	7.6940E+06	1.4734E-05	4.4604E-01	1.8040E+01
29	8.5250E+05	7.6555E-06	2.2298E+00	5.2990E+01	7.4	8.0880E+06	1.2665E-05	5.6539E-01	1.7620E+01
30	8.9620E+05	8.0157E-06	4.3564E-01	5.2160E+01	7.5	8.5030E+06	9.6774E-06	1.9480E+01	1.7220E+01
31	9.4210E+05	8.2942E-06	2.4136E-01	5.1340E+01	7.6	8.9390E+06	8.2574E-06	8.5035E-01	1.6780E+01
32	9.9040E+05	9.0032E-06	1.9618E-01	5.0470E+01	7.7	9.3970E+06	1.0513E-05	1.1018E+00	1.6360E+01
33	1.0410E+06	1.0479E-05	1.5911E-01	4.9577E+01	7.8	9.8790E+06	1.4335E-05	8.1458E-01	1.5930E+01
34	1.0950E+06	1.2997E-05	1.1780E-01	4.8664E+01	7.9	1.0390E+07	5.2481E-05	8.7837E-01	1.5470E+01
35	1.1510E+06	1.6664E-05	8.5254E-02	4.7590E+01	8.0	1.0920E+07	5.6719E-06	8.5035E-01	1.5070E+01
36	1.2100E+06	2.1418E-05	6.9285E-02	4.6510E+01	8.1	1.1480E+07	8.2574E-06	1.2641E+00	1.4760E+01
37	1.2720E+06	2.6972E-05	6.6220E-02	4.5400E+01	8.2	1.2070E+07	-2.2376E-05	1.0000E+00	1.4540E+01
38	1.3370E+06	3.2810E-05	6.8244E-02	4.4210E+01	8.3	1.2680E+07	-5.2481E-05	1.0000E+00	1.4420E+01
39	1.4060E+06	3.8166E-05	7.0789E-02	4.2950E+01	8.4	1.3340E+07	1.0396E-04	2.8180E-01	1.4400E+01
40	1.4780E+06	4.1990E-05	7.1458E-02	4.1720E+01	8.5	1.4020E+07	8.1125E-04	1.1950E-02	1.4400E+01
41	1.5530E+06	4.3254E-05	6.9276E-02	4.0570E+01	8.6	1.4740E+07	1.4861E-03	5.7789E-02	1.4400E+01
42	1.6330E+06	4.1382E-05	6.4059E-02	3.9530E+01	8.7	1.5490E+07	9.8413E-04	3.4504E-02	1.4400E+01
43	1.7170E+06	3.6622E-05	5.8889E-02	3.8560E+01	8.8	1.6290E+07	8.5276E-05	5.5053E-01	1.4400E+01
44	1.8050E+06	3.0285E-05	6.4501E-02	3.7690E+01	8.9	1.7120E+07	-1.7585E-04	1.0000E+00	1.4400E+01
45	1.8970E+06	2.4441E-05	9.2888E-02	3.6866E+01	9.0	1.8000E+07	-1.0188E-04	1.0000E+00	1.4400E+01

* ERR X 100 = %
 ** WIND = % [FWHM]
 *** [EN/CM**2/LET/HARGY/SOURCE]

Table 6.3 (b) Integrated spectrum

60 CM LI20 ASSEMBLY -- 14 PHI NE213 -- [Z=21.6 CM]
 *** RUNNING INTEGRAL ***

J	ENERGY (EV)	INTEGRAL	MAXIMUM	MINIMUM	J	ENERGY (EV)	INTEGRAL	MAXIMUM	MINIMUM
1	1.7556E+07	-5.1940E-06	-1.0138E-05	4.6	1	1.8502E+06	7.5791E-05	2.3052E-04	1.5358E-04
2	1.6697E+07	-1.292E-05	-2.773E-05	4.7	1	1.7642E+05	7.4799E-05	2.3214E-04	1.5500E-04
3	1.5238E+07	-1.292E-05	6.5111E-06	-2.557E-05	4.8	1	1.6746E+06	7.8361E-05	2.3408E-04
4	1.5108E+07	-1.0826E-05	5.7515E-05	2.1552E-05	4.9	1	1.5927E+06	7.9329E-05	2.3628E-04
5	1.4576E+07	4.5832E-05	1.3511E-04	9.163E-05	5.0	1	1.5147E+06	8.0336E-05	1.5866E-04
6	1.3674E+07	6.5075E-05	1.7875E-04	1.3015E-04	5.1	1	1.4415E+06	8.1310E-05	1.6067E-04
7	1.3011E+07	6.6941E-05	1.3011E-04	1.3389E-04	5.2	1	1.3713E+06	8.2197E-05	1.6262E-04
8	1.2367E+07	6.4317E-05	1.8542E-04	1.2863E-04	5.3	1	1.2640E+06	8.2961E-05	1.6439E-04
9	1.1772E+07	6.3198E-05	1.3542E-04	1.2640E-04	5.4	1	1.2406E+06	8.3591E-05	2.4607E-04
10	1.1197E+07	6.2885E-05	1.8542E-04	1.2578E-04	5.5	1	1.1801E+05	8.4089E-05	2.4722E-04
11	1.0650E+07	6.2697E-05	1.8636E-04	1.2539E-04	5.6	1	1.1226E+06	8.4470E-05	2.4812E-04
12	1.0153E+07	6.2743E-05	1.8776E-04	1.2549E-04	5.7	1	1.0680E+06	8.4757E-05	2.4885E-04
13	9.6551E+06	6.2269E-05	1.3907E-04	1.2562E-04	5.8	1	1.0153E+06	8.4977E-05	2.4946E-04
14	9.1650E+06	6.2782E-05	1.9017E-04	1.2556E-04	5.9	9	6.5935E+05	8.5158E-05	2.4999E-04
15	8.7183E+06	6.2723E-05	1.9111E-04	1.2546E-04	6.0	9	1.1384E+05	8.5315E-05	2.5051E-04
16	8.2931E+06	6.2764E-05	1.9200E-04	1.2553E-04	6.1	8	7.7407E+05	8.5429E-05	2.5108E-04
17	7.3883E+06	6.2902E-05	1.9299E-04	1.2580E-04	6.2	8	3.145E+05	8.5193E-05	2.5232E-04
18	7.5040E+06	6.3106E-05	1.7406E-04	1.2621E-04	6.3	7	9.088E+05	8.3164E-05	2.5699E-04
19	7.1373E+06	6.3369E-05	1.9515E-04	1.2674E-04	6.4	7	5.5266E+05	7.4352E-05	2.7467E-04
20	6.7891E+06	6.3671E-05	1.9623E-04	1.2734E-04	6.5	7	1.1558E+05	7.3613E-05	2.7467E-04
21	6.4535E+06	6.3976E-05	1.9731E-04	1.2795E-04	6.6	6	6.8067E+05	7.1132E-05	2.7467E-04
22	6.1435E+06	6.4260E-05	1.9830E-04	1.2852E-04	6.7	6	6.4751E+05	6.5167E-05	2.7467E-04
23	5.8441E+06	6.4496E-05	1.9935E-04	1.2899E-04	6.8	6	6.1591E+05	5.3444E-05	2.7467E-04
24	5.5593E+06	6.4794E-05	1.9995E-04	1.2942E-04	6.9	5	5.8587E+05	5.3276E-05	2.7467E-04
25	5.2381E+06	6.4982E-05	2.0088E-04	1.2998E-04	7.0	5	5.5729E+05	5.16799E-06	2.7467E-04
26	5.0297E+06	6.5470E-05	2.0205E-04	1.3081E-04	7.1	5	5.3018E+05	4.2872E-05	2.7467E-04
27	4.7849E+06	6.5975E-05	2.0349E-04	1.3195E-04	7.2	5	5.0424E+05	1.0209E-04	2.7467E-04
28	4.5508E+06	6.6642E-05	1.9935E-04	1.3238E-04	7.3	4	4.7966E+05	5.77454E-05	2.7467E-04
29	4.3294E+06	6.7336E-05	2.0636E-04	1.3266E-04	7.4	4	4.5625E+05	5.5714E-05	2.7467E-04
30	4.1178E+06	6.7959E-05	2.0853E-04	1.3600E-04	7.5	4	3.3401E+05	5.3401E+05	2.7467E-04
31	3.9168E+06	6.8557E-05	2.1000E-04	1.3718E-04	7.6	4	1.2825E+05	4.4212E-04	2.7467E-04
32	3.7267E+06	6.9089E-05	2.1124E-04	1.3818E-04	7.7	3	9.2766E+05	5.3636E-04	2.7467E-04
33	3.5443E+06	6.9423E-05	2.1231E-04	1.3897E-04	7.8	3	7.3545E+05	6.2751E-04	2.7467E-04
34	3.3716E+06	6.9514E-05	2.1334E-04	1.3963E-04	7.9	3	5.540E+05	5.5714E-04	2.7467E-04
35	3.2068E+06	7.0158E-05	2.1443E-04	1.4032E-04	8.0	3	3.804E+05	7.9118E-04	2.7467E-04
36	3.0508E+06	7.0582E-05	2.1564E-04	1.4116E-04	8.1	3	2.156E+05	6.6085E-04	2.7467E-04
37	2.9015E+06	7.1130E-05	2.1703E-04	1.4226E-04	8.2	3	0.556E+05	9.2185E-04	2.7467E-04
38	2.7601E+06	7.1803E-05	2.1863E-04	1.4351E-04	8.3	2	9.093E+05	9.7458E-04	2.7467E-04
39	2.6255E+06	7.2569E-05	2.2038E-04	1.4514E-04	8.4	2	7.679E+05	1.0197E-03	2.7467E-04
40	2.4978E+06	7.3364E-05	2.2220E-04	1.4673E-04	8.5	2	6.324E+05	1.0575E-03	2.7467E-04
41	2.3759E+06	7.4119E-05	2.2393E-04	1.4824E-04	8.6	2	5.046E+05	1.0890E-03	2.7467E-04
42	2.2598E+06	7.4775E-05	2.2548E-04	1.4955E-04	8.7	2	3.17E+05	1.1153E-03	2.7467E-04
43	2.1496E+06	7.5316E-05	2.2682E-04	1.5063E-04	8.8	2	2.656E+05	1.1368E-03	2.7467E-04
44	2.0452E+06	7.5776E-05	2.2801E-04	1.5155E-04	8.9	2	1.554E+05	1.1547E-03	2.7467E-04
45	1.9457E+06	7.6237E-05	2.2919E-04	1.5247E-04	9.0	2	0.501E+05	1.1693E-03	2.7467E-04

* ENERGY = LOWER BOUNDARY

Table 6.4 In-system neutron spectrum in the Li₂O assembly (z = 31.5 cm).

(a) scalar spectrum

60 CM Li₂O ASSEMBLY -- 14 PHI NE213 -- [Z=31.5 CM]

** UNFOLDED SPECTRUM ***

J	ENERGY(eV)	PWID	ERR	WIND	J	ENERGY(eV)	PWID	ERR	WIND	J	ENERGY(eV)	PWID	ERR	WIND
1	2.1020E+05	5.892E-04	2.1141E+01	8.168E+01	4.6	1.995E+06	1.8865E-05	5.3073E-02	5.6000E+01	1.8865E-05	5.3073E-02	5.6000E+01	1.8865E-05	5.3073E-02
2	2.2100E+05	7.1804E-04	2.1157E+01	8.051E+01	4.7	2.097E+06	1.9200E-05	5.2648E-02	5.5140E+01	2.097E+06	1.9200E-05	5.2648E-02	5.5140E+01	2.097E+06
3	2.3230E+05	8.7314E-04	2.1154E+01	7.934E+01	4.8	2.204E+06	2.0359E-05	5.4310E+01	4.889E-02	2.204E+06	2.0359E-05	5.4310E+01	4.889E-02	2.204E+06
4	2.4420E+05	1.0561E-03	2.1180E+01	7.816E+01	4.9	2.317E+06	2.1773E-05	4.4742E-02	3.3550E+01	2.317E+06	2.1773E-05	4.4742E-02	3.3550E+01	2.317E+06
5	2.5630E+05	1.2724E-03	2.1183E+01	7.700E+01	5.0	2.4360E+06	2.2733E-05	4.2172E-02	3.2800E+01	2.4360E+06	2.2733E-05	4.2172E-02	3.2800E+01	2.4360E+06
6	2.6990E+05	1.5227E-03	2.1166E+01	7.582E+01	5.1	2.5610E+06	2.2711E-05	4.1986E-02	3.2040E+01	2.5610E+06	2.2711E-05	4.1986E-02	3.2040E+01	2.5610E+06
7	2.8380E+05	1.8060E-03	2.1160E+01	7.466E+01	5.2	2.6920E+06	2.1554E-05	4.4470E-02	3.1250E+01	2.6920E+06	2.1554E-05	4.4470E-02	3.1250E+01	2.6920E+06
8	2.9830E+05	2.1220E+03	2.1220E+01	7.348E+01	5.3	2.8300E+06	2.0490E+01	3.0490E+01	3.0490E+01	2.8300E+06	2.0490E+01	3.0490E+01	3.0490E+01	2.8300E+06
9	3.1360E+05	2.4418E-03	2.1218E+01	7.2320E+01	5.4	2.9750E+06	1.6948E-05	2.9740E+01	2.9740E+01	2.9750E+06	1.6948E-05	2.9740E+01	2.9740E+01	2.9750E+06
10	3.2970E+05	2.8005E-03	2.1067E+01	7.1140E+01	5.5	3.1280E+06	1.4593E+01	2.9020E+01	2.9020E+01	3.1280E+06	1.4593E+01	2.9020E+01	2.9020E+01	3.1280E+06
11	3.4666E+05	3.0913E-03	2.1317E+01	6.9980E+01	5.6	3.2880E+06	1.2878E-05	2.8300E+01	2.8300E+01	3.2880E+06	1.2878E-05	2.8300E+01	2.8300E+01	3.2880E+06
12	3.6444E+05	3.4047E-03	2.1336E+01	6.8800E+01	5.7	3.4570E+06	1.2333E-05	2.7580E+01	2.7580E+01	3.4570E+06	1.2333E-05	2.7580E+01	2.7580E+01	3.4570E+06
13	3.8300E+05	3.6058E-03	2.1226E+01	6.7680E+01	5.8	3.6344E+06	1.2170E-05	2.6820E+01	2.6820E+01	3.6344E+06	1.2170E-05	2.6820E+01	2.6820E+01	3.6344E+06
14	4.0270E+05	3.7342E-03	2.1137E+01	6.6600E+01	5.9	3.8210E+06	1.2090E-05	2.6060E+01	2.6060E+01	3.8210E+06	1.2090E-05	2.6060E+01	2.6060E+01	3.8210E+06
15	4.2330E+05	3.7155E-03	2.1129E+01	6.5630E+01	6.0	4.0160E+06	1.7206E-05	2.5270E+01	2.5270E+01	4.0160E+06	1.7206E-05	2.5270E+01	2.5270E+01	4.0160E+06
16	4.4500E+05	3.5279E-03	2.1250E+01	6.4690E+01	6.1	4.2220E+06	1.3493E-05	2.4510E+01	2.4510E+01	4.2220E+06	1.3493E-05	2.4510E+01	2.4510E+01	4.2220E+06
17	4.6780E+05	3.2087E-03	2.1270E+01	6.3830E+01	6.2	4.4390E+06	1.8407E-05	2.3940E+01	2.3940E+01	4.4390E+06	1.8407E-05	2.3940E+01	2.3940E+01	4.4390E+06
18	4.9180E+05	2.7814E-03	2.1158E+01	6.2960E+01	6.3	4.6660E+06	1.7260E-05	2.3330E+01	2.3330E+01	4.6660E+06	1.7260E-05	2.3330E+01	2.3330E+01	4.6660E+06
19	5.1700E+05	2.2507E-03	2.1179E+01	6.2100E+01	6.4	4.9360E+06	1.5779E-05	2.2720E+01	2.2720E+01	4.9360E+06	1.5779E-05	2.2720E+01	2.2720E+01	4.9360E+06
20	5.4360E+05	1.6963E-03	2.1181E+01	6.1200E+01	6.5	5.1570E+06	1.4377E-05	2.2180E+01	2.2180E+01	5.1570E+06	1.4377E-05	2.2180E+01	2.2180E+01	5.1570E+06
21	5.7140E+05	1.1810E-03	2.1144E+01	6.0300E+01	6.6	5.4220E+06	1.3145E-05	2.1670E+01	2.1670E+01	5.4220E+06	1.3145E-05	2.1670E+01	2.1670E+01	5.4220E+06
22	6.0070E+05	7.4836E-04	2.1114E+01	5.9360E+01	6.7	5.7000E+06	1.2334E-05	2.1100E+01	2.1100E+01	5.7000E+06	1.2334E-05	2.1100E+01	2.1100E+01	5.7000E+06
23	6.3150E+05	4.2734E-04	2.1029E+01	5.8430E+01	6.8	5.9920E+06	1.2292E-05	2.0560E+01	2.0560E+01	5.9920E+06	1.2292E-05	2.0560E+01	2.0560E+01	5.9920E+06
24	6.6390E+05	2.1855E-04	2.0992E+01	5.7490E+01	6.9	6.2990E+06	1.2097E-05	2.0020E+01	2.0020E+01	6.2990E+06	1.2097E-05	2.0020E+01	2.0020E+01	6.2990E+06
25	6.9790E+05	9.9295E-05	1.9915E+01	5.6560E+01	7.0	6.6220E+06	1.1943E-05	1.9430E+01	1.9430E+01	6.6220E+06	1.1943E-05	1.9430E+01	1.9430E+01	6.6220E+06
26	7.3370E+05	4.1600E-05	1.7672E+01	5.5620E+01	7.1	6.9610E+06	1.1774E-05	1.8970E+01	1.8970E+01	6.9610E+06	1.1774E-05	1.8970E+01	1.8970E+01	6.9610E+06
27	7.7130E+05	1.8236E-05	1.2401E+01	5.4720E+01	7.2	7.3180E+06	1.2413E-05	1.8900E+01	1.8900E+01	7.3180E+06	1.2413E-05	1.8900E+01	1.8900E+01	7.3180E+06
28	8.1090E+05	1.0653E-05	1.0100E-05	5.3860E+00	7.3	7.6940E+06	1.2353E-05	1.8040E+01	1.8040E+01	7.6940E+06	1.2353E-05	1.8040E+01	1.8040E+01	7.6940E+06
29	8.5250E+05	8.8053E-06	1.2327E+00	5.2990E+01	7.4	8.0380E+06	1.2367E-05	1.7620E+01	1.7620E+01	8.0380E+06	1.2367E-05	1.7620E+01	1.7620E+01	8.0380E+06
30	8.9620E+05	8.5703E-06	2.3224E-01	5.2160E+01	7.5	8.5030E+06	1.4324E-05	1.7220E+01	1.7220E+01	8.5030E+06	1.4324E-05	1.7220E+01	1.7220E+01	8.5030E+06
31	9.4210E+05	8.7672E-06	9.2873E-02	5.1340E+01	7.6	8.9390E+06	1.3503E-05	1.6780E+01	1.6780E+01	8.9390E+06	1.3503E-05	1.6780E+01	1.6780E+01	8.9390E+06
32	9.9040E+05	9.2462E-06	7.3622E-02	5.0470E+01	7.7	9.3700E+06	1.3674E-05	1.6360E+01	1.6360E+01	9.3700E+06	1.3674E-05	1.6360E+01	1.6360E+01	9.3700E+06
33	1.0410E+06	1.0100E-05	6.7124E-02	4.9570E+01	7.8	9.8790E+06	1.3567E-05	1.5930E+01	1.5930E+01	9.8790E+06	1.3567E-05	1.5930E+01	1.5930E+01	9.8790E+06
34	1.0950E+06	1.1402E-05	5.9823E-02	4.8640E+01	7.9	1.0390E+07	1.7184E-05	1.5470E+01	1.5470E+01	1.0390E+07	1.7184E-05	1.5470E+01	1.5470E+01	1.0390E+07
35	1.1510E+06	1.3129E-05	5.3056E-02	4.7590E+01	8.0	1.0920E+07	1.4511E-05	1.5070E+01	1.5070E+01	1.0920E+07	1.4511E-05	1.5070E+01	1.5070E+01	1.0920E+07
36	1.2100E+06	1.5203E-05	4.7775E-02	4.6510E+01	8.1	1.1480E+07	1.3503E-05	1.4640E+01	1.4640E+01	1.1480E+07	1.3503E-05	1.4640E+01	1.4640E+01	1.1480E+07
37	1.2720E+06	1.7464E-05	4.4545E-02	4.5400E+01	8.2	1.2070E+07	1.3413E-05	1.4240E+01	1.4240E+01	1.2070E+07	1.3413E-05	1.4240E+01	1.4240E+01	1.2070E+07
38	1.3370E+06	1.9697E-05	4.2618E-02	4.4210E+01	8.3	1.2680E+07	1.3333E-05	1.3840E+01	1.3840E+01	1.2680E+07	1.3333E-05	1.3840E+01	1.3840E+01	1.2680E+07
39	1.4060E+06	2.1686E-05	4.2680E-02	4.2950E+01	8.4	1.3344E+07	1.3233E-05	1.3440E+01	1.3440E+01	1.3344E+07	1.3233E-05	1.3440E+01	1.3440E+01	1.3344E+07
40	1.4780E+06	2.3131E-05	4.2967E-02	4.1720E+01	8.5	1.4020E+07	1.3133E-05	1.3070E+01	1.3070E+01	1.4020E+07	1.3133E-05	1.3070E+01	1.3070E+01	1.4020E+07
41	1.5530E+06	2.3778E-05	4.2071E-02	4.0570E+01	8.6	1.4740E+07	1.3033E-05	1.2730E+01	1.2730E+01	1.4740E+07	1.3033E-05	1.2730E+01	1.2730E+01	1.4740E+07
42	1.6330E+06	2.3530E-05	4.1462E-02	3.9530E+01	8.7	1.5490E+07	1.2933E-05	1.2430E+01	1.2430E+01	1.5490E+07	1.2933E-05	1.2430E+01	1.2430E+01	1.5490E+07
43	1.7170E+06	2.2449E-05	4.0875E-02	3.8560E+01	8.8	1.6290E+07	1.2833E-05	1.2130E+01	1.2130E+01	1.6290E+07	1.2833E-05	1.2130E+01	1.2130E+01	1.6290E+07
44	1.8050E+06	2.0917E-05	3.1866E-02	3.7690E+01	8.9	1.7122E+07	1.2733E-05	1.1830E+01	1.1830E+01	1.7122E+07	1.2733E-05	1.1830E+01	1.1830E+01	1.7122E+07
45	1.8970E+06	1.9525E-05	4.8759E-02	3.6860E+01	9.0	1.8000E+07	1.2633E-05	1.1530E+01	1.1530E+01	1.8000E+07	1.2633E-05	1.1530E+01	1.1530E+01	1.8000E+07

* ERR X 100 = %

** WIND = % [FWHM]

*** [CN/CM**2/LETHARGY/SOURCE]

Table 6.4 (b) Integrated spectrum

60 CM LI2D ASSEMBLY -- 14 PHI NE213 -- C Z=31.5 CM 3
*** RUNNING INTEGRAL ***

J	ENERGY (EV)	INTEGRAL	MAXIMUM	VINYL	J	ENERGY (EV)	INTEGRAL	MAXIMUM	VINYL	J	ENERGY (EV)	INTEGRAL	MAXIMUM	VINYL
1	1.7556E+07	-1.4652E-06	0.0000E+00	-2.9303E-06	46	1.8502E+06	3.0625E-05	8.5435E-05	6.1369E-05	42	1.6245E+06	3.1185E-05	8.6526E-05	6.2370E-05
2	1.6697E+07	-4.8050E-06	0.3000E+00	-9.6100E-06	47	1.7604E-06	3.1723E-05	8.7695E-05	6.3445E-05	43	1.6746E+06	3.2257E-05	8.8920E-05	6.4574E-05
3	1.5838E+07	-6.1640E-06	0.0000E+00	-1.2328E-05	48	1.5921E+06	3.5147E+06	8.0159E-05	6.5713E-05	49	1.0987E-05	3.5147E+06	8.1365E-05	6.6820E-05
4	1.5103E+07	-1.0439E-06	1.6225E+06	-2.0879E-05	50	1.4415E+06	3.6100E-05	9.1365E-05	6.7858E-05	50	1.7227E-05	3.6100E-05	9.2370E-05	6.8801E-05
5	1.4376E+07	-8.4141E-06	3.1729E-05	-1.6528E-05	51	1.4415E+06	3.6100E-05	9.1365E-05	6.7858E-05	51	2.4714E-05	3.6100E-05	9.2370E-05	6.8801E-05
6	1.3674E+07	-1.4745E-05	4.5324E-05	-2.9491E-05	52	1.4415E+06	3.6100E-05	9.1365E-05	6.7858E-05	52	3.2970E-05	3.6100E-05	9.2370E-05	6.8801E-05
7	1.3011E+07	-1.6485E-05	4.7504E-05	-3.2941E-05	53	1.3715E+06	3.3929E-05	9.2496E-05	6.8801E-05	53	3.2553E-05	3.3929E-05	9.3523E-05	6.9635E-05
8	1.2367E+07	-1.6776E-05	5.0692E-05	-3.6692E-05	54	1.3040E+06	3.4400E-05	9.3523E-05	7.1517E-05	54	3.1727E-05	3.4400E-05	9.4435E-05	7.2416E-05
9	1.1772E+07	-1.7053E-05	5.1727E-05	-3.4116E-05	55	1.2405E+06	3.4818E-05	9.4435E-05	7.3559E-05	55	3.2754E-05	3.4818E-05	9.5231E-05	7.4981E-05
10	1.1197E+07	-1.7357E-05	5.2754E-05	-3.4754E-05	56	1.1801E+06	3.5179E-05	9.5231E-05	7.5921E-05	56	3.3768E-05	3.5179E-05	9.6527E-05	7.7198E-05
11	1.0650E+07	-1.7683E-05	5.3768E-05	-3.5372E-05	57	1.1225E+06	3.5490E-05	9.6527E-05	7.8144E-05	57	1.6927E-05	3.5490E-05	9.7562E-05	7.9521E-05
12	1.0133E+07	-1.8013E-05	5.4831E-05	-3.6931E-05	58	1.0680E+06	3.5755E-05	9.7562E-05	7.9548E-05	58	2.9308E-05	3.5755E-05	9.8041E-05	8.0401E-05
13	9.6351E+06	-1.8318E-05	5.6925E-05	-3.6637E-05	59	1.0153E+06	3.5994E-05	9.8041E-05	8.1423E-05	59	3.6672E-05	3.5994E-05	9.8765E-05	8.2416E-05
14	9.1650E+06	-1.8570E-05	5.8672E-05	-3.7141E-05	60	9.6595E+05	3.6208E-05	9.9521E-05	8.3424E-05	60	3.7650E-05	3.6208E-05	9.9521E-05	8.4241E-05
15	8.7183E+06	-1.8825E-05	5.9812E-05	-3.8240E-05	61	9.1834E+05	3.6407E-05	9.9521E-05	8.5146E-05	61	3.8240E-05	3.6407E-05	9.9521E-05	8.5921E-05
16	8.2931E+06	-1.9120E-05	6.1912E-05	-3.9375E-05	62	8.7402E+05	3.6722E-05	9.9521E-05	8.6844E-05	62	3.9277E-05	3.6722E-05	9.9548E-05	8.7304E-05
17	7.8383E+06	-1.9450E-05	6.3943E-05	-4.0277E-05	63	8.3145E+05	3.7048E-05	9.9548E-05	8.8345E-05	63	4.0277E-05	3.7048E-05	9.9548E-05	8.9345E-05
18	7.5040E+06	-1.9803E-05	6.6214E-05	-4.1960E-05	64	7.9088E+05	3.7320E-05	1.0287E-04	9.0735E-05	64	4.1960E-05	3.7320E-05	1.0287E-04	9.1735E-05
19	7.1373E+06	-2.0162E-05	6.1134E-05	-4.3232E-05	65	7.5226E+05	3.7619E-05	1.0195E-04	9.0390E-05	65	4.3232E-05	3.7619E-05	1.0195E-04	9.1390E-05
20	6.7891E+06	-2.0504E-05	6.2200E-05	-4.4008E-05	66	7.1552E+05	3.7855E-05	1.0393E-04	9.2144E-05	66	4.4008E-05	3.7855E-05	1.0393E-04	9.3144E-05
21	6.4535E+06	-2.0813E-05	6.3240E-05	-4.4832E-05	67	6.8067E+05	3.8098E-05	2.5777E-04	9.3196E-05	67	4.4832E-05	3.8098E-05	2.5777E-04	9.4196E-05
22	6.1435E+06	-2.1104E-05	6.3554E-05	-4.5525E-05	68	6.4751E+05	3.8351E-05	2.5777E-04	9.4172E-05	68	4.5525E-05	3.8351E-05	2.5777E-04	9.5172E-05
23	5.8441E+06	-2.1374E-05	6.4252E-05	-4.6274E-05	69	6.1591E+05	3.8653E-05	2.5777E-04	9.6140E-05	69	4.6274E-05	3.8653E-05	2.5777E-04	9.7140E-05
24	5.5593E+06	-2.1645E-05	6.4923E-05	-4.7289E-05	70	5.8587E+05	3.8953E-05	2.5777E-04	9.7193E-05	70	4.7289E-05	3.8953E-05	2.5777E-04	9.8193E-05
25	5.2382E+06	-2.1937E-05	6.5665E-05	-4.8275E-05	71	5.5729E+05	3.9255E-05	2.5777E-04	9.9196E-05	71	4.8275E-05	3.9255E-05	2.5777E-04	1.0196E-04
26	5.0297E+06	-2.2263E-05	6.6438E-05	-4.9256E-05	72	5.3012E+05	3.9557E-05	2.5777E-04	1.0182E-04	72	4.9256E-05	3.9557E-05	2.5777E-04	1.0385E-04
27	4.7849E+06	-2.2626E-05	6.7229E-05	-4.9291E-05	73	5.0424E+05	3.9859E-05	2.5777E-04	1.0182E-04	73	5.0424E+05	3.9859E-05	2.5777E-04	1.0385E-04
28	4.5508E+06	-2.3026E-05	6.8252E-05	-4.9653E-05	74	4.7966E+05	4.0161E-05	2.5777E-04	1.0360E-04	74	5.9276E-05	4.0161E-05	2.5777E-04	1.0555E-04
29	4.3294E+06	-2.3456E-05	6.9198E-05	-4.9911E-05	75	4.5625E+05	4.0460E-05	2.5777E-04	1.04640E-04	75	6.9198E-05	4.0460E-05	2.5777E-04	1.06440E-04
30	4.1178E+06	-2.3883E-05	7.0182E-05	-4.7776E-05	76	4.3401E+05	4.0759E-05	2.5777E-04	1.0535E-04	76	7.0182E-05	4.0759E-05	2.5777E-04	1.0735E-04
31	3.9168E+06	-2.4291E-05	7.1097E-05	-4.8581E-05	77	4.1285E+05	4.1058E-05	2.5777E-04	1.0624E-04	77	8.1097E-05	4.1058E-05	2.5777E-04	1.0824E-04
32	3.7267E+06	-2.4664E-05	7.1993E-05	-4.9291E-05	78	3.9276E-05	4.1358E-05	2.5777E-04	1.0713E-04	78	9.2676E-05	4.1358E-05	2.5777E-04	1.0913E-04
33	3.5443E+06	-2.4944E-05	7.2616E-05	-4.9889E-05	79	3.7354E+05	4.1657E-05	2.5777E-04	1.0803E-04	79	1.0447E-05	4.1657E-05	2.5777E-04	1.1003E-04
34	3.3716E+06	-2.5223E-05	7.3291E-05	-5.0447E-05	80	3.5540E+05	4.1956E-05	2.5777E-04	1.0902E-04	80	1.1030E-05	4.1956E-05	2.5777E-04	1.1102E-04
35	3.2068E+06	-2.5515E-05	7.3996E-05	-5.1030E-05	81	3.3804E+05	4.2257E-05	2.5777E-04	1.0991E-04	81	1.1702E-05	4.2257E-05	2.5777E-04	1.1391E-04
36	3.0508E+06	-2.5851E-05	7.4783E-05	-5.1702E-05	82	3.2156E+05	4.2556E-05	2.5777E-04	1.0980E-04	82	1.2394E-05	4.2556E-05	2.5777E-04	1.1591E-04
37	2.9015E+06	-2.6249E-05	7.5585E-05	-5.2498E-05	83	3.0586E+05	4.2854E-05	2.5777E-04	1.0969E-04	83	1.3093E-05	4.2854E-05	2.5777E-04	1.1799E-04
38	2.7601E+06	-2.6712E-05	7.6709E-05	-5.3423E-05	84	2.9093E+05	4.3153E-05	2.5777E-04	1.0958E-04	84	1.4091E-05	4.3153E-05	2.5777E-04	1.1998E-04
39	2.6255E+06	-2.7227E-05	7.7335E-05	-5.4433E-05	85	2.7679E+05	4.3452E-05	2.5777E-04	1.0947E-04	85	1.5091E-05	4.3452E-05	2.5777E-04	1.2197E-04
40	2.4978E+06	-2.7771E-05	7.7901E-05	-5.5541E-05	86	2.6324E+05	4.3751E-05	2.5777E-04	1.0936E-04	86	1.6206E-05	4.3751E-05	2.5777E-04	1.2396E-04
41	2.3759E+06	-2.8315E-05	7.8463E-05	-5.6630E-05	87	2.5046E+05	4.4050E-05	2.5777E-04	1.0925E-04	87	1.7283E-05	4.4050E-05	2.5777E-04	1.2595E-04
42	2.2598E+06	-2.9015E-05	7.9035E-05	-5.7670E-05	88	2.3817E+05	4.4359E-05	2.5777E-04	1.0914E-04	88	1.8282E-05	4.4359E-05	2.5777E-04	1.2794E-04
43	2.1496E+06	-2.9319E-05	8.0408E-05	-5.8638E-05	89	2.2656E+05	4.4658E-05	2.5777E-04	1.0903E-04	89	1.9298E-05	4.4658E-05	2.5777E-04	1.2993E-04
44	2.0452E+06	-2.9774E-05	8.1418E-05	-5.9547E-05	90	2.1554E+05	4.4957E-05	2.5777E-04	1.0892E-04	90	2.0301E+05	4.5256E-05	2.5777E-04	1.3191E-04
45	1.9457E+06	-3.0220E-05	8.2441E-05	-6.0441E-05	91	2.0501E+05	4.5565E-05	2.5777E-04	1.0881E-04	91	2.1441E-05	4.5565E-05	2.5777E-04	1.3391E-04

* ENERGY = LOWER BOUNDARY

Table 6.5 In-system neutron spectrum in the Li₂O assembly (z = 41.6 cm).

(a) scalar spectrum

60 CM Li₂O ASSEMBLY -- 14 PHI NE213 -- [Z=41.6 CM]
** UNFOLDED SPECTRUM ***

J	ENERGY (EV)	PWID	ERR	WIND	J	ENERGY (EV)	PWID	ERR	WIND
1	2.1020E+05	5.8943E-04	1.0995E+01	3.1680E+01	4.6	1.9950E+06	1.0540E-05	4.0011E-02	3.6000E+01
2	2.2100E+05	7.1982E-04	1.0978E+01	8.0510E+01	4.7	2.0970E+06	1.0723E-05	3.9370E-02	3.5140E+01
3	2.3230E+05	8.7522E-04	1.0977E+01	7.9340E+01	4.8	2.2040E+06	1.1112E-05	3.7935E-02	3.4310E+01
4	2.4420E+05	1.0605E-03	1.0974E+01	7.8160E+01	4.9	2.3170E+06	1.1507E-05	3.6340E-02	3.3550E+01
5	2.5680E+05	1.2777E-03	1.0974E+01	7.7000E+01	5.0	2.4360E+06	1.1674E-05	3.5259E-02	3.2800E+01
6	2.6990E+05	1.5273E-03	1.0977E+01	7.5820E+01	5.1	2.5610E+06	1.1448E-05	3.5548E-02	3.2040E+01
7	2.8380E+05	1.8120E-03	1.0971E+01	7.4660E+01	5.2	2.6920E+06	1.0787E-05	3.7861E-02	3.1250E+01
8	2.9830E+05	2.1212E-03	1.0986E+01	7.3480E+01	5.3	2.8300E+06	9.7772E-06	4.1831E-02	3.0490E+01
9	3.1360E+05	2.4556E-03	1.0980E+01	7.2320E+01	5.4	2.9750E+06	8.5969E-06	4.9017E-02	2.9740E+01
10	3.2970E+05	2.7949E-03	1.0981E+01	7.1140E+01	5.5	3.1280E+06	7.4758E-06	5.8363E-02	2.9020E+01
11	3.4660E+05	3.1201E-03	1.0987E+01	6.9980E+01	5.6	3.2880E+06	6.6573E-06	6.7472E-02	2.8300E+01
12	3.6440E+05	3.4087E-03	1.0983E+01	6.8800E+01	5.7	3.4570E+06	6.3558E-06	7.0044E-02	2.7580E+01
13	3.8300E+05	3.6212E-03	1.0992E+01	6.7680E+01	5.8	3.6340E+06	6.6342E-06	6.5774E-02	2.6820E+01
14	4.0270E+05	3.7351E-03	1.0992E+01	6.6600E+01	5.9	3.8210E+06	7.3217E-06	5.8912E-02	2.6060E+01
15	4.2330E+05	3.7161E-03	1.0992E+01	6.5630E+01	6.0	4.0160E+06	8.0418E-06	5.6373E-02	2.5270E+01
16	4.4500E+05	3.5452E-03	1.1002E+01	6.4690E+01	6.1	4.2220E+06	8.4482E-06	5.6414E-02	2.4550E+01
17	4.6780E+05	3.2256E-03	1.1008E+01	6.3830E+01	6.2	4.4390E+06	8.4324E-06	5.8289E-02	2.3940E+01
18	4.9180E+05	2.7829E-03	1.1000E+01	6.2960E+01	6.3	4.6600E+06	8.1323E-06	6.1335E-02	2.3330E+01
19	5.1700E+05	2.2527E-03	1.1007E+01	6.2100E+01	6.4	4.9060E+06	7.7427E-06	6.6970E-02	2.2720E+01
20	5.4360E+05	1.6963E-03	1.1023E+01	6.1200E+01	6.5	5.1570E+06	7.2879E-06	7.4536E-02	2.2130E+01
21	5.7140E+05	1.1791E-03	1.1014E+01	6.0300E+01	6.6	5.4220E+06	6.7213E-06	8.4972E-02	2.1670E+01
22	6.0070E+05	7.4678E-04	1.1007E+01	5.9360E+01	6.7	5.7000E+06	6.1959E-06	9.6574E-02	2.1100E+01
23	6.3150E+05	4.2455E-04	1.1011E+01	5.8430E+01	6.8	5.9920E+06	6.1335E-06	9.8379E-02	2.0560E+01
24	6.6390E+05	2.1481E-04	1.0951E+01	5.7490E+01	6.9	6.2990E+06	6.6024E-06	9.6035E-02	2.0020E+01
25	6.9790E+05	9.6395E-05	1.0671E+01	5.6560E+01	7.0	6.6220E+06	7.1976E-06	9.9822E-02	1.9480E+01
26	7.3370E+05	3.8510E-05	9.9260E+00	5.5620E+01	7.1	6.9610E+06	7.6366E-06	9.2673E-02	1.8970E+01
27	7.7150E+05	1.5190E-05	7.7404E+00	5.4720E+01	7.2	7.3180E+06	8.2620E-06	9.3364E-02	1.8490E+01
28	8.1090E+05	7.5679E-06	3.8351E+00	5.3860E+01	7.3	7.6940E+06	8.9154E-06	9.7798E-02	1.8040E+01
29	8.5220E+05	5.6987E-06	9.3922E+00	5.2990E+01	7.4	8.0880E+06	8.9882E-06	9.9897E-02	1.7620E+01
30	8.9622E+05	5.4560E-06	1.7775E-01	5.2160E+01	7.5	8.5030E+06	8.5311E-06	1.1352E-01	1.7220E+01
31	9.4210E+05	5.5925E-06	6.7587E-02	5.1340E+01	7.6	8.9390E+06	7.9170E-06	1.4613E-01	1.6730E+01
32	9.9000E+05	5.8642E-06	5.2580E-02	5.0470E+01	7.7	9.3970E+06	7.4646E-06	1.6582E-01	1.6360E+01
33	1.0410E+06	6.2649E-06	4.9701E-02	4.9570E+01	7.8	9.8790E+06	7.9225E-06	1.6963E-01	1.5930E+01
34	1.0930E+06	6.8017E-06	4.6880E-02	4.8640E+01	7.9	1.0390E+07	8.9822E-06	1.7812E-01	1.5470E+01
35	1.1510E+06	7.4573E-06	4.4279E-02	4.7590E+01	8.0	1.0920E+07	8.6674E-06	1.5481E-01	1.5070E+01
36	1.2100E+06	8.2068E-06	4.1874E-02	4.6510E+01	8.1	1.1480E+07	1.0096E-05	1.2844E-01	1.4760E+01
37	1.2720E+06	9.0032E-06	3.9618E-02	4.5400E+01	8.2	1.2070E+07	1.2106E-05	1.2295E-01	1.4540E+01
38	1.3370E+06	9.7822E-06	3.7910E-02	4.4210E+01	8.3	1.2680E+07	1.3786E-05	8.9974E-02	1.4320E+01
39	1.4000E+06	1.0499E-05	3.7073E-02	4.2950E+01	8.4	1.3340E+07	4.1330E-05	1.7825E-02	1.4300E+01
40	1.4780E+06	1.1520E-05	3.6923E-02	4.1720E+01	8.5	1.4020E+07	8.4535E-05	3.0050E-02	1.4300E+01
41	1.5530E+06	1.377E-05	3.6804E-02	4.0570E+01	8.6	1.4740E+07	1.0296E-04	4.1894E-02	1.4300E+01
42	1.6333E+06	1.445E-05	3.6315E-02	3.9530E+01	8.7	1.5490E+07	4.7524E-05	3.8669E-02	1.4300E+01
43	1.7170E+06	1.1264E-05	3.6168E-02	3.8560E+01	8.8	1.6290E+07	-1.0726E-05	1.0000E+00	1.4400E+01
44	1.8050E+06	1.0934E-05	3.5914E-02	3.7690E+01	8.9	1.7120E+07	-1.3486E-05	1.0000E+00	1.4400E+01
45	1.8970E+06	1.0633E-05	3.8738E-02	3.6860E+01	9.0	1.8000E+07	-8.6842E-06	1.0000E+00	1.4400E+01

* ERR X 100 = %

** WIND = % [FWHM]

*** [N/CM**2/LET/HARGY/SOURCE]

Table 6.5

(b) Integrated spectrum

60 CM LI20 ASSEMBLY -- 14 PHI NE213 -- [Z=41.6 CM]
 *** RUNNING INTEGRAL ***

J	ENERGY(EV)	INTEGRAL	MAXIMUM	MINIMUM	J ENERGY(EV)	INTEGRAL	MAXIMUM	MINIMUM
1	1.7556E+07	-4.3421E-07	0.0000E+00	-3.6842E-07	4.6	1.8502E+06	1.2633E-05	2.5366E-05
2	1.6697E+07	-1.3585E-06	0.0000E+00	-2.7170E-06	4.7	1.7604E+06	1.2946E-05	2.5893E-05
3	1.5888E+07	-1.8944E-06	0.0000E+00	-3.7396E-06	4.8	1.6746E+06	1.3218E-05	3.4127E-05
4	1.5108E+07	-7.5265E-07	2.4681E-06	-1.5053E-06	4.9	1.5927E+06	1.3494E-05	3.4720E-05
5	1.4376E+07	1.7133E-06	7.8318E-06	3.4270E-06	5.0	1.5147E+06	1.3768E-05	2.7535E-05
6	1.3674E+07	3.7634E-06	1.1866E-05	7.5268E-06	5.1	1.4415E+06	1.4034E-05	2.8067E-05
7	1.3011E+07	4.7475E-06	1.4350E-05	9.4949E-06	5.2	1.3713E+06	1.4286E-05	2.8573E-05
8	1.2367E+07	5.1749E-06	1.5374E-05	1.0350E-05	5.3	1.3040E+06	1.4522E-05	2.9044E-05
9	1.1772E+07	5.4403E-06	1.6054E-05	1.0881E-05	5.4	1.2406E+06	1.4738E-05	2.9476E-05
10	1.1197E+07	5.6603E-06	1.6624E-05	1.1321E-05	5.5	1.1801E+06	1.5113E-05	2.9869E-05
11	1.0650E+07	5.8434E-06	1.7124E-05	1.1226E-05	5.6	1.1226E+06	1.5220E-05	3.0226E-05
12	1.0133E+07	6.0062E-06	1.7591E-05	1.2012E-05	5.7	1.0680E+06	1.5275E-05	3.0550E-05
13	9.6351E+06	6.1623E-06	1.8030E-05	1.2325E-05	5.8	1.0153E+06	1.5424E-05	3.0847E-05
14	9.1650E+06	6.3180E-06	1.8466E-05	1.2636E-05	5.9	9.6595E+05	1.5563E-05	3.1125E-05
15	8.7183E+06	6.4870E-06	1.8919E-05	1.2974E-05	6.0	9.1884E+05	1.5693E-05	3.1386E-05
16	8.2931E+06	6.6761E-06	1.9394E-05	1.3352E-05	6.1	8.7407E+05	1.5803E-05	3.1610E-05
17	7.8835E+06	6.8779E-06	1.9889E-05	1.3757E-05	6.2	8.3145E+05	1.5807E-05	3.1613E-05
18	7.5040E+06	7.0796E-06	2.0377E-05	1.4159E-05	6.3	7.9088E+05	1.5270E-05	3.0540E-05
19	7.1373E+06	7.2669E-06	2.0829E-05	1.4534E-05	6.4	7.5226E+05	1.2711E-05	2.5421E-05
20	6.7891E+06	7.4491E-06	2.1246E-05	1.4880E-05	6.5	7.1558E+05	4.1170E-06	6.9906E-05
21	6.4585E+06	7.6027E-06	2.1641E-05	1.5205E-05	6.6	6.3067E+05	1.2616E-04	5.8378E-05
22	6.1435E+06	7.7519E-06	2.2003E-05	1.5504E-05	6.7	6.4751E+05	7.2628E-05	2.5425E-04
23	5.8441E+06	7.3897E-06	2.2339E-05	1.5779E-05	6.8	6.1591E+05	7.8888E-04	5.0483E-04
24	5.5593E+06	8.0297E-06	2.2678E-05	1.6059E-05	6.9	5.8587E+05	7.6571E-04	5.7781E-04
25	5.2881E+06	8.1834E-06	2.3043E-05	1.6367E-05	7.0	5.5729E+05	6.6090E-04	1.6661E-03
26	5.0297E+06	8.3520E-06	2.3434E-05	1.6704E-05	7.1	5.3018E+05	1.10859E-03	2.63858E-03
27	4.7849E+06	8.5327E-06	2.3847E-05	1.7055E-05	7.2	5.0424E+05	1.6495E-03	4.3882E-03
28	4.5508E+06	8.7234E-06	2.4279E-05	1.7447E-05	7.3	4.7966E+05	2.3452E-03	5.7080E-03
29	4.3294E+06	8.9219E-06	2.4725E-05	1.7844E-05	7.4	4.5625E+05	2.1523E-03	7.6446E-03
30	4.1178E+06	9.1212E-06	2.5172E-05	1.8242E-05	7.5	4.3401E+05	4.0388E-03	9.7721E-03
31	3.9168E+06	9.3119E-06	2.5596E-05	1.8622E-05	7.6	4.1285E+05	4.9670E-03	1.9001E-03
32	3.7227E+06	9.4382E-06	2.5984E-05	1.8966E-05	7.7	3.9276E+05	5.9001E-03	1.4240E-02
33	3.5443E+06	9.6381E-06	2.6338E-05	1.9276E-05	7.8	3.7354E+05	6.8046E-03	1.6411E-02
34	3.3771E+06	9.7859E-06	2.6678E-05	1.9575E-05	7.9	3.5540E+05	7.6554E-03	1.8453E-02
35	3.2068E+06	9.9411E-06	2.7033E-05	1.9882E-05	8.0	3.3804E+05	8.4334E-03	2.0323E-02
36	3.0508E+06	1.0117E-05	2.7429E-05	2.0234E-05	8.1	3.2156E+05	9.1318E-03	2.1998E-02
37	2.9015E+06	1.0321E-05	2.7879E-05	2.0643E-05	8.2	3.0586E+05	9.7445E-03	2.3469E-02
38	2.7601E+06	1.056E-05	2.8389E-05	2.1111E-05	8.3	2.9093E+05	1.0274E-02	2.4740E-02
39	2.6255E+06	1.0815E-05	2.8949E-05	2.1630E-05	8.4	2.7679E+05	1.0726E-02	2.5824E-02
40	2.4978E+06	1.1091E-05	2.9541E-05	2.2182E-05	8.5	2.6324E+05	1.1107E-02	2.6739E-02
41	2.3759E+06	1.1373E-05	3.0146E-05	2.2745E-05	8.6	2.5046E+05	1.1425E-02	2.7504E-02
42	2.2598E+06	1.1650E-05	3.0742E-05	2.3300E-05	8.7	2.3877E+05	1.1690E-02	2.8139E-02
43	2.1496E+06	1.1917E-05	3.1319E-05	2.3834E-05	8.8	2.2656E+05	1.1908E-02	2.8663E-02
44	2.0452E+06	1.2175E-05	3.1876E-05	2.4349E-05	8.9	2.1554E+05	1.2088E-02	2.9094E-02
45	1.9457E+06	1.2428E-05	3.2424E-05	2.4835E-05	9.0	2.0501E+05	1.2235E-02	2.9448E-02

* ENERGY = LOWER BOUNDARY

Table 6.6 In-system neutron spectrum in the Li₂O assembly ($z = 51.7$ cm).

(a) scalar spectrum

60 CM LI₂O ASSEMBLY --14 PHI NE213 -- [Z=51.7 CM]

** UNFOLDED SPECTRUM ***

J	ENERGY (EV)	PM10	ERR	WIND	J	ENERGY (EV)	PM10	ERR	WIND
1	2.11020E+05	-8.6034E-05	1.0000E+00	8.1680E+01	4.6	1.995E+06	5.0693E-06	5.5318E-02	3.6000E+01
2	2.2100E+05	-1.0455E-04	1.0000E+00	8.0510E+01	4.7	2.097E+06	5.1411E-06	3.4768E-02	3.5140E+01
3	2.3230E+05	-1.2643E-04	1.0000E+00	7.9340E+01	4.8	2.204E+06	5.2527E-06	3.3874E-02	3.4310E+01
4	2.4420E+05	-1.5405E-04	1.0000E+00	7.8160E+01	4.9	2.317E+06	5.3376E-06	3.3550E+01	3.3089E-02
5	2.5680E+05	-1.8514E-04	1.0000E+00	7.7000E+01	5.0	2.436E+06	5.4354E-06	3.2800E+01	3.2800E+01
6	2.6990E+05	-2.2093E-04	1.0000E+00	7.5820E+01	5.1	2.5610E+06	5.1400E-06	3.2040E+01	3.2040E+01
7	2.8380E+05	-2.6215E-04	1.0000E+00	7.4660E+01	5.2	2.6920E+06	4.8227E-06	3.5422E+02	3.1250E+01
8	2.9830E+05	-3.0803E-04	1.0000E+00	7.3480E+01	5.3	2.8300E+06	4.4143E-06	3.8517E-02	3.0470E+01
9	3.1360E+05	-3.5563E-04	1.0000E+00	7.2320E+01	5.4	2.9750E+06	3.9780E-06	4.2965E-02	2.9740E+01
10	3.2970E+05	-4.0359E-04	1.0000E+00	7.1140E+01	5.5	3.1280E+06	3.5647E-06	4.9094E-02	2.9020E+01
11	3.4666E+05	-4.5161E-04	1.0000E+00	6.9980E+01	5.6	3.2880E+06	3.2248E-06	5.5130E-02	2.8300E+01
12	3.6440E+05	-4.9259E-04	1.0000E+00	6.8800E+01	5.7	3.4570E+06	3.0219E-06	5.8419E-02	2.7580E+01
13	3.8300E+05	-5.2349E-04	1.0000E+00	6.7680E+01	5.8	3.6340E+06	3.0047E-06	5.9037E-02	2.6820E+01
14	4.0270E+05	-5.3983E-04	1.0000E+00	6.6600E+01	5.9	3.8210E+06	3.1522E-06	5.5985E-02	2.6060E+01
15	4.2330E+05	-5.3725E-04	1.0000E+00	6.5630E+01	6.0	4.0160E+06	3.3538E-06	5.4856E-02	2.5270E+01
16	4.4500E+05	-5.1131E-04	1.0000E+00	6.4690E+01	6.1	4.2220E+06	3.4909E-06	5.5404E-02	2.4550E+01
17	4.6780E+05	-4.6550E-04	1.0000E+00	6.3830E+01	6.2	4.4390E+06	3.5183E-06	5.6471E-02	2.3940E+01
18	4.9180E+05	-3.9885E-04	1.0000E+00	6.2960E+01	6.3	4.6660E+06	3.4773E-06	5.9102E-02	2.3330E+01
19	5.1700E+05	-3.2226E-04	1.0000E+00	6.2100E+01	6.4	4.9060E+06	3.3968E-06	6.2422E-02	2.2720E+01
20	5.4360E+05	-2.4290E-04	1.0000E+00	6.1530E+01	6.5	5.1570E+06	3.2495E-06	6.7755E-02	2.2180E+01
21	5.7140E+05	-1.6735E-04	1.0000E+00	6.0300E+01	6.6	5.4220E+06	3.0219E-06	7.5928E-02	2.1670E+01
22	6.0070E+05	-1.0466E-04	1.0000E+00	5.9360E+01	6.7	5.7000E+06	2.8173E-06	8.5163E-02	2.1100E+01
23	6.3150E+05	-5.8333E-05	1.0000E+00	5.8430E+01	6.8	5.9920E+06	2.8276E-06	8.5860E-02	2.0560E+01
24	6.6390E+05	-2.7920E-05	1.0000E+00	5.7490E+01	6.9	6.2990E+06	3.1354E-06	7.9964E-02	2.0020E+01
25	6.9790E+05	-1.0875E-05	1.0000E+00	5.6560E+01	7.0	6.6220E+06	3.5326E-06	7.6337E-02	1.9480E+01
26	7.3370E+05	-2.4795E-06	1.0000E+00	5.5620E+01	7.1	6.9610E+06	3.6994E-06	7.4966E-02	1.8970E+01
27	7.7130E+05	9.9627E-07	5.5971E+01	5.4720E+01	7.2	7.3180E+06	5.6418E-06	8.0119E-02	1.8490E+01
28	8.1090E+05	2.2106E-06	6.2228E+00	5.3860E+01	7.3	7.6940E+06	3.6440E-06	8.9511E-02	1.8040E+01
29	8.5250E+05	2.5809E-06	1.0359E+00	5.2990E+01	7.4	8.0880E+06	3.7726E-06	9.5119E-02	1.7620E+01
30	8.9620E+05	2.7094E-06	1.0000E+00	5.2160E+01	7.5	8.5030E+06	3.7666E-06	9.6720E-02	1.7220E+01
31	9.4210E+05	3.8102E-06	6.0564E-02	5.1340E+01	7.6	8.9390E+06	3.4408E-06	1.4747E-01	1.6780E+01
32	9.9040E+05	2.9096E-06	4.6779E-02	5.0470E+01	7.7	9.3970E+06	5.1496E-06	7.2777E-02	1.6360E+01
33	1.0410E+06	3.0658E-06	4.4753E-02	4.9570E+01	7.8	9.8790E+06	3.3760E-06	1.3965E-01	1.5930E+01
34	1.0950E+06	3.2749E-06	4.3063E-02	4.8640E+01	7.9	1.0590E+07	3.9037E-06	1.3392E-01	1.5470E+01
35	1.1510E+06	3.5263E-06	4.1549E-02	4.7590E+01	8.0	1.0920E+07	4.4830E-06	1.0802E-01	1.5070E+01
36	1.2100E+06	3.8102E-06	3.9828E-02	4.6510E+01	8.1	1.1480E+07	5.3297E-06	8.5895E-02	1.4210E+01
37	1.2720E+06	4.1072E-06	3.8028E-02	4.5400E+01	8.2	1.2070E+07	6.9126E-06	1.4475E-01	1.4210E+01
38	1.3370E+06	4.3979E-06	3.6530E-02	4.4210E+01	8.3	1.2680E+07	1.0270E-05	5.4242E-02	1.4230E+01
39	1.4060E+06	4.6639E-06	3.5771E-02	4.2950E+01	8.4	1.3340E+07	1.7487E-05	5.5233E-02	1.4210E+01
40	1.4780E+06	4.8822E-06	3.5580E-02	4.1720E+01	8.5	1.4020E+07	2.7338E-05	2.9463E-02	1.4210E+01
41	1.5530E+06	5.0555E-06	3.5321E-02	4.0570E+01	8.6	1.4740E+07	4.8077E-05	4.8077E-02	1.4210E+01
42	1.6330E+06	5.1195E-06	3.4615E-02	3.9530E+01	8.7	1.5490E+07	1.1032E-05	5.1616E-02	1.4210E+01
43	1.7170E+06	5.1333E-06	3.4162E-02	3.8560E+01	8.8	1.6290E+07	-3.2333E-05	1.0000E+00	1.4400E+01
44	1.8050E+06	5.0982E-06	3.4299E-02	3.7690E+01	8.9	1.7120E+07	-4.6099E-06	1.0000E+00	1.4400E+01
45	1.8970E+06	5.0596E-06	3.5056E-02	3.6866E+01	9.0	1.8000E+07	-2.0696E-06	1.0000E+00	1.4400E+01

* ERR X 100 = %

** WIND = % [FWHM]

*** [N/CM*2/LETHARGY/SOURCE]

Table 6.6 (b) Integrated spectrum

60 CM LI20 ASSEMBLY --14 PHI NE213 -- [Z=51.7 CM]
*** RUNNING INTEGRAL ***

J	ENERGY (EV)	INTEGRAL	MAXIMUM	MINIMUM	J	ENERGY (EV)	INTEGRAL	MAXIMUM	MINIMUM
1	1.7556E+07	-1.0348E-07	0.0000E+00	-2.0696E-07	4.6	1.8502E+06	5.2621E-06	1.2904E-05	1.0524E-05
2	1.6697E+07	-3.3397E-07	0.0000E+00	-6.7795E-07	4.7	1.7604E+06	5.3852E-06	1.3168E-05	1.0770E-05
3	1.5388E+07	-4.9164E-07	0.0000E+00	-9.9178E-07	4.8	1.6746E+06	5.5092E-06	1.3433E-05	1.1013E-05
4	1.5108E+07	-2.3408E-07	5.8007E-07	-4.6815E-07	4.9	1.5927E+06	5.6327E-06	1.3698E-05	1.1265E-05
5	1.4376E+07	4.2347E-07	2.0280E-06	8.4693E-07	5.0	1.5147E+06	5.7542E-06	1.3959E-05	1.1508E-05
6	1.3674E+07	1.0863E-06	3.4352E-06	2.1736E-06	5.1	1.4415E+06	5.8719E-06	1.4212E-05	1.1744E-05
7	1.3011E+07	1.5086E-06	4.3403E-06	3.0171E-06	5.2	1.3713E+06	5.9843E-06	1.4453E-05	1.1969E-05
8	1.2367E+07	1.7514E-06	4.817E-06	3.5027E-06	5.3	1.3040E+06	6.0902E-06	1.4668E-05	1.2130E-05
9	1.1772E+07	1.9116E-06	5.2525E-06	3.8232E-06	5.4	1.2406E+06	6.1890E-06	1.4894E-05	1.2378E-05
10	1.1191E+07	2.0334E-06	5.5418E-06	4.0568E-06	5.5	1.1801E+06	6.2805E-06	1.5092E-05	1.2561E-05
11	1.0650E+07	2.1334E-06	5.7902E-06	4.2668E-06	5.6	1.1226E+06	6.3650E-06	1.5227E-05	1.2730E-05
12	1.0133E+07	2.2179E-06	6.0115E-06	4.4358E-06	5.7	1.0680E+06	6.4433E-06	1.5447E-05	1.2837E-05
13	9.6335E+06	2.2905E-06	6.3842E-06	4.5810E-06	5.8	1.0153E+06	6.5165E-06	1.5607E-05	1.3033E-05
14	9.1650E+06	2.3579E-06	6.5778E-06	4.7157E-06	5.9	9.6595E+05	6.5259E-06	1.5759E-05	1.3172E-05
15	8.7183E+06	2.4331E-06	6.8661E-06	4.8661E-06	6.0	9.1884E+05	6.6516E-06	1.5908E-05	1.3303E-05
16	8.2931E+06	2.5181E-06	5.7344E-06	5.0362E-06	6.1	8.7407E+05	6.7079E-06	1.6066E-05	1.3416E-05
17	7.8882E+06	2.6040E-05	5.9399E-06	5.2080E-06	6.2	8.1145E+05	6.7056E-06	1.6328E-05	1.3411E-05
18	7.5040E+06	2.6869E-06	7.3854E-06	5.3739E-06	6.3	7.9028E+05	6.4166E-06	1.6712E-05	1.2832E-05
19	7.1373E+06	2.7770E-06	7.5843E-06	5.5410E-06	6.4	7.5226E+05	5.0475E-06	1.6975E-05	1.0095E-05
20	6.7391E+06	2.8561E-06	7.7744E-06	5.7121E-06	6.5	7.1558E+05	4.9235E-06	1.7066E-05	9.8470E-06
21	6.4585E+06	2.9376E-06	7.9376E-06	5.8753E-06	6.6	6.8067E+05	4.3798E-06	1.9965E-05	8.7595E-06
22	6.1435E+06	3.0093E-06	7.9437E-06	6.0195E-06	6.7	5.4751E+05	2.9838E-06	1.9965E-05	5.9675E-06
23	5.8441E+06	3.0744E-06	8.0972E-06	6.1457E-06	6.8	5.1125E+05	6.7112E-06	1.9965E-05	1.3422E-05
24	5.5593E+06	3.1328E-06	8.2101E-06	6.2776E-06	6.9	5.8587E+05	5.1659E-06	1.9965E-05	1.0332E-05
25	5.2881E+06	3.2026E-06	8.4126E-06	6.4172E-06	7.0	5.5729E+05	1.3534E-05	1.9965E-05	2.7068E-05
26	5.0297E+06	3.2844E-06	8.5861E-06	6.5687E-06	7.1	5.3018E+05	2.5679E-05	1.9965E-05	1.3358E-05
27	4.7849E+06	3.3640E-06	8.7666E-06	6.7279E-06	7.2	5.0424E+05	4.1792E-05	1.9965E-05	1.9965E-05
28	4.5508E+06	3.4453E-06	8.9507E-06	6.8915E-06	7.3	4.7966E+05	6.1736E-05	1.9965E-05	1.2342E-05
29	4.3294E+06	3.5283E-06	9.1366E-06	7.0575E-06	7.4	4.5625E+05	5.8501E-05	1.9965E-05	1.0022E-05
30	4.1178E+06	3.6112E-06	9.3208E-06	7.2224E-06	7.5	4.3401E+05	1.3534E-05	1.9965E-05	2.1155E-04
31	3.9168E+06	3.6904E-06	9.4977E-06	7.3809E-06	7.6	4.1285E+05	1.1058E-04	1.9965E-05	2.7488E-04
32	3.7267E+06	3.7648E-06	9.5641E-06	7.5297E-06	7.7	3.9276E+05	1.3744E-04	1.9965E-05	1.3384E-05
33	3.5443E+06	3.8355E-06	9.3232E-06	7.6710E-06	7.8	3.7354E+05	1.6443E-05	1.9965E-05	1.2342E-05
34	3.3716E+06	3.9066E-06	9.9831E-06	7.8133E-06	7.9	3.5540E+05	8.5011E-05	1.9965E-05	1.7002E-04
35	3.2068E+06	3.9828E-06	1.0153E-05	7.9657E-06	8.0	3.3804E+05	2.1523E-04	1.9965E-05	4.7563E-04
36	3.0508E+06	4.0676E-06	1.0340E-05	8.1351E-06	8.1	3.2156E+05	2.3778E-04	1.9965E-05	1.5999E-04
37	2.9015E+06	4.1627E-06	1.0548E-05	8.3255E-06	8.2	3.0586E+05	2.7578E-04	1.9965E-05	5.5155E-04
38	2.7601E+06	4.2689E-06	1.0777E-05	8.5377E-06	8.3	2.9093E+05	3.1216E-04	1.9965E-05	3.8235E-04
39	2.6255E+06	4.3851E-06	1.1027E-05	8.7703E-06	8.4	2.7679E+05	4.0285E-04	1.9965E-05	4.3047E-04
40	2.4978E+06	4.5093E-06	1.1292E-05	9.0187E-06	8.5	2.6324E+05	1.5333E-04	1.9965E-05	6.3066E-04
41	2.3759E+06	4.6379E-06	1.1567E-05	9.2757E-06	8.6	2.5046E+05	2.4595E-04	1.9965E-05	6.4918E-04
42	2.2598E+06	4.7662E-06	1.1842E-05	9.5338E-06	8.7	2.3817E+05	3.3229E-04	1.9965E-05	6.6458E-04
43	2.1496E+06	4.8918E-06	1.2114E-05	9.7875E-06	8.8	2.2656E+05	3.3861E-04	1.9965E-05	6.7723E-04
44	2.0452E+06	5.0178E-06	1.2380E-05	1.0036E-05	8.9	2.1554E+05	4.3844E-04	1.9965E-05	6.8769E-04
45	1.9457E+06	5.1401E-06	1.2642E-05	1.0230E-05	9.0	2.0501E+05	3.4814E-04	1.9965E-05	6.9629E-04

* ENERGY = LOWER BOUNDARY

Table 6.7 In-system neutron spectrum in the Li₂O assembly ($z = 61.8$ cm).

(a) scalar spectrum

60 CM LI₂O ASSEMBLY -- 14 PHI NE213 -- [Z=61.8 CM]

** UNFOLDED SPECTRUM *** *

J	ENERGY(EV)	PWID	ERR	WIND	J	ENERGY(EV)	PWID	ERR	WIND	J	ENERGY(EV)	PWID	ERR	WIND	
1	2.1020E+05	-3.4037E-05	1.0000E+00	8.1680E+01	4.6	1.9950E+06	2.2116E-06	3.2745E-02	3.6000E+01	2	2.1100E+05	-4.1310E-05	1.0000E+00	8.0510E+01	3.2107E-02
3	2.3230E+05	-5.0239E-05	1.0000E+00	7.9340E+01	4.7	2.0970E+06	2.2359E-06	3.5140E+01	2.3230E+05	4	2.4420E+05	-6.0774E-05	1.0000E+00	7.8160E+01	2.2637E-06
5	2.5680E+05	-7.3398E-05	1.0000E+00	7.7000E+01	4.8	2.3170E+06	2.2705E-06	3.4310E+01	2.5680E+05	6	2.6990E+05	-8.7702E-05	1.0000E+00	7.5820E+01	2.3350E-06
7	2.8380E+05	-1.0394E-04	1.0000E+00	7.4660E+01	5.0	2.4360E+06	2.2281E-06	3.1369E-02	2.8380E+05	8	2.9830E+05	-1.2189E-04	1.0000E+00	7.3480E+01	2.2800E+01
9	3.1360E+05	-1.4075E-04	1.0000E+00	7.3200E+01	5.1	2.5610E+06	2.1214E-06	3.2040E+01	3.1360E+05	10	3.2970E+05	-1.6052E-04	1.0000E+00	7.2320E+01	3.1250E+01
11	3.4650E+05	-1.7892E-04	1.0000E+00	7.1140E+01	5.5	2.8300E+06	2.1214E-06	3.4490E+01	3.4650E+05	12	3.6440E+05	-1.9524E-04	1.0000E+00	6.9800E+01	3.4472E-02
13	3.8300E+05	-2.0770E-04	1.0000E+00	6.8800E+01	5.7	3.4570E+06	1.2792E-06	2.7580E+01	3.8300E+05	14	4.0270E+05	-2.1357E-04	1.0000E+00	6.7680E+01	5.3745E-02
15	4.2330E+05	-2.1253E-04	1.0000E+00	6.6600E+01	5.8	3.6340E+06	1.2830E-06	5.4613E-02	4.2330E+05	16	4.4500E+05	-2.0263E-04	1.0000E+00	6.5630E+01	6.6320E+01
17	4.6780E+05	-1.8404E-04	1.0000E+00	6.4690E+01	6.1	4.2220E+06	1.3521E-06	2.9020E+01	4.6780E+05	18	4.9180E+05	-1.5820E-04	1.0000E+00	6.3230E+01	5.1502E-02
19	5.1700E+05	-1.2754E-04	1.0000E+00	6.2960E+01	6.3	4.6660E+06	1.4164E-06	2.8300E+01	5.1700E+05	20	5.4360E+05	-9.5705E-05	1.0000E+00	6.2100E+01	5.5177E-02
21	5.7140E+05	-6.5823E-05	1.0000E+00	6.1200E+01	6.4	4.9060E+06	1.4416E-06	5.5920E+01	5.7140E+05	22	6.0700E+05	-4.1780E-05	1.0000E+00	5.9360E+01	5.5177E-02
23	6.3150E+05	-2.2922E-05	1.0000E+00	5.8430E+01	6.8	5.9920E+06	1.4466E-06	5.5920E+01	6.3150E+05	24	6.6390E+05	-1.0967E-05	1.0000E+00	5.7490E+01	5.2333E-02
25	6.9790E+05	-4.1714E-06	1.0000E+00	5.6560E+01	6.9	6.2990E+06	1.4561E-06	5.7488E-02	6.9790E+05	25	7.3370E+05	-8.6115E-07	1.0000E+00	5.5620E+01	5.3752E-02
26	7.7130E+05	5.1969E-07	4.5806E+01	5.4720E+01	7.1	6.9610E+06	1.4751E-06	5.4197E-02	7.7130E+05	27	8.1090E+05	1.0410E+06	4.1819E-02	5.0470E+01	5.5177E-02
28	8.5250E+05	1.0605E-06	9.8370E-01	5.2990E+01	7.3	7.6940E+06	1.5651E-06	7.4462E-02	8.5250E+05	29	9.1050E+05	1.4435E-06	4.9570E+01	5.2990E+01	5.0560E+01
30	8.9620E+05	1.2180E-06	1.5896E-01	5.2160E+01	7.4	8.0890E+06	1.5619E-06	7.4899E-02	8.9620E+05	31	9.4210E+05	1.2572E-06	5.6438E-02	5.1570E+01	5.2218E-01
32	9.9040E+05	1.3028E-06	4.3457E-02	5.1340E+01	7.5	8.5930E+06	1.5371E-06	7.4840E-02	9.9040E+05	33	1.0410E+06	1.3635E-06	4.1819E-02	5.0470E+01	5.3370E-01
34	1.0950E+06	1.4435E-06	4.0725E-02	4.8640E+01	7.6	9.3970E+06	1.4810E-06	7.1497E-02	1.0950E+06	35	1.1510E+06	1.5384E-06	4.7590E+01	5.0470E+01	5.4370E-01
36	1.2100E+06	1.6443E-06	3.8338E-02	5.1340E+01	7.7	1.1480E+07	1.4810E-06	7.0824E-02	1.2100E+06	37	1.2720E+06	1.7542E-06	3.6879E-02	5.0470E+01	5.4370E-01
38	1.3370E+06	1.8625E-06	3.5419E-02	4.4210E+01	7.8	1.2680E+07	1.5290E-06	7.1100E-02	1.3370E+06	39	1.4060E+06	1.9650E-06	3.4681E-02	4.8640E+01	5.5619E-01
40	1.4780E+06	2.0544E-06	3.4402E-02	4.7590E+01	7.9	1.3340E+07	1.5329E-06	7.2220E-02	1.4780E+06	41	1.5530E+06	2.1249E-06	3.3995E-02	4.1720E+01	5.6780E-01
42	1.6333E+06	2.1731E-06	3.3238E-02	4.6510E+01	8.0	1.4020E+07	1.4900E-06	7.0795E-02	1.6333E+06	43	1.7170E+06	2.1963E-06	3.2538E-02	4.5400E+01	5.2416E-01
44	1.8050E+06	2.2013E-06	3.2258E-02	3.8560E+01	8.1	1.4740E+07	1.4810E-06	7.0957E-02	1.8050E+06	45	1.8970E+06	2.2009E-06	3.2596E-02	3.6860E+01	5.3364E-01

* ERR X 100 = %

** WIND = % [FWHM]

*** [CN/CM*2/LETTHARGY/SOURCE]

Table 6.7

(b) Integrated spectrum

60 CM LI120 ASSEMBLY -- 14 PHI NE213 -- E Z=61.8 CM]
*** RUNNING INTEGRAL ***

J	ENERGY (EV)	INTEGRAL	MAXIMUM	MINIMUM	J	ENERGY (EV)	INTEGRAL	MAXIMUM	MINIMUM
1	1.7556E+07	-2.6628E-08	0.0000E+00	-5.3364E-03	4.6	1.2502E+06	2.0797E-06	4.9168E-06	4.1594E-06
2	1.6697E+07	-3.6152E-08	0.0000E+00	-1.7230E-07	4.7	1.7604E+06	2.1330E-06	4.2659E-06	4.0304E-06
3	1.5888E+07	-1.3169E-07	0.0000E+00	-2.6339E-07	4.8	1.6746E+06	2.1861E-06	4.3722E-06	5.1438E-06
4	1.5108E+07	-6.6117E-03	1.4767E-07	-1.3223E-07	4.9	1.5927E+06	2.2386E-06	4.4772E-06	5.2560E-06
5	1.4376E+07	1.1570E-07	5.5071E-07	2.3140E-07	5.0	1.5147E+06	2.2899E-06	4.5798E-06	5.3659E-06
6	1.3674E+07	3.2109E-07	9.5571E-07	6.4217E-07	5.1	1.4415E+06	2.3395E-06	4.6790E-06	4.6721E-06
7	1.3011E+07	4.7708E-07	1.3168E-06	9.5416E-07	5.2	1.3713E+06	2.3869E-06	4.7739E-06	4.7538E-06
8	1.2367E+07	5.6603E-07	1.5529E-06	1.1722E-06	5.3	1.3040E+06	2.4318E-06	4.8637E-06	5.0722E-06
9	1.1772E+07	6.6196E-07	1.7214E-06	1.3239E-06	5.4	1.2406E+06	2.4741E-06	4.9482E-06	5.0712E-06
10	1.1197E+07	7.1591E-07	1.3412E-06	1.4273E-06	5.5	1.1501E+06	2.5136E-06	5.8465E-06	5.0272E-06
11	1.0650E+07	7.5273E-07	1.9360E-06	1.5055E-06	5.6	1.1226E+06	2.5505E-06	5.9265E-06	5.1011E-06
12	1.0133E+07	7.8779E-07	2.0248E-06	1.0248E-06	5.7	1.0620E+06	2.5852E-06	6.0016E-06	5.1703E-06
13	9.6351E+06	8.2173E-06	1.1977E-06	1.6436E-06	5.8	1.0153E+06	2.6178E-06	6.0277E-06	5.2357E-06
14	9.1650E+06	8.5469E-07	2.1920E-06	1.7094E-06	5.9	9.6595E+05	2.6490E+05	6.1406E-06	5.2980E-06
15	8.7163E+06	8.8805E-07	2.2743E-06	1.7761E-06	6.0	9.1884E+05	2.6786E-06	6.2070E-06	5.3573E-06
16	8.2931E+06	9.2503E-07	2.3576E-06	1.8461E-06	6.1	8.7407E+05	2.7042E-06	6.2776E-06	5.4085E-06
17	7.8863E+06	9.5896E-07	2.4420E-06	1.9177E-06	6.2	8.3145E+05	2.7404E-06	6.3927E-06	5.4095E-06
18	7.5040E+06	9.9503E-07	2.5263E-06	1.6991E-06	6.3	7.9088E+05	2.5830E-06	6.7367E-06	5.1660E-06
19	7.1373E+06	1.0307E-06	2.6091E-06	2.0615E-06	6.4	7.5226E+05	2.0009E-06	7.9529E-06	4.0017E-06
20	6.7889E+06	1.0650E-06	2.6380E-06	2.1300E-06	6.5	7.1553E+05	1.9578E-06	7.9529E-06	3.9156E-06
21	6.4585E+06	1.0967E-06	2.7617E-06	2.1934E-06	6.6	6.8967E+05	1.7492E-06	7.9529E-06	3.4985E-06
22	6.1435E+06	1.1262E-06	2.5303E-06	2.2524E-06	6.7	6.4751E+05	1.2009E-06	7.9529E-06	2.4013E-06
23	5.8441E+06	1.1551E-06	2.3974E-06	2.3103E-06	6.8	6.1591E+05	5.4739E-08	1.0958E-07	4.0684E-06
24	5.5939E+06	1.1854E-06	2.9672E-06	2.3798E-06	6.9	5.8587E+05	2.0342E-06	7.9529E-06	4.0684E-06
25	5.2888E+06	1.2177E-06	3.0408E-06	2.4355E-06	7.0	5.5729E+05	5.3254E-06	7.9529E-06	1.0651E-05
26	5.0297E+06	1.2515E-06	3.1170E-06	2.5031E-06	7.1	5.3018E+05	1.0111E-05	7.9529E-06	2.0221E-05
27	4.7849E+06	1.2859E-06	3.1940E-06	2.5717E-06	7.2	5.0424E+05	-1.6438E-05	7.9529E-06	3.2975E-05
28	4.5503E+06	1.3270E-06	2.7071E-06	2.6393E-06	7.3	4.7966E+05	2.4398E-05	7.9529E-06	4.8795E-05
29	4.3294E+06	1.3533E-06	3.3449E-06	2.7067E-06	7.4	4.5625E+05	3.3600E-05	7.9529E-06	6.7199E-05
30	4.1178E+06	1.3862E-06	3.4180E-06	2.7723E-06	7.5	4.3401E+05	4.3731E-05	7.9529E-06	8.7462E-05
31	3.9168E+06	1.4182E-06	3.4894E-06	2.8365E-06	7.6	4.1285E+05	5.4358E-05	7.9529E-06	1.0872E-04
32	3.7267E+06	1.4493E-06	3.5587E-06	2.8986E-06	7.7	3.9276E+05	6.5036E-05	7.9529E-06	1.3007E-04
33	3.56443E+06	1.4796E-06	3.6262E-06	2.9591E-06	7.8	3.7354E+05	7.5421E-05	7.9529E-06	1.5084E-04
34	3.3716E+06	1.5098E-06	3.6936E-06	3.0196E-06	7.9	3.5804E+05	8.5183E-05	7.9529E-06	1.7037E-04
35	3.2063E+06	1.5414E-06	3.7633E-06	3.0828E-06	8.0	3.4201E+05	9.4129E-05	7.9529E-06	1.8826E-04
36	3.0508E+06	1.5757E-06	3.3390E-06	3.1514E-06	8.1	3.2156E+05	-1.0216E-04	7.9529E-06	2.0431E-04
37	2.9015E+06	1.6138E-06	3.9219E-06	3.2277E-06	8.2	3.0586E+05	-1.0919E-04	7.9529E-06	2.1839E-04
38	2.7601E+06	1.6565E-06	4.0139E-06	3.3130E-06	8.3	2.9093E+05	-1.1529E-04	7.9529E-06	2.3057E-04
39	2.6255E+06	1.7038E-06	4.1153E-06	3.4076E-06	8.4	2.7679E+05	-1.2048E-04	7.9529E-06	2.4097E-04
40	2.49978E+06	1.7551E-06	4.2248E-06	3.5103E-06	8.5	2.6324E+05	-1.2487E-04	7.9529E-06	2.4974E-04
41	2.3759E+06	1.8091E-06	4.3397E-06	3.6182E-06	8.6	2.5046E+05	-1.2854E-04	7.9529E-06	2.5708E-04
42	2.2598E+06	1.8641E-06	4.4568E-06	3.7282E-06	8.7	2.3817E+05	-1.3158E-04	7.9529E-06	2.6316E-04
43	2.1496E+06	1.9189E-06	4.5735E-06	3.8378E-06	8.8	2.2656E+05	-1.3409E-04	7.9529E-06	2.6818E-04
44	2.0452E+06	1.9730E-06	4.6389E-06	3.9460E-06	8.9	2.1553E+05	-1.3616E-04	7.9529E-06	2.7231E-04
45	1.9457E+06	2.0265E-06	4.8031E-06	4.0530E-06	9.0	2.0501E+05	-1.3786E-04	7.9529E-06	2.7571E-04

* ENERGY = LOWER BOUNDARY

Table 6.8 In-system neutron spectrum in the Li₂O assembly (z = 72.0 cm).

(a) scalar spectrum

60 CM Li₂O ASSEMBLY -- 14 PHI NE213 -- E Z=72.0 CM]
** UNFOLDED SPECTRUM ***

J	ENERGY(EV)	PWID	ERR	WIND	J	ENERGY(EV)	PMID	ERR	WIND
1	2.1020E+05	-4.9072E-05	1.0000E+00	8.1680E+01	4.6	1.9950E+06	9.11160E-07	3.1360E-02	3.6000E+01
2	2.2100E+05	-5.9871E-05	1.0000E+00	8.0510E+01	4.7	2.0970E+06	9.11604E-07	3.0907E-02	3.5140E+01
3	2.3230E+05	-7.2747E-05	1.0000E+00	7.9340E+01	4.8	2.2040E+06	9.1944E-07	3.0487E-02	3.4310E+01
4	2.4420E+05	-8.8067E-05	1.0000E+00	7.8150E+01	4.9	2.3170E+06	9.1456E-07	3.0343E-02	3.3550E+01
5	2.5680E+05	-1.0614E-04	1.0000E+00	7.7000E+01	5.0	2.4360E+06	9.9313E-07	3.2800E+01	
6	2.6990E+05	-1.2696E-04	1.0000E+00	7.5820E+01	5.1	2.5610E+06	8.5040E-07	3.1481E-02	3.2040E+01
7	2.8380E+05	-1.5043E-04	1.0000E+00	7.4660E+01	5.2	2.6920E+06	7.8780E-07	3.3487E-02	3.1250E+01
8	2.9830E+05	-1.7631E-04	1.0000E+00	7.3480E+01	5.3	2.8300E+06	7.1429E-07	3.6411E-02	3.0490E+01
9	3.1360E+05	-2.0392E-04	1.0000E+00	7.2320E+01	5.4	2.9750E+06	6.41152E-07	4.0194E-02	2.9740E+01
10	3.2970E+05	-2.3206E-04	1.0000E+00	7.1140E+01	5.5	3.1280E+06	5.8037E-07	4.4601E-02	2.9020E+01
11	3.4660E+05	-2.5966E-04	1.0000E+00	6.9930E+01	5.6	3.2380E+06	5.3689E-07	4.8811E-02	2.8300E+01
12	3.6440E+05	-2.8331E-04	1.0000E+00	6.8800E+01	5.7	3.4570E+06	5.1434E-07	5.1522E-02	2.7580E+01
13	3.8300E+05	-3.0094E-04	1.0000E+00	6.7630E+01	5.8	3.6340E+06	5.1139E-07	5.2925E-02	2.6820E+01
14	4.0270E+05	-3.1062E-04	1.0000E+00	6.6600E+01	5.9	3.8210E+06	5.2323E-07	5.2799E-02	2.6060E+01
15	4.2330E+05	-3.0790E-04	1.0000E+00	6.5630E+01	6.0	4.0160E+06	5.3874E-07	5.2597E-02	2.5227E+01
16	4.4500E+05	-2.9383E-04	1.0000E+00	6.4690E+01	6.1	4.2220E+06	5.4725E-07	5.5071E-02	2.4550E+01
17	4.6780E+05	-2.6711E-04	1.0000E+00	6.3830E+01	6.2	4.4390E+06	5.4618E-07	5.5571E-02	2.3940E+01
18	4.9180E+05	-2.2984E-04	1.0000E+00	6.2960E+01	6.3	4.6660E+06	5.4139E-07	5.7808E-02	2.3330E+01
19	5.1700E+05	-1.8577E-04	1.0000E+00	6.2100E+01	6.4	4.9060E+06	5.3633E-07	6.0558E-02	2.2720E+01
20	5.4360E+05	-1.3969E-04	1.0000E+00	6.1200E+01	6.5	5.1570E+06	5.2401E-07	6.3866E-02	2.2180E+01
21	5.7140E+05	-9.6813E-05	1.0000E+00	6.0300E+01	6.6	5.4220E+06	5.0569E-07	6.8460E-02	2.1670E+01
22	6.0070E+05	-6.0961E-05	1.0000E+00	5.9360E+01	6.7	5.7000E+06	4.9754E-07	7.2801E-02	2.1100E+01
23	6.3150E+05	-3.4243E-05	1.0000E+00	5.8430E+01	6.8	5.9920E+06	5.1227E-07	7.1883E-02	2.0560E+01
24	6.6390E+05	-1.6944E-05	1.0000E+00	5.7490E+01	6.9	6.2990E+06	5.4884E-07	6.8733E-02	2.0020E+01
25	6.9790E+05	-7.1128E-06	1.0000E+00	5.6560E+01	7.0	6.6220E+06	5.9633E-07	6.6938E-02	1.9480E+01
26	7.3370E+05	-2.3456E-06	1.0000E+00	5.5620E+01	7.1	6.9610E+06	6.3598E-07	6.4023E-02	1.8370E+01
27	7.7130E+05	-4.0312E-07	1.0000E+00	5.4720E+01	7.2	7.3130E+06	6.4496E-07	6.6680E-02	1.3490E+01
28	8.1090E+05	-2.5288E-07	9.3212E+00	5.3860E+01	7.3	7.6940E+06	6.3707E-07	7.3063E-02	1.8040E+01
29	8.5250E+05	4.3500E-07	1.0520E+00	5.2990E+01	7.4	8.0880E+06	6.2693E-07	7.5799E-02	1.7620E+01
30	8.9620E+05	4.8316E-07	1.6061E-01	5.2160E+01	7.5	8.5030E+06	6.4744E-07	7.7680E-02	1.7220E+01
31	9.4210E+05	5.0434E-07	5.6057E-02	5.1340E+01	7.6	8.9390E+06	6.7172E-07	8.7115E-02	1.6780E+01
32	9.9040E+05	5.2519E-07	4.2957E-02	5.0470E+01	7.7	9.3970E+06	6.4724E-07	9.4473E-02	1.6360E+01
33	1.0410E+06	5.5075E-07	4.1409E-02	4.9570E+01	7.8	9.8790E+06	6.0944E-07	1.0336E-01	1.5930E+01
34	1.0950E+06	5.8280E-07	4.0426E-02	4.8640E+01	7.9	1.0390E+07	6.5301E-07	1.0520E-01	1.5470E+01
35	1.1510E+06	6.1988E-07	3.9385E-02	4.7590E+01	8.0	1.0920E+07	7.8063E-07	8.0119E-02	1.5070E+01
36	1.2100E+06	6.6113E-07	3.8023E-02	4.6510E+01	8.1	1.1480E+07	9.6047E-07	5.9920E-02	1.4760E+01
37	1.2720E+06	7.0515E-07	3.6455E-02	4.5400E+01	8.2	1.2070E+07	1.2769E-06	4.7345E-02	1.4220E+01
38	1.3370E+06	7.4998E-07	3.4863E-02	4.4210E+01	8.3	1.2680E+07	1.8275E-06	3.4149E-02	1.3690E+01
39	1.4060E+06	7.9358E-07	3.4030E-02	4.2950E+01	8.4	1.3340E+07	2.5106E-06	2.7077E-02	1.3660E+01
40	1.4780E+06	8.3255E-07	3.3635E-02	4.1720E+01	8.5	1.4020E+07	2.7988E-06	2.7275E-02	1.3660E+01
41	1.5530E+06	8.6411E-07	3.3112E-02	4.0570E+01	8.6	1.4740E+07	2.0627E-06	5.0731E-02	1.3660E+01
42	1.6330E+06	8.8712E-07	3.2310E-02	3.9530E+01	8.7	1.5490E+07	6.2804E-07	7.0362E-02	1.3990E+01
43	1.7170E+06	9.0071E-07	3.1551E-02	3.8560E+01	8.8	1.6290E+07	-2.1448E-07	1.0000E+00	1.4400E+01
44	1.8050E+06	9.0663E-07	3.1217E-02	3.7690E+01	8.9	1.7120E+07	-2.5792E-07	1.0000E+00	1.4400E+01
45	1.8970E+06	9.0855E-07	3.14666E-02	3.6860E+01	9.0	1.8000E+07	-1.1256E-07	1.0000E+00	1.4400E+01

* ERR X 100 = %

** WIND = % [FWHM]

*** [N/CM**2/LETHARGY/SOURCE]

Table 6.8

(b) Integrated spectrum

60 CM LI20 ASSEMBLY -- 14 PHI N=213 -- [Z=72.0 CM]
 *** RUNNING INTEGRAL ***

J	ENERGY (EV)	INTEGRAL	MAXIMUM	MINIMUM	J	ENERGY (EV)	INTEGRAL	MAXIMUM	MINIMUM
1	1.7556E+07	-5.6282E-09	0.0000E+00	-1.1256E-08	4.6	1.8502E+06	3.1698E-07	1.8717E-06	1.6340E-06
2	1.6697E+07	-1.8524E-08	0.0000E+00	-3.7042E-08	4.7	1.7604E+06	3.3894E-07	1.9185E-06	1.6779E-06
3	1.5888E+07	-2.9248E-08	0.0000E+00	-5.8496E-08	4.8	1.6746E+06	3.6075E-07	1.9649E-06	1.7215E-06
4	1.5108E+07	-1.4652E-08	3.5612E-08	-2.9304E-08	4.9	1.5927E+06	8.8221E-07	2.0107E-06	1.7644E-06
5	1.4376E+07	3.4500E-08	1.4198E-07	6.8579E-08	5.0	1.5147E+06	9.0310E-07	2.0554E-06	1.8062E-06
6	1.3674E+07	1.0241E-07	2.8573E-07	2.8573E-07	5.1	1.4415E+06	9.2321E-07	2.0984E-06	1.8464E-06
7	1.3011E+07	1.6342E-07	4.1465E-07	3.2684E-07	5.2	1.3713E+06	9.4237E-07	2.1394E-06	1.8847E-06
8	1.2367E+07	2.0755E-07	5.9615E-07	4.1510E-07	5.3	1.3040E+06	9.5047E-07	2.1782E-06	1.9209E-06
9	1.1772E+07	2.3796E-07	5.7602E-07	4.7592E-07	5.4	1.2406E+06	9.7746E-07	2.2148E-06	1.9549E-06
10	1.1197E+07	2.6053E-07	6.2692E-07	5.2102E-07	5.5	1.1801E+06	9.9336E-07	2.2491E-06	1.9867E-06
11	1.0650E+07	2.7849E-07	6.6908E-07	5.5697E-07	5.6	1.1226E+06	1.00832E-06	2.2633E-06	2.0165E-06
12	1.0133E+07	2.9319E-07	7.0516E-07	5.2611E-07	5.7	1.0680E+06	1.0222E-06	2.3116E-06	2.0444E-06
13	9.6531E+06	3.0675E-07	7.3878E-07	6.1351E-07	5.8	1.0153E+06	1.0354E-06	2.35403E-06	2.0708E-06
14	9.1650E+06	3.2141E-07	7.7420E-07	6.4283E-07	5.9	9.6595E+05	1.0480E-06	2.3677E-06	2.0960E-06
15	8.7183E+06	3.3674E-07	8.1072E-07	6.7347E-07	6.0	9.1884E+05	1.0599E-06	2.3943E-06	2.1198E-06
16	8.2931E+06	3.5167E-07	8.4560E-07	7.0333E-07	6.1	8.7407E+05	1.0700E-06	2.4224E-06	2.1401E-06
17	7.8833E+06	3.6615E-07	8.7932E-07	7.3230E-07	6.2	8.3145E+05	1.0695E-06	2.4670E-06	2.1389E-06
18	7.5040E+06	3.8091E-07	9.1351E-07	7.6183E-07	6.3	7.9905E+05	1.0169E-06	2.5975E-06	2.0337E-06
19	7.1373E+06	3.9607E-07	9.4315E-07	7.9214E-07	6.4	7.5226E+05	9.9670E-07	2.5975E-06	1.9934E-06
20	6.7891E+06	4.1095E-07	9.5199E-07	8.2191E-07	6.5	7.1553E+05	8.7942E-07	2.5975E-06	1.7528E-06
21	6.4585E+06	4.2485E-07	1.01338E-06	8.4973E-07	6.6	6.2067E+05	5.23738E-07	2.5975E-06	1.0476E-06
22	6.1435E+06	4.3764E-07	1.04313E-06	8.7523E-07	6.7	6.4751E+05	-3.2342E-07	2.5975E-06	6.4684E-07
23	5.8441E+06	4.4953E-06	1.0706E-06	8.9905E-06	6.8	6.1591E+05	-2.0356E-06	2.5975E-06	4.0711E-06
24	5.5593E+06	4.6106E-07	1.0973E-06	9.2212E-07	6.9	5.8587E+05	-5.0336E-06	2.5975E-06	1.0167E-05
25	5.2821E+06	4.7284E-07	1.1243E-06	9.4572E-07	7.0	5.5729E+05	-9.9243E-06	2.5975E-06	1.9849E-05
26	5.0297E+06	4.8510E-07	1.1522E-06	9.7020E-07	7.1	5.3018E+05	-1.6909E-05	2.5975E-06	3.3818E-05
27	4.7349E+06	4.9770E-07	1.1806E-06	9.9539E-07	7.2	5.0424E+05	-2.5197E-05	2.5975E-06	5.2395E-05
28	4.5508E+06	5.1045E-07	1.2092E-06	1.0467E-06	7.3	4.7962E+05	-3.7639E-05	2.5975E-06	7.5379E-05
29	4.3294E+06	5.2334E-07	1.2381E-06	1.0467E-06	7.4	4.5625E+05	-5.1045E-05	2.5975E-06	1.0209E-04
30	4.1178E+06	5.3630E-07	1.2669E-06	1.0726E-06	7.5	4.3401E+05	-6.5736E-05	2.5975E-06	1.3147E-04
31	3.9168E+06	5.4905E-07	1.2952E-06	1.0981E-06	7.6	4.1285E+05	-8.1131E-05	2.5975E-06	1.6226E-04
32	3.7267E+06	5.6145E-07	1.3228E-06	1.1229E-06	7.7	3.9276E+05	-9.6662E-05	2.5975E-06	1.9332E-04
33	3.5443E+06	5.7356E-07	1.3497E-06	1.1471E-06	7.8	3.7354E+05	-1.1171E-04	2.5975E-06	2.342E-04
34	3.3716E+06	5.8575E-07	1.3767E-06	1.1715E-06	7.9	3.5540E+05	-2.5387E-04	2.5975E-06	2.5175E-04
35	3.2068E+06	5.9852E-07	1.4049E-06	1.1970E-06	8.0	3.3804E+05	-1.3886E-04	2.5975E-06	2.7772E-04
36	3.0508E+06	6.1238E-07	1.4352E-06	1.2243E-06	8.1	3.2156E+05	-1.5046E-04	2.5975E-06	3.0092E-04
37	2.9015E+06	6.2778E-07	1.4686E-06	1.2556E-06	8.2	3.0586E+05	-1.6066E-04	2.5975E-06	3.2131E-04
38	2.7601E+06	6.4498E-07	1.5056E-06	1.2900E-06	8.3	2.9093E+05	-1.6947E-04	2.5975E-06	3.3894E-04
39	2.6255E+06	6.6402E-07	1.5463E-06	1.3230E-06	8.4	2.7679E+05	-1.7699E-04	2.5975E-06	3.5399E-04
40	2.4978E+06	6.8461E-07	1.5902E-06	1.3692E-06	8.5	2.6324E+05	-1.8334E-04	2.5975E-06	3.6668E-04
41	2.3759E+06	7.0626E-07	1.6362E-06	1.4125E-06	8.6	2.5046E+05	-1.8865E-04	2.5975E-06	3.7730E-04
42	2.2598E+06	7.2843E-07	1.6833E-06	1.4569E-06	8.7	2.3817E+05	-1.9305E-04	2.5975E-06	3.8610E-04
43	2.1496E+06	7.5071E-07	1.7307E-06	1.5014E-06	8.8	2.2656E+05	-1.9669E-04	2.5975E-06	3.9338E-04
44	2.0452E+06	7.7291E-07	1.7779E-06	1.5453E-06	8.9	2.1554E+05	-1.9968E-04	2.5975E-06	3.9937E-04
45	1.9457E+06	7.9493E-07	1.8249E-06	1.5900E-06	9.0	2.0501E+05	-2.0214E-04	2.5975E-06	4.0427E-04

* ENERGY = LOWER BOUNDARY

Table 6.9 In-system neutron spectrum in the Li₂O assembly ($z = 82.1$ cm).

(a) scalar spectrum

60 CM Li₂O ASSEMBLY -- 14 PHI NE213 -- [Z=82.1 CM]

** UNFOLDED SPECTRUM ***

J	ENERGY (EV)	PMID	ERR	WIND	J	ENERGY (EV)	PMID	ERR	WIND	J	ENERGY (EV)	PMID	ERR	WIND
1	2.1020E+05	-3.8325E-07	1.0000E+00	8.1680E+01	4.6	1.9950E+06	3.0509E-07	3.1873E-02	3.6000E+01	3.1873E-02	3.0509E-07	3.6000E+01	3.1873E-02	3.6000E+01
2	2.2100E+05	-4.5666E-07	1.0000E+00	8.0510E+01	4.7	2.0970E+06	3.0845E-07	3.1320E-02	3.5140E+01	3.1320E-02	3.0845E-07	3.5140E+01	3.1320E-02	3.5140E+01
3	2.3230E+05	-5.3650E-07	1.0000E+00	7.9340E+01	4.8	2.2040E+06	3.1093E-07	3.0846E-02	3.4310E+01	3.0846E-02	3.1093E-07	3.4310E+01	3.0846E-02	3.4310E+01
4	2.4420E+05	-6.5302E-07	1.0000E+00	7.8160E+01	4.9	2.3170E+06	3.0990E-07	3.0534E-02	3.3550E+01	3.0534E-02	3.0990E-07	3.3550E+01	3.0534E-02	3.3550E+01
5	2.5630E+05	-7.8035E-07	1.0000E+00	7.7000E+01	5.0	2.4360E+06	3.0251E-07	3.0831E-02	3.2800E+01	3.0831E-02	3.0251E-07	3.2800E+01	3.0831E-02	3.2800E+01
6	2.6990E+05	-9.1858E-07	1.0000E+00	7.5820E+01	5.1	2.5610E+06	2.8739E-07	3.1846E-02	3.2040E+01	3.1846E-02	2.8739E-07	3.2040E+01	3.1846E-02	3.2040E+01
7	2.8380E+05	-1.1039E-06	1.0000E+00	7.4660E+01	5.2	2.6920E+06	2.6564E-07	3.3999E-02	3.1250E+01	3.3999E-02	2.6564E-07	3.1250E+01	3.3999E-02	3.1250E+01
8	2.9830E+05	-1.3053E-06	1.0000E+00	7.3480E+01	5.3	2.8300E+06	2.4065E-07	3.7164E-02	3.0490E+01	3.7164E-02	2.4065E-07	3.0490E+01	3.7164E-02	3.0490E+01
9	3.1360E+05	-1.4866E-06	1.0000E+00	7.2320E+01	5.4	2.9750E+06	2.1621E-07	4.0977E-02	2.9740E+01	4.0977E-02	2.1621E-07	2.9740E+01	4.0977E-02	2.9740E+01
10	3.2970E+05	-1.7232E-06	1.0000E+00	7.1140E+01	5.5	3.1280E+06	1.9512E-07	4.5596E-02	2.9020E+01	4.5596E-02	1.9512E-07	2.9020E+01	4.5596E-02	2.9020E+01
11	3.4660E+05	-1.6852E-06	1.0000E+00	6.9980E+01	5.6	3.2380E+06	1.7869E-07	5.0324E-02	2.8300E+01	5.0324E-02	1.7869E-07	2.8300E+01	5.0324E-02	2.8300E+01
12	3.6440E+05	-2.1446E-06	1.0000E+00	6.8800E+01	5.7	3.4570E+06	1.6821E-07	5.4209E-02	2.7580E+01	5.4209E-02	1.6821E-07	2.7580E+01	5.4209E-02	2.7580E+01
13	3.8300E+05	-2.3277E-06	1.0000E+00	6.7680E+01	5.8	3.6340E+06	1.6441E-07	5.6959E-02	2.6820E+01	5.6959E-02	1.6441E-07	2.6820E+01	5.6959E-02	2.6820E+01
14	4.0270E+05	-1.9579E-06	1.0000E+00	6.6600E+01	5.9	3.8210E+06	1.6646E-07	5.7478E-02	2.6060E+01	5.7478E-02	1.6646E-07	2.6060E+01	5.7478E-02	2.6060E+01
15	4.2330E+05	-2.1610E-06	1.0000E+00	6.5630E+01	6.0	4.0160E+06	1.7144E-07	5.7517E-02	2.5270E+01	5.7517E-02	1.7144E-07	2.5270E+01	5.7517E-02	2.5270E+01
16	4.4500E+05	-2.0013E-06	1.0000E+00	6.4690E+01	6.1	4.2220E+06	1.7597E-07	5.8034E-02	2.4550E+01	5.8034E-02	1.7597E-07	2.4550E+01	5.8034E-02	2.4550E+01
17	4.6780E+05	-1.8196E-06	1.0000E+00	6.3830E+01	6.2	4.4390E+06	1.7930E-07	5.9675E-02	2.3940E+01	5.9675E-02	1.7930E-07	2.3940E+01	5.9675E-02	2.3940E+01
18	4.9180E+05	-1.4945E-06	1.0000E+00	6.2960E+01	6.3	4.6660E+06	1.8194E-07	6.1097E-02	2.3330E+01	6.1097E-02	1.8194E-07	2.3330E+01	6.1097E-02	2.3330E+01
19	5.1700E+05	-1.1311E-06	1.0000E+00	6.2100E+01	6.4	4.9060E+06	1.8641E-07	6.2060E-02	2.2720E+01	6.2060E-02	1.8641E-07	2.2720E+01	6.2060E-02	2.2720E+01
20	5.4360E+05	-8.5897E-07	1.0000E+00	6.1200E+01	6.5	5.1570E+06	1.9075E-07	6.2767E-02	2.2180E+01	6.2767E-02	1.9075E-07	2.2180E+01	6.2767E-02	2.2180E+01
21	5.7140E+05	-4.8618E-07	1.0000E+00	6.0300E+01	6.6	5.4220E+06	1.9159E-07	6.5015E-02	2.1670E+01	6.5015E-02	1.9159E-07	2.1670E+01	6.5015E-02	2.1670E+01
22	6.0070E+05	-2.1905E-07	1.0000E+00	5.9360E+01	6.7	5.7000E+06	1.8748E-07	6.9475E-02	2.1100E+01	6.9475E-02	1.8748E-07	2.1100E+01	6.9475E-02	2.1100E+01
23	6.3150E+05	-9.2111E-07	1.0000E+00	5.8430E+01	6.8	5.9920E+06	1.8150E-07	7.2231E-02	2.0560E+01	7.2231E-02	1.8150E-07	2.0560E+01	7.2231E-02	2.0560E+01
24	6.6390E+05	-1.6139E-08	3.6110E+03	5.7490E+01	6.9	6.2990E+06	1.7947E-07	7.5085E-02	2.0020E+01	7.5085E-02	1.7947E-07	2.0020E+01	7.5085E-02	2.0020E+01
25	7.6346E+05	-3.3367E-02	5.6560E+01	7.0	6.6220E+06	1.8642E-07	7.6857E-02	1.9480E+01	7.6857E-02	1.8642E-07	7.6857E-02	1.9480E+01	7.6857E-02	1.9480E+01
26	7.3370E+05	8.6317E+01	5.5620E+01	7.1	6.9610E+06	2.0205E-07	7.2027E-02	1.8970E+01	7.2027E-02	1.8970E+01	7.2027E-02	1.8970E+01	7.2027E-02	1.8970E+01
27	7.7130E+05	2.3702E+01	5.4720E+01	7.2	7.3176E-07	2.1766E-07	7.3176E-02	1.8490E+01	7.3176E-02	1.8490E+01	7.3176E-02	1.8490E+01	7.3176E-02	1.8490E+01
28	8.1090E+05	1.2991E-07	5.3860E+01	7.3	7.6940E+06	2.2464E-07	7.5570E-02	1.8040E+01	7.5570E-02	1.8040E+01	7.5570E-02	1.8040E+01	7.5570E-02	1.8040E+01
29	8.5250E+05	1.3467E-07	1.03360E+00	5.2990E+01	7.4	8.0880E+06	2.2346E-07	7.8751E-02	1.7620E+01	7.8751E-02	1.7620E+01	7.8751E-02	1.7620E+01	7.8751E-02
30	8.9620E+05	1.3916E-07	1.7072E-01	5.2160E+01	7.5	8.5030E+06	2.2170E-07	8.4382E-02	1.7220E+01	8.4382E-02	2.2170E-07	1.7220E+01	8.4382E-02	1.7220E+01
31	9.4210E+05	1.4446E-07	6.1435E-02	5.1340E+01	7.6	8.9390E+06	2.2425E-07	9.5983E-02	1.6780E+01	9.5983E-02	2.2425E-07	1.6780E+01	9.5983E-02	1.6780E+01
32	9.9040E+05	1.5148E-07	4.72836E-02	5.0470E+01	7.7	9.3970E+06	2.2536E-07	1.086E-01	1.6360E+01	1.086E-01	2.2536E-07	1.086E-01	1.086E-01	1.6360E+01
33	1.0410E+06	1.6075E-07	4.5340E-02	4.9570E+01	7.8	9.8790E+06	2.2389E-07	1.0593E-01	1.5930E+01	1.0593E-01	2.2389E-07	1.0593E-01	1.0593E-01	1.5930E+01
34	1.0950E+06	1.7235E-07	4.3942E-02	4.8640E+01	7.9	1.0390E+07	2.4850E-07	1.0287E-01	1.5470E+01	1.0287E-01	2.4850E-07	1.0287E-01	1.0287E-01	1.5470E+01
35	1.1510E+06	1.8561E-07	4.2738E-02	4.7590E+01	8.0	1.0920E+07	3.1550E-07	1.0570E-01	1.5070E+01	1.0570E-01	3.1550E-07	1.0570E-01	1.0570E-01	1.5070E+01
36	1.2100E+06	2.0005E-07	4.1170E-02	4.6510E+01	8.1	1.1480E+07	3.9377E-07	5.3862E-02	1.4760E+01	5.3862E-02	3.9377E-07	5.3862E-02	1.4760E+01	5.3862E-02
37	1.2720E+06	2.1511E-07	3.9316E-02	4.5400E+01	8.2	1.2070E+07	4.82338E-07	4.82338E-02	1.4300E+01	4.82338E-02	4.82338E-07	4.82338E-02	4.82338E-07	1.4300E+01
38	1.3370E+06	2.3043E-07	3.7450E-02	4.4210E+01	8.3	1.2680E+07	6.5703E-07	5.5421E-02	1.3560E+01	5.5421E-02	6.5703E-07	5.5421E-02	6.5703E-07	1.3560E+01
39	1.4060E+06	2.4585E-07	3.6424E-02	4.2950E+01	8.4	1.3340E+07	9.2391E-07	7.6678E-02	1.3540E+01	7.6678E-02	9.2391E-07	7.6678E-02	9.2391E-07	1.3540E+01
40	1.4780E+06	2.6073E-07	3.5761E-02	4.1720E+01	8.5	1.4020E+07	1.0569E-06	8.7088E-02	1.3540E+01	8.7088E-02	1.0569E-06	8.7088E-02	1.0569E-06	1.3540E+01
41	1.5530E+06	2.7414E-07	3.4910E-02	4.0570E+01	8.6	1.4740E+07	7.9530E-07	5.6544E-02	1.3540E+01	5.6544E-02	7.9530E-07	5.6544E-02	7.9530E-07	1.3540E+01
42	1.6330E+06	2.8540E-07	3.3802E-02	3.9530E+01	8.7	1.5490E+07	2.3754E-07	7.4984E-02	1.3960E+01	7.4984E-02	2.3754E-07	7.4984E-02	2.3754E-07	1.3960E+01
43	1.7170E+06	2.9362E-07	3.2639E-02	3.8560E+01	8.8	1.6290E+07	-1.0536E-07	1.4400E+01	1.4400E+01	1.4400E+01	-1.0536E-07	1.4400E+01	1.4400E+01	1.4400E+01
44	1.8050E+06	2.9862E-07	3.2106E-02	3.7690E+01	8.9	1.7120E+07	-1.1938E-07	1.4400E+01	1.4400E+01	1.4400E+01	-1.1938E-07	1.4400E+01	1.4400E+01	1.4400E+01
45	1.8970E+06	3.0191E-07	3.2002E-02	3.6860E+01	9.0	1.8000E+07	-6.0014E-08	1.4400E+01	1.4400E+01	1.4400E+01	-6.0014E-08	1.4400E+01	1.4400E+01	1.4400E+01

* ERR × 100 ≈ %

** WIND = % [FWHM]

*** [N/CM*2/LET/HARGY/SOURCE]

Table 6.9

(b) Integrated spectrum

60 CM LI20 ASSEMBLY -- 14 PHI NE213 -- [Z=82.1 CM]
*** RUNNING INTEGRAL ***

J	ENERGY(EV)	INTEGRAL	MAXIMUM	MINIMUM	J	ENERGY(EV)	INTEGRAL	MAXIMUM	MINIMUM
1	1.7556E+07	-3.0037E-09	0.0000E+00	-6.0014E-09	4.6	1.8502E+06	2.8474E-07	5.6338E-07	5.6943E-07
2	1.6697E+07	-8.9697E-09	0.0030E+00	-1.7939E-08	4.7	1.7604E+06	2.9197E-07	5.6393E-07	5.7879E-07
3	1.5888E+07	-1.4238E-03	0.0000E+00	-2.8475E-08	4.8	1.6746E+06	2.9907E-07	5.9813E-07	5.9813E-07
4	1.5108E+07	-8.7445E-09	1.2768E-08	-1.7439E-08	4.9	1.5927E+06	3.0596E-07	7.0870E-07	6.1192E-07
5	1.4376E+07	1.0014E-08	5.4781E-08	2.028E-08	5.0	1.5147E+06	3.1257E-07	7.2289E-07	6.2515E-07
6	1.3674E+07	3.5721E-08	1.0906E-07	7.1441E-08	5.1	1.4415E+06	3.1886E-07	7.3639E-07	6.3772E-07
7	1.3011E+07	5.8348E-08	1.6679E-07	1.670E-07	5.2	1.4478E+06	7.4913E-07	6.4956E-07	6.4956E-07
8	1.2367E+07	7.4192E-02	1.9081E-02	1.4838E-07	5.3	1.3040E+06	3.2033E-07	7.6108E-07	6.6065E-07
9	1.1772E+07	8.5701E-03	2.1003E-07	1.7140E-07	5.4	1.2406E+06	3.3549E-07	7.7226E-07	6.7098E-07
10	1.1197E+07	9.5015E-08	2.3673E-07	1.9003E-07	5.5	1.1801E+06	3.4029E-07	7.8267E-07	6.8057E-07
11	1.0650E+07	1.0232E-07	2.5371E-07	2.0464E-07	5.6	1.1226E+06	3.4447E-07	7.9235E-07	6.8946E-07
12	1.0133E+07	1.6742E-07	2.6742E-07	2.1579E-07	5.7	1.0680E+06	3.4885E-07	8.0135E-07	6.9770E-07
13	9.6351E+06	1.1260E-05	1.2798E-07	2.2530E-07	5.8	1.0150E+06	3.5269E-07	7.0537E-07	6.9537E-07
14	9.1650E+06	1.1797E-07	2.9220E-07	2.3593E-07	5.9	9.6595E+05	3.5629E-07	8.1768E-07	7.1259E-07
15	8.7123E+06	1.2503E-07	3.0449E-07	2.4607E-07	6.0	9.1884E+05	3.5968E-07	8.2535E-07	7.1937E-07
16	8.2931E+06	1.2811E-07	3.1651E-07	2.5622E-07	6.1	8.7407E+05	3.6257E-07	8.3349E-07	7.2514E-07
17	7.8333E+06	1.3326E-07	2.8356E-07	2.6551E-07	6.2	8.3145E+05	3.6244E-07	8.4720E-07	7.2439E-07
18	7.5040E+06	1.3845E-07	3.4095E-07	2.7680E-07	6.3	7.9056E+05	3.6472E-07	8.8956E-07	6.9544E-07
19	7.1373E+06	1.4349E-07	3.5232E-07	2.8699E-07	6.4	7.5226E+05	2.7802E-07	8.1041E-06	5.5604E-07
20	6.7891E+06	1.4813E-07	3.6315E-07	2.9536E-07	6.5	7.1553E+05	4.4050E-08	1.5202E-06	8.8119E-08
21	6.4535E+06	1.5243E-07	3.7332E-07	3.0497E-07	6.6	6.8067E+05	5.3089E-07	2.7978E-06	-1.1818E-06
22	6.1435E+06	1.5663E-07	3.8233E-07	3.1327E-07	6.7	6.4751E+05	5.7125E-06	5.7125E-06	-4.0949E-06
23	5.8441E+06	1.6069E-07	3.4052E-07	3.2169E-07	6.8	6.1591E+05	6.0474E-06	5.7125E-06	-4.1041E-06
24	5.5593E+06	1.6520E-07	4.0259E-07	3.3041E-07	6.9	5.8587E+05	6.0520E-06	5.7125E-06	-4.1260E-06
25	5.2831E+06	1.6963E-07	4.1279E-07	3.3937E-07	7.0	5.5729E+05	6.0873E-06	5.7125E-06	-4.1746E-06
26	5.0297E+06	1.7415E-07	4.2293E-07	3.4830E-07	7.1	5.3018E+05	6.1303E-06	5.7125E-06	-4.2605E-06
27	4.7849E+06	4.7852E-07	4.3262E-07	3.5795E-07	7.2	5.0624E+05	6.1868E-06	5.7125E-06	-4.3736E-06
28	4.5508E+06	1.8279E-07	4.4248E-07	3.6559E-07	7.3	4.7966E+05	6.2615E-06	5.7125E-06	-4.5231E-06
29	4.3294E+06	1.8700E-07	4.5196E-07	3.7400E-07	7.4	4.5625E+05	6.3525E-06	5.7125E-06	-4.7050E-06
30	4.1178E+06	1.9115E-07	4.6127E-07	3.8229E-07	7.5	4.3401E+05	6.4524E-06	5.7125E-06	-4.9052E-06
31	3.9168E+06	1.9519E-07	4.7034E-07	3.9037E-07	7.6	4.1285E+05	6.5606E-06	5.7125E-06	-5.1213E-06
32	3.7267E+06	1.9911E-07	4.7914E-07	3.9822E-07	7.7	3.9276E+05	6.6585E-06	5.7125E-06	-5.3170E-06
33	3.5443E+06	2.0293E-07	4.8783E-07	4.0597E-07	7.8	3.7354E+05	6.7744E-06	5.7125E-06	-5.5498E-06
34	3.3716E+06	2.0696E-07	4.9669E-07	4.1592E-07	7.9	3.5540E+05	6.8856E-06	5.7125E-06	-5.7713E-06
35	3.2068E+06	2.1120E-07	5.0608E-07	4.2241E-07	8.0	3.3804E+05	6.9699E-06	5.7125E-06	-5.9398E-06
36	3.0508E+06	2.1536E-07	5.1628E-07	4.3172E-07	8.1	3.2156E+05	7.0561E-06	5.7125E-06	-6.1121E-06
37	2.9015E+06	2.2104E-07	5.2753E-07	4.4209E-07	8.2	3.0586E+05	7.1304E-06	5.7125E-06	-6.2608E-06
38	2.7601E+06	2.2684E-07	5.4001E-07	4.5367E-07	8.3	2.9093E+05	7.1957E-06	5.7125E-06	-6.3913E-06
39	2.6255E+06	2.3325E-07	5.5375E-07	4.6650E-07	8.4	2.7679E+05	7.2508E-06	5.7125E-06	-6.5017E-06
40	2.4978E+06	2.4021E-07	5.6857E-07	4.8041E-07	8.5	2.6324E+05	7.2968E-06	5.7125E-06	-6.5936E-06
41	2.3759E+06	2.4754E-07	5.8416E-07	4.9507E-07	8.6	2.5046E+05	7.3358E-06	5.7125E-06	-6.6716E-06
42	2.2598E+06	2.2104E-07	5.0013E-07	5.1010E-07	8.7	2.3817E+05	7.3684E-06	5.7125E-06	-6.7369E-06
43	2.1496E+06	2.6258E-07	6.1616E-07	5.2516E-07	8.8	2.2656E+05	7.3953E-06	5.7125E-06	-6.7905E-06
44	2.0452E+06	2.7005E-07	6.3206E-07	5.4010E-07	8.9	2.1554E+05	7.4181E-06	5.7125E-06	-6.8362E-06
45	1.9457E+06	2.7744E-07	6.4780E-07	5.5487E-07	9.0	2.0501E+05	7.4373E-06	5.7125E-06	-6.8745E-06

* ENERGY = LOWER BOUNDARY

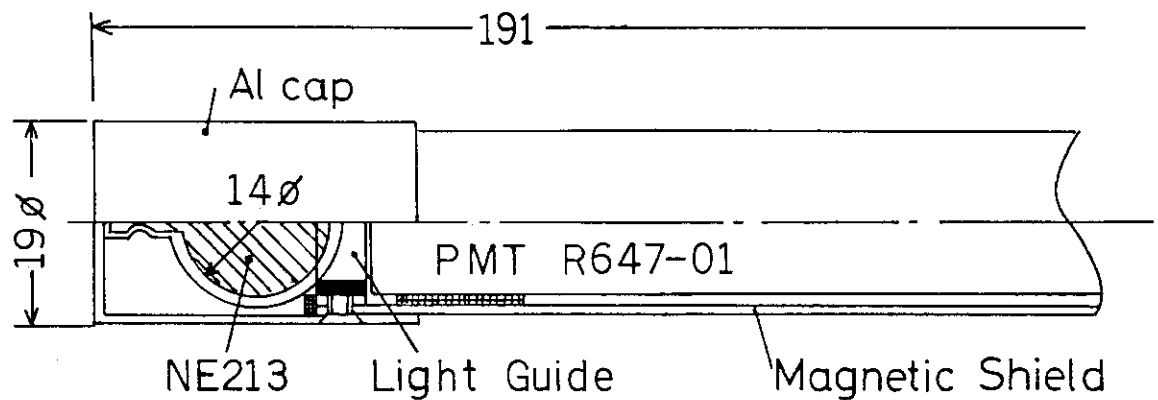


Fig. 6.1 Sectional view of the small spherical NE213 spectrometer.

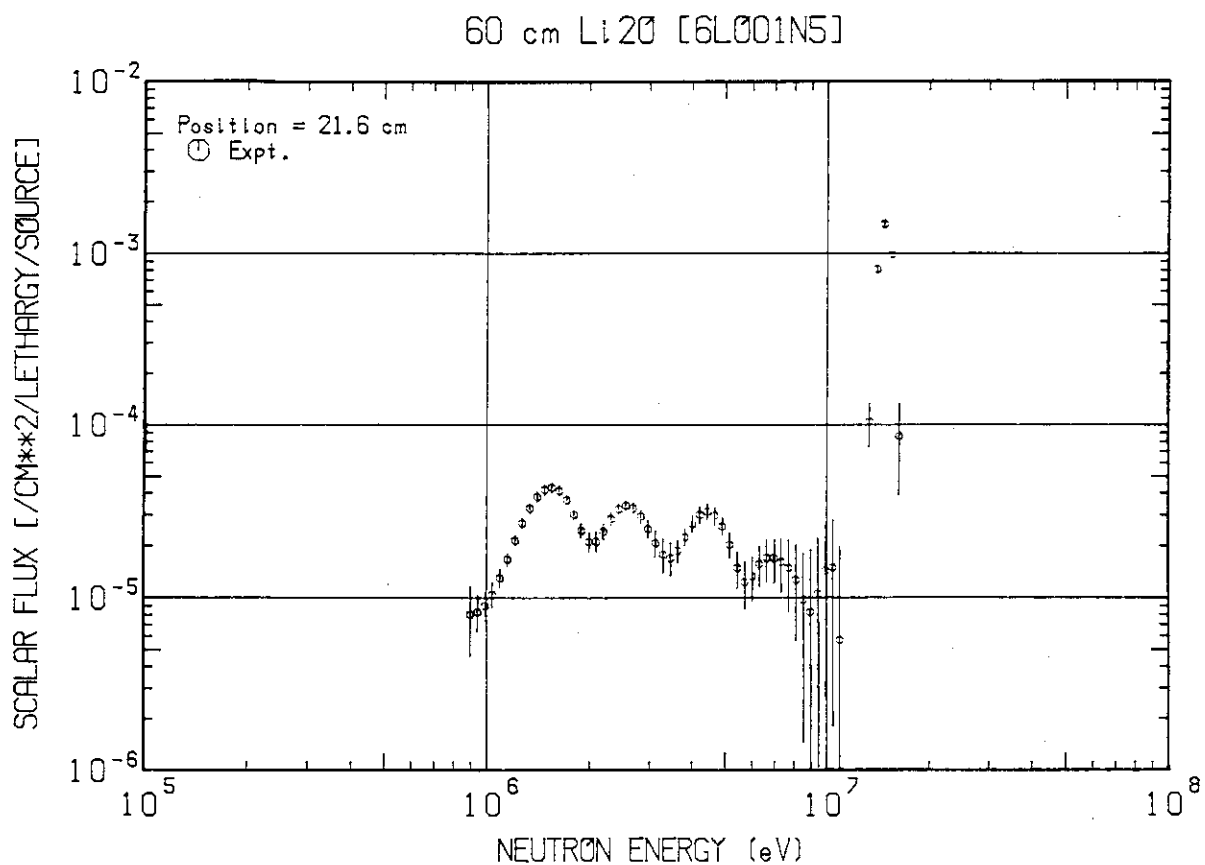


Fig. 6.2 Measured neutron scalar spectrum in the Li_2O assembly
($z = 21.6$ cm).

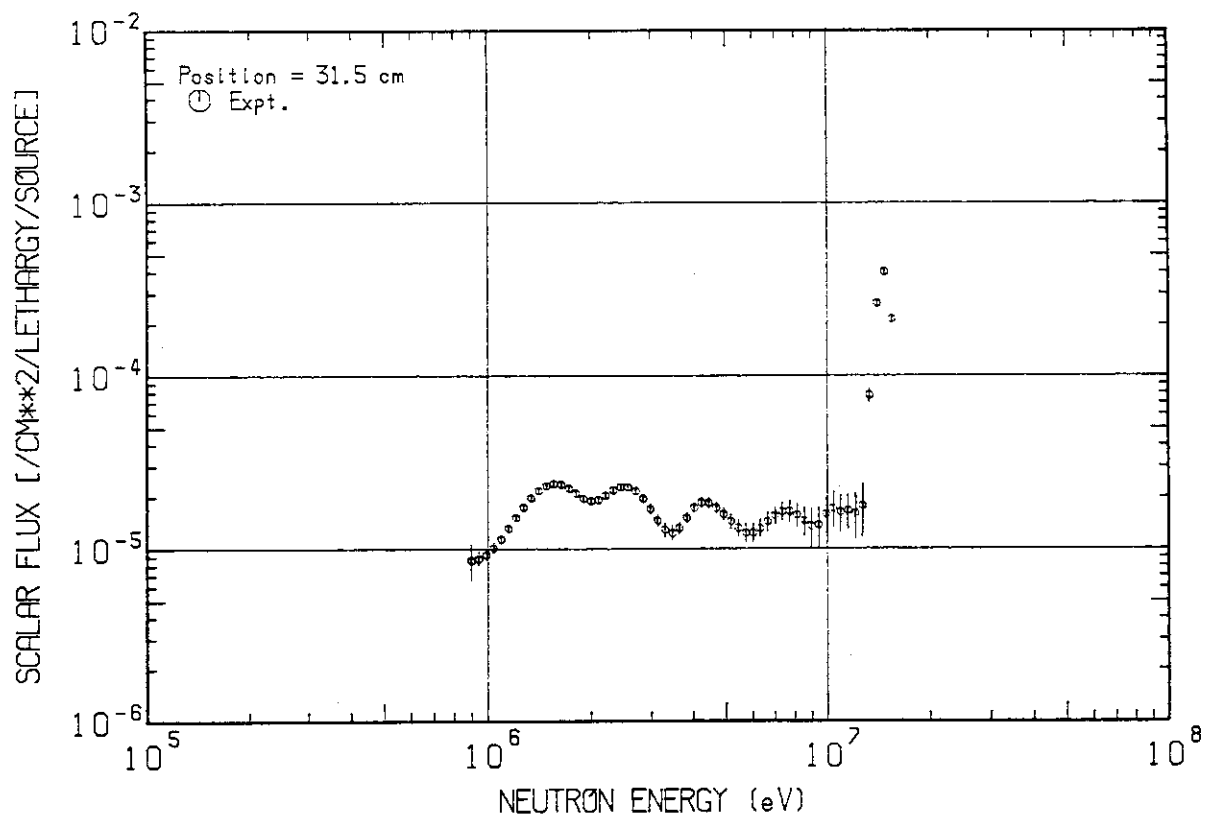
60 cm Li₂O [6L002N5]

Fig. 6.3 Measured neutron scalar spectrum in the Li₂O assembly
(z = 31.5 cm).

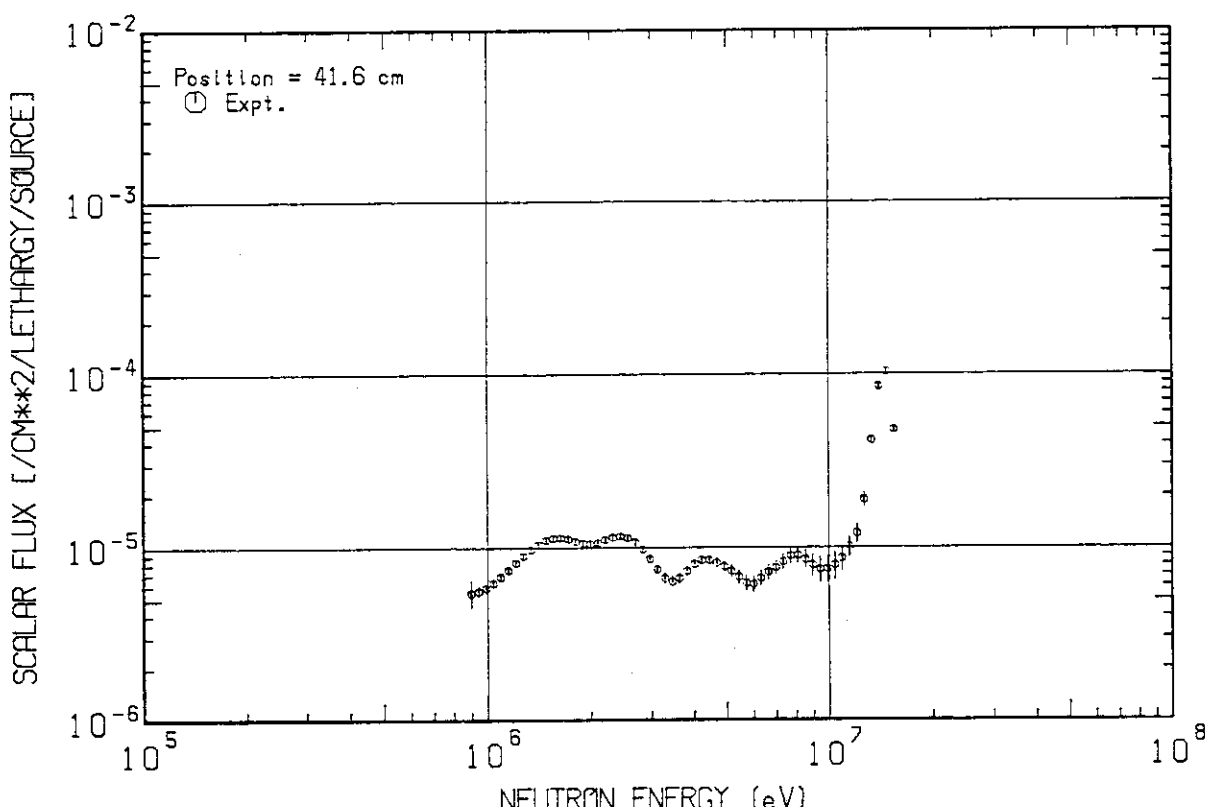
60 cm Li₂O [6L003N5]

Fig. 6.4 Measured neutron scalar spectrum in the Li₂O assembly
(z = 41.6 cm).

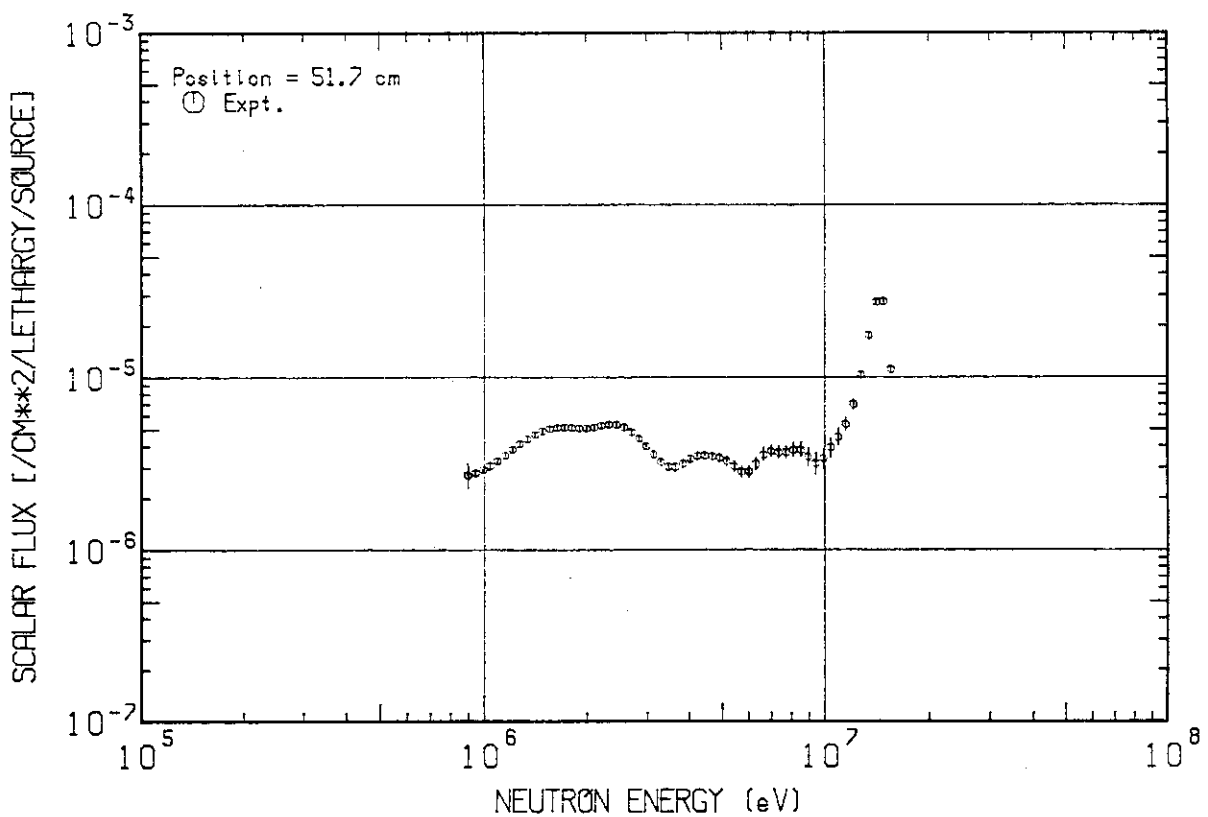
60 cm Li₂O [6L004N5]

Fig. 6.5 Measured neutron scalar spectrum in the Li₂O assembly
(z = 51.7 cm).

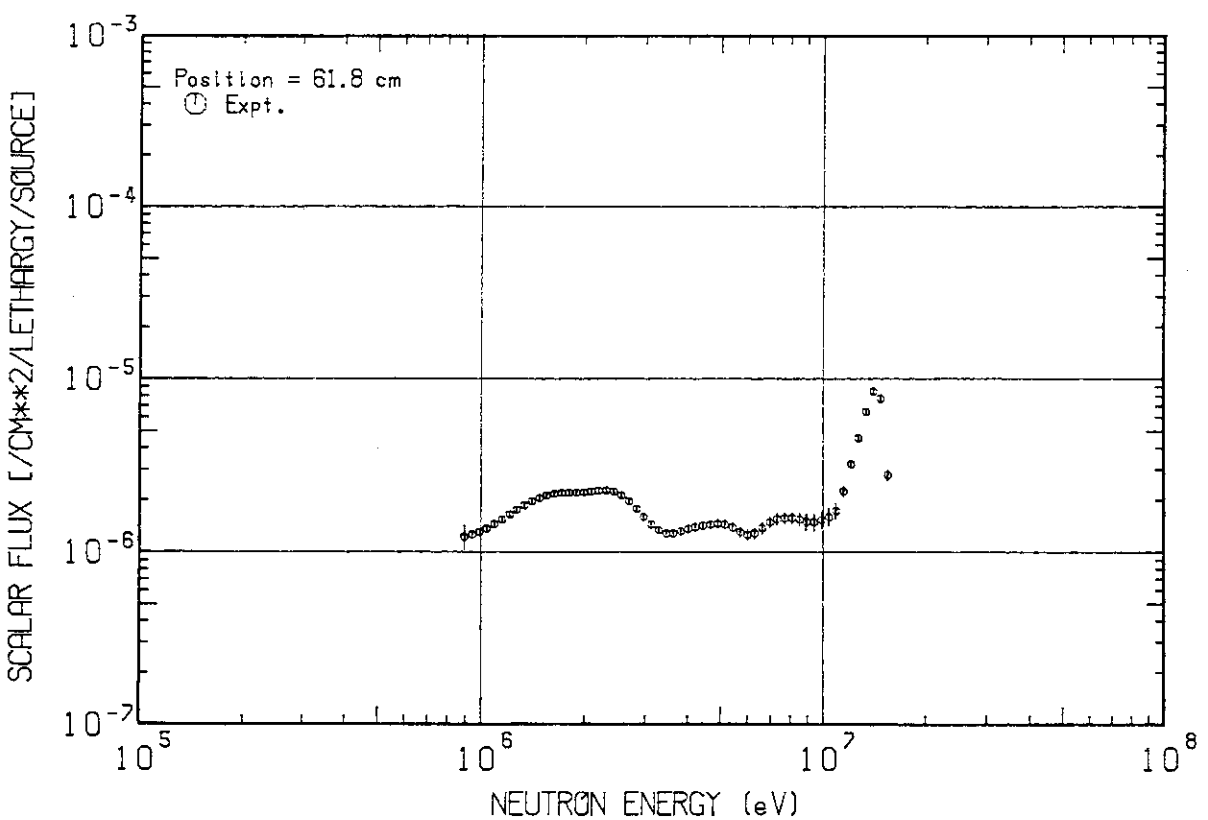
60 cm Li₂O [6L005N5]

Fig. 6.6 Measured neutron scalar spectrum in the Li₂O assembly
(z = 61.8 cm).

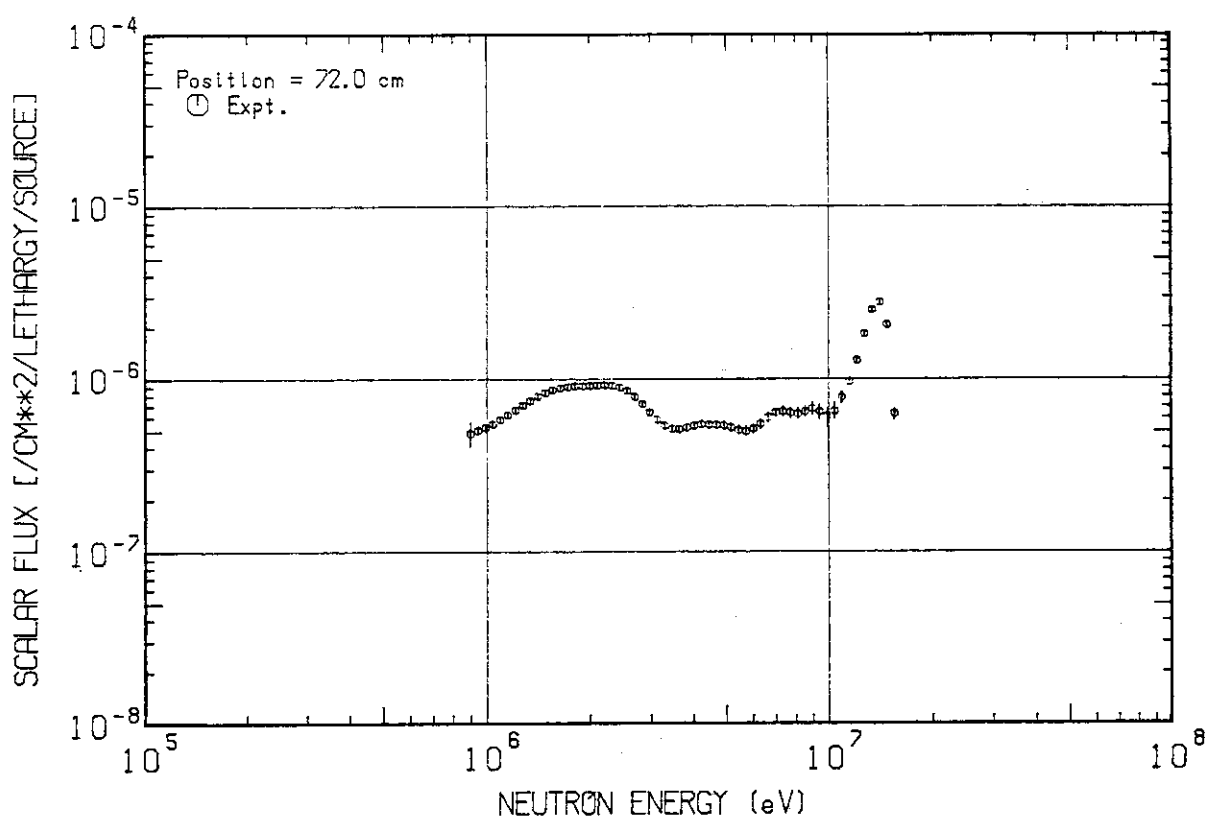
60 cm Li₂O [6L006N5]

Fig. 6.7 Measured neutron scalar spectrum in the Li₂O assembly
(z = 72.0 cm).

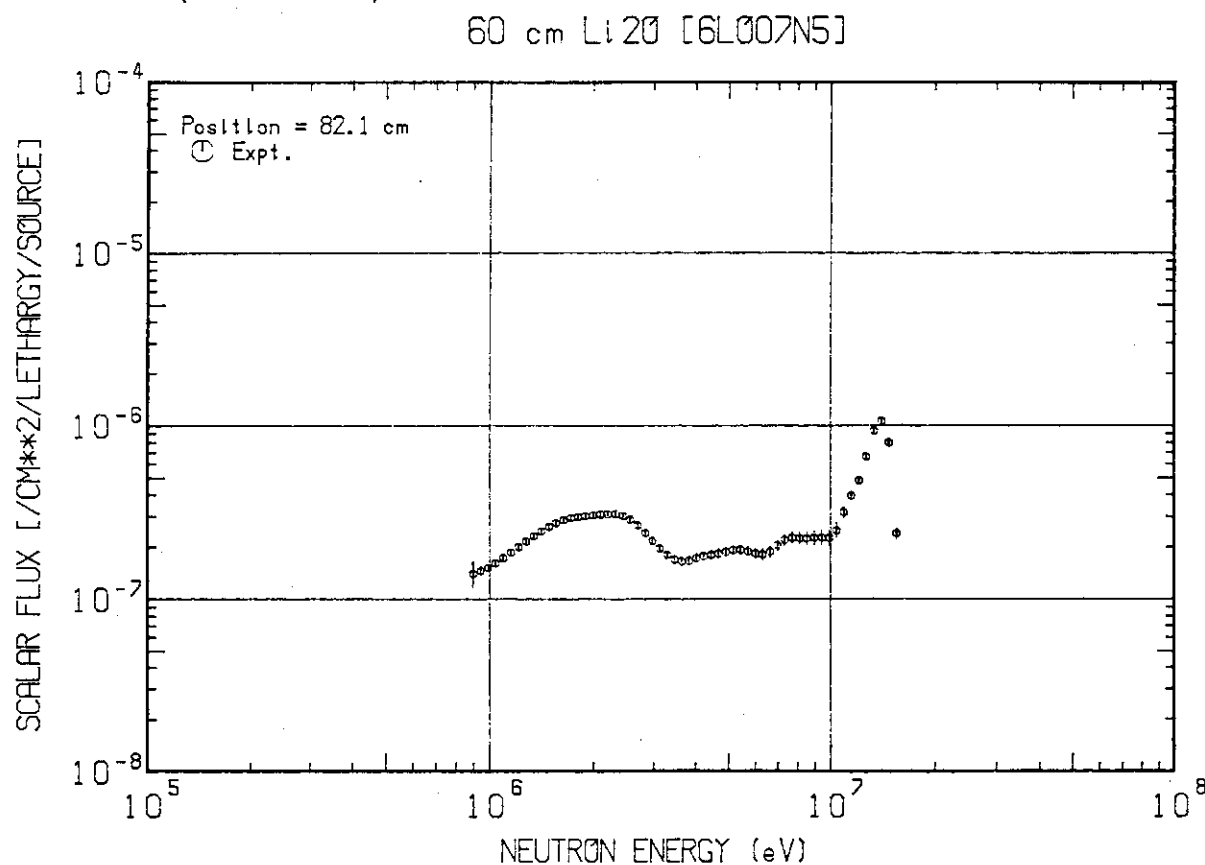


Fig. 6.8 Measured neutron scalar spectrum in the Li₂O assembly
(z = 82.1 cm).

7. Discussions and Concluding Remarks

To confirm the reliability of measured data, they were intercompared. First, the ${}^6\text{Li}$ TPR's (T_6) measured by the ${}^6\text{Li}_2\text{O}$ pellet were compared with those determined by the Li-glass scintillation method. This comparison is shown in Fig. 7.1. The Li_2O pellet data plotted in the figure are corrected for the self-shielding and room-return effects, while the Li-glass data are uncorrected for them. Since the ${}^6\text{Li}$ atom density in ${}^6\text{Li}$ -glass scintillator is about one order smaller than that in the ${}^6\text{Li}_2\text{O}$ pellet and since the self-shielding for the ${}^6\text{Li}_2\text{O}$ pellet in the Li_2O assembly was estimated to be $2 \sim 3\%$ except near the surfaces, the correction for the Li-glass data might be small. Figure 7.1 indicates that, though data were measured independently by quite different methods, they agree well within experimental errors except in the vicinity of surfaces, where both the room-returned soft-neutron effect and the self-shielding effect would be expected to be large. For the glass scintillator, there are large experimental error in the measured data due to a relatively large background to signal ratio. High-energy D-T neutrons are dominant in the region near the front surface and the contribution of ${}^7\text{Li}(n,n't){}^4\text{He}$ reaction is the almost same order as that of ${}^6\text{Li}(n,t){}^4\text{He}$ reaction. Therefore, the measured data might be oversubtracted by the contribution of ${}^7\text{Li}(n,n't){}^4\text{He}$ reaction.

The ${}^7\text{Li}$ TPRs (T_7) measured by the ${}^7\text{Li}_2\text{O}$ pellet and the NE213 spectrometer are shown in Fig. 7.2. The agreement between two method is very well within the experimental errors. The data obtained by the NE213 spectrometer, however, is a little lower than that by the ${}^7\text{Li}_2\text{O}$ pellet. The data of JENDL-3PR1 were used for calculation of T_7 , as the ${}^7\text{Li}(n,n't){}^4\text{He}$ cross section. Recent cross section measurement⁽²⁷⁾ recommends that the value of JENDL-3PR1 for ${}^7\text{Li}(n,n't){}^4\text{He}$ cross section around 14 MeV had better increase by about 7 %. If this revised data are used, the agreement between two methods is expected to improve almost perfectly.

Another set of comparisons was provided for the measured fission rates and reaction rates, and calculated predictions. As, here, measurements of different type are to be compared, it was expedient to express results in terms of a suitable indexing scheme such as the Calculated to Experimental ratio (C/E). The C/E plots of reaction rates for ${}^{238}\text{U}(n,f)$ and ${}^{27}\text{Al}(n,\alpha){}^{24}\text{Na}$ are presented in Fig 7.3. The

calculation used in C/E is described in Appendix A.4. The plots indicate agreement of either measurement with its predicted values, within the experimental error.

Both the TPR and the C/E comparisons support the view that the reliability of the measured data is adequate for use in benchmark verification of calculational methods and nuclear data.

Since April 1982, JENDL-2 has been distributed and widely used as a Japanese standard nuclear data library. As JENDL-2 was evaluated for applying mainly to fission reactors, the accuracy of evaluated data above 5 MeV was pointed out to be insufficient for fusion neutronics studies.

Therefore, a strong request for a newly evaluated nuclear data file was submitted to the Japanese Nuclear Data Committee. In Dec. 1983, eight selected nuclei have been evaluated and released as JENDL-3PR1.

As a useful exercise, we examined JENDL-3PR1 by providing this database, as well as ENDF/B-IV, in the analysis of the present benchmark experiments.(28)

A sample of calculational procedure is provided in Appendix A. 4. The T_6 predictions based on JENDL-3PR1 clearly are in good agreement with measured values. Recently, an updated data file JENDL-3PR2, has been released. In that set, ^6Li ^7Li and C data have been modified from those in JENDL-3PR1 ; in this new evaluation, the present benchmark results were duly considered.

The next experiments in this series of benchmark measurements, using a 60 cm cylindrical graphite assembly, as well as a set of measurements with a 40-cm long Li_2O cylinder with 20-cm long graphite reflector, have been completed ; results will be reported in the near future.

Concluding Remarks

- (1) Fusion blanket benchmark experiments on a 60 cm-thick lithium-oxide cylindrical assembly have been carried out using the FNS. Measured data are very reliable and can be used for testing methods and data as the benchmark data.
- (2) Preliminary versions of the JENDL-3 nuclear data file and the newly developed transport codes BERMUDA and MORSE-DD, are being evaluated using present benchmark data. They are also useful for evaluations of not only the JENDL-3 file but the other files such as the ENDF/B-VI, JEF (Joint European File) and EFF (European Fusion File).

Acknowledgement

The authors are deeply indebted to Messrs. J. Kusano, C. Kutsukake and S. Tanaka for their operation of the FNS accelerator. They are also grateful to Mr. T. Takahashi for his preparation of Li₂O pellets and Drs. H. Kudo, K. Okuno and Y. Nagame for their evaluation of escaped tritium from Li₂O pellets.

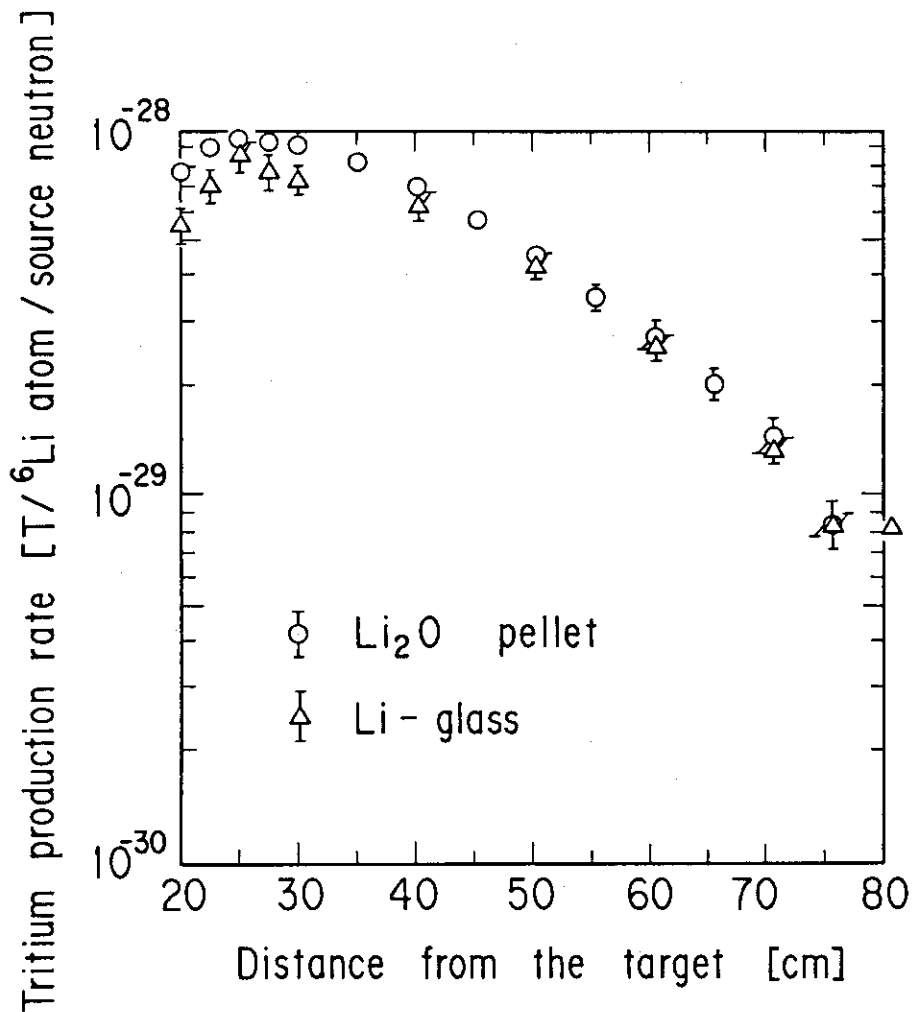


Fig. 7.1 Comparison ${}^6\text{Li}$ of TPRs (T_6) measured by ${}^6\text{Li}_2\text{O}$ pellets and Li-glass scintillators.

The ${}^6\text{Li}_2\text{O}$ pellet data are corrected for the self-shielding effect.

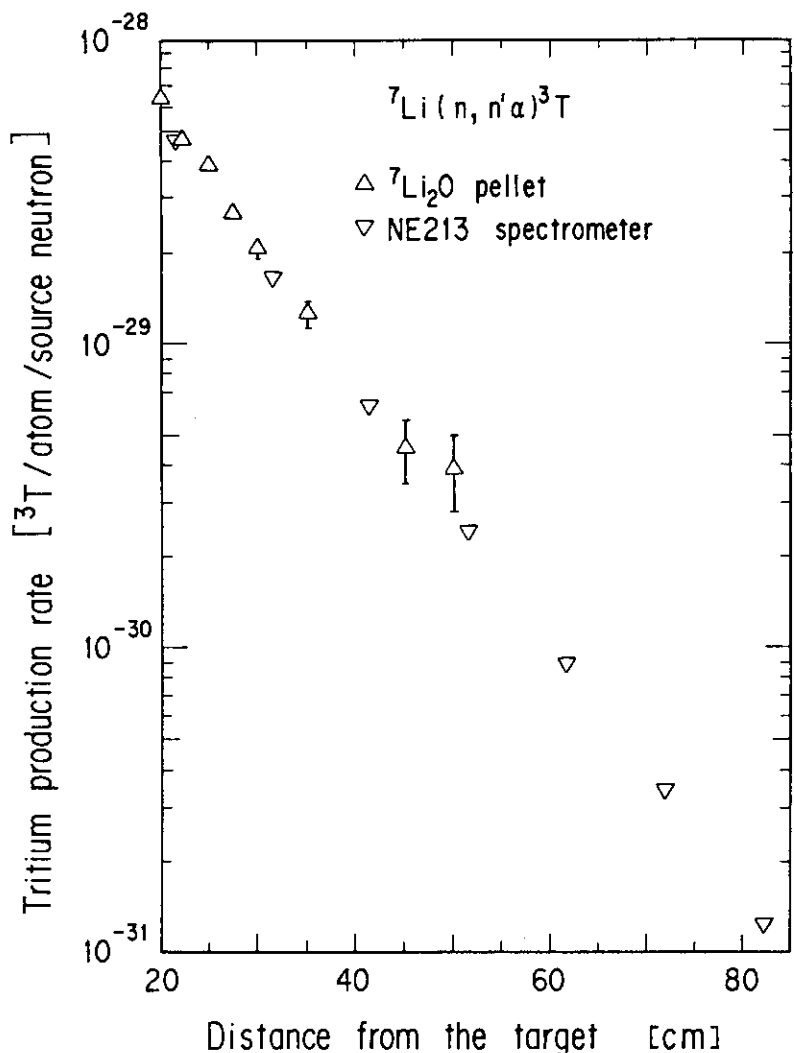


Fig. 7.2 Comparison of ^7Li TPRs (T_7) measured by $^7\text{Li}_2\text{O}$ pellets and NE213 spectrometer.

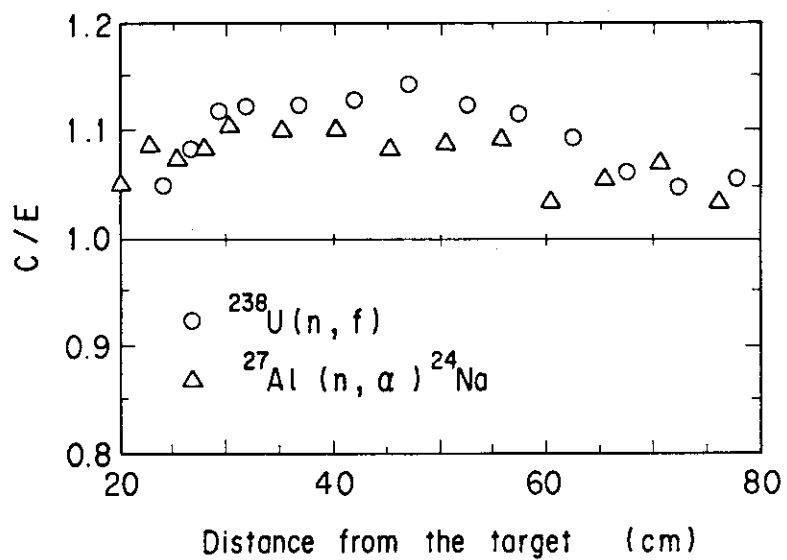


Fig. 7.3 Comparison of C/E values for $^{238}\text{U}(n, f)$ and $^{27}\text{Al}(n, \alpha)^{24}\text{Na}$ reactions.

References

- (1) Hiraoka T., et al.: "Integral Experiments on a Spherical Lithium Metal Blanket System," Proc. Symp. Fusion Reactor Design Problems, CONF-740131, pp363-376, IAEA (1974).
- (2) Maekawa H., et al.: Nucl. Sci. Eng., 57, 335 (1975).
- (3) Maekawa H., Kusano J., Seki Y.: JAERI-M 6811; NEACRP-L-165 (1976).
- (4) Maekawa H., Seki Y.: J. Nucl. Sci. Technol. 14, 97 (1977).
- (5) idem.: ibid. 14, 219 (1977).
- (6) Itoh S., Seki Y., Maekawa H.: "Measurement and Calculation of Fast Neutron Spectra in a Graphite-Reflected Lithium Assembly," Proc. Third ANS Topical Mtg. on Fusion Technology, CONF-780508 Vol. 1, 385 (1978).
- (7) Maekawa H., et al.: J. Nucl. Sci. Technol., 16, 377 (1979).
- (8) Nakamura T., et al.: "Fusion Neutronics Source (FNS)," Proc. Third Symp. on Accelerator Sci. & Technol., Osaka Univ., Aug. 27-29, 1980, pp55-56.
- (9) Nakamura T., et al.: "Present Status of the Fusion Neutronics Source (FNS), Proc. 4th Symp. on Accelerator Sci. & Technol., RIKEN, Saitama, Nov. 24-26, 1982, pp155-156.
- (10) Maekawa H. et al.: JAERI-M 83-196 (1983); NEACRP-L-268.
- (11) Sako K., et al.: "Conceptual Design of a Gas-Cooled Tokamak Reactor," Proc. Symp. Fusion Reactor Design Problems, CONF-740131, pp27-49, IAEA. (1974); JAERI-M 5502, (1973).
- (12) Suzuki T. et al.: JAERI-M 82-190 (1982) (in Japanese); Proc. 6th Int. Conf. on Radiation Shielding, Vol. 1 246-258, Tokyo (1983).
- (13) Nakagawa M., Mori T.: JAERI-M 84-126 (1984); ibid. Vol. 1 171-179, Tokyo (1983).
- (14) Ikeda Y., et al: To be published in JAERI-M report.
- (15) Seki Y., et al.: J. Nucl. Sci. Technol., 20, 686 (1983).
- (16) Rhoades W. A., Mynatt F. R.: ORNL/TM-4280 (1979).
- (17) Seki M., et al.: J. Nucl. Sci. Technol., 16, 838 (1979).
- (18) Maekawa H., et al.: JAERI-M 83-219 (1983).
- (19) Oyama Y., Maekawa H.: Nucl. Instr. Meth. A245, 173 (1986).
- (20) Oyama Y., et al.: JAERI-M84-124 (in Japanese) (1984); To be published in Nucl. Instr. Meth.
- (21) Mori T., M. Nakagawa : Private communication.

- (22) Yamaguchi S., et al.: JAERI-M 85-086 (1985) (in Japanese); To be published in Nucl. Instr. Meth.
- (23) Baba H.: JAERI-M 7017 (1977).
- (24) Lederer C. M., Shirley V. S. (edited): "Table of Isotopes," Seventh Edition, John Wiley and Sons, Inc., New York (1978).
- (25) Kinbara S., Kumahara T.: Nucl. Instr. Meth., 70, 173 (1969).
- (26) "FORIST Spectra Unfolding Code," Radiation Shielding Information Center, Oak Ridge National Laboratory, PSR-92 (1975).
- (27) Maekawa H., et al.: JAERI-M 86-125, pp130-132 (1986).
- (28) Maekawa H., et al.: "Integral Test of JENDL-3PR1 Through Benchmark Experiments on Li₂O Slab Assemblies," Int. Conf. on Nuclear Data for Basic and Applied Science, May 13-17, 1985, Santa Fe, New Mexico, U.S.A. Vol. pp101-106.
- (29) Narita M., et al.: "Some Applications of Solid State Nuclear Track Detectors to Fast Reactor Physics Experiments [1]," Bull. of Faculty of Engineering, Hokaido University, No 103, pp. 27-39 (1981) (in Japanese).
- (30) Ikeda Y., et al.: To be submitted to Nucl. Instr. Meth.
- (31) Kosako K., et al.: JAERI-M 86-125, pp157-159 (1986).
- (32) Hasegawa A.: To be published in JAERI report.
- (33) Kawasaki H., Seki Y.: JAERI-M 82-091 (1982).

Appendix

A.1 Fission Rate distributions Measured by Fission Track Recorders (FTD)

Solid state track recorders (SSTR) were used to measure fission rates in an effort to examine their applicability to fusion neutronics experiments, where the SSTRs were coupled with fission foils to form fission track detector (FTD). This study is a result of collaboration with Hokkaido University, where considerable research has been done on the SSTR technique. In contrast to the micro-fission chambers, FTDs have an advantage of being small, thus affording good spatial resolution and little perturbation to the environment. Polycarbonate film (Takiron PC-1600) of 24 mm × 19 mm and 0.5 mm thickness was used as the solid state track recorder, with fission foils of both thorium and depleted uranium. The foils were standard diameter, and were mounted at the center of the polycarbonate films.

Detectors were inserted into gaps between the Li_2O blocks loaded in the central experimental drawer. Detector locations are shown in Fig. A.1.1. A stepwise irradiation was performed to keep track densities as uniform as practicable throughout the drawer. The required source intensities and irradiation times were evaluated by pre-experiment analysis. The track densities thus obtained ranged from 8500 to 54000 per square centimeter.

Irradiated films were treated for etched in 30 w/o KOH bath for 30 minutes at 60°C, washed in water, rinsed and dried.

Etch-pit tracks were measured by a semi-automatic image processing apparatus, LUZEX 450 (Toyo Ink Co.), with an optical field of 100 $\mu\text{m} \times 100 \mu\text{m}$. The track size spectrum was measured, affording discrimination against small-sized pits due to recoil protons. One to two thousands tracks were accumulated by scanning a number of fields. Details of the chemical processing and reported elsewhere.⁽²⁹⁾

The calibration of FTD was performed by directly irradiating different detectors of the same type in a 15 MeV neutron beam. The neutron flux in this case was determined by the absolute yield monitor, an associated α -particle detector, while the neutron spectrum was calculated by 3-D Monte Carlo analysis⁽¹⁵⁾ and confirmed by time-of-flight experiments. The prime sensitivity for the each type of FTD was determined by taking the effective fission cross section at the source field. Table A.1.1 gives the prime sensitivity that was

used in the present experiment.

Measured values are summarized in Table A.1.2 ; numbers in parentheses are statistical errors in etch-pit counting. As the systematic errors, 2 ~ 3 % and ~ 2.4 % are assigned to the prime sensitivity and the absolute neutron yield, respectively. Overall accuracy of the fission rates in the present experiment is estimated to be approximately 9 %. The fission rates distributions in the Li₂O assembly are shown in Fig. A.1.2 with those of micro-fission chambers (mfc). In the case of U-238, the data of FTD agree well with those of mfc. While in the case of Th-232, some data of FTD deviate from those of mfc. This deviation might be attributed to the change of condition during the etching and to the miscontact between the fission foil and polycarbonate film during the irradiation.

The results indicate that FTD allows a sensitive and useful measurement of the local fission rate as the spectrum index in fusion blanket neutronics experiments, and that irradiation, chemical processing and calibration are handled with proper care.

Table A.1.1 Measured prime sensitivity of the FTDs.

Radiator	Fissionable material	Prime sensitivity k [cm ⁻²]
Th	Th-232	(1.03 ± 0.02) × 10 ¹⁹
DU	U-238	(7.39 ± 0.18) × 10 ¹⁸

Table A.1.2 Absolute fission rates in Li₂O assembly measured with FTD method.

Position *1	Absolute fission rate [fissions/atom/source neutron]		
	Th-232	U-238	
24.8 ₆	4.37 -29 ^{*2} (2.9%) ^{*3}	1.53 ₈ -28 (2.4%)	
29.9 ₂	1.58 ₃ -29 (2.1%)	9.71 -29 (3.0%)	
34.9 ₈	1.28 ₁ -29 (2.6%)	5.51 -29 (3.9%)	
40.0 ₄	7.97 -30 (2.6%)	3.00 -29 (2.4%)	
45.1 ₀	5.62 -30 (3.0%)	1.93 ₇ -29 (2.6%)	
50.1 ₆	2.91 -30 (2.7%)	1.22 ₈ -29 (3.3%)	
55.2 ₂	1.77 ₉ -30 (2.8%)	7.77 -30 (3.3%)	
60.2 ₈	1.15 ₄ -30 (3.0%)	5.09 -30 (2.2%)	
65.3 ₄	7.05 -31 (2.9%)	2.74 -30 (3.1%)	
70.4 ₀	-----	1.77 ₄ -30 (3.8%)	

*1 Distance from the target.

*2 Read as 4.37×10^{-29} .

*3 Experimental error due to the statistics of etch-pit counting.

The errors of source neutron ($\sim 2.4\%$), prime sensitivity ($2 \sim 3\%$) and unknown factors are excluded.

DU & Th

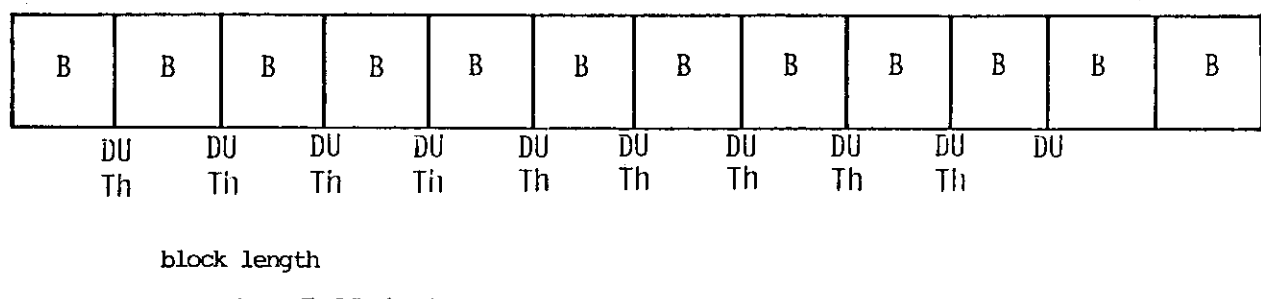


Fig. A.1.1 Loading pattern of the experimental drawer and FTD locations.

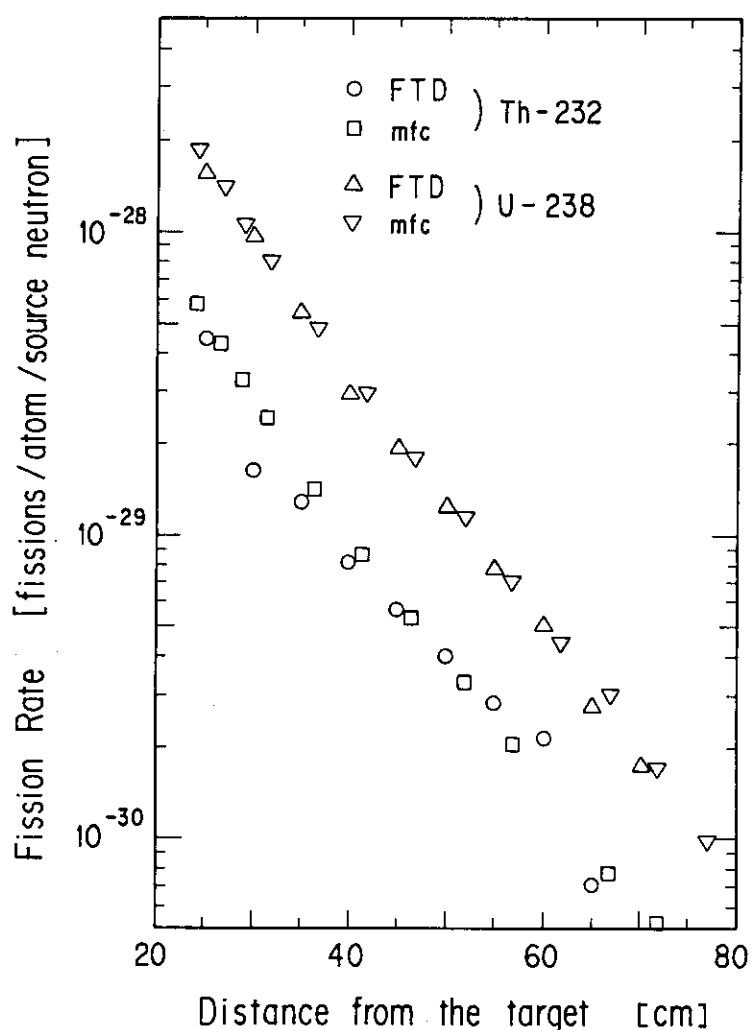


Fig. A.1.2 Fission rate distributions measured by FTDs in the Li_2O assembly.

A.2 Response Distribution of PIN Diode

A PIN diode measurement was carried out along the central axis of the Li₂O assembly in addition to the fission rates and reaction rates measurements. With a low threshold energy of 0.2 MeV, the PIN diode is suitable to measure the intermediate energy neutron flux.

The PIN diode, Studsvik Type 5430, was set in the space between the special-sized Li₂O blocks in the same manner as the reaction-rate measurement. Total neutron yield at the target was 1.178×10^{15} during the irradiation. After the irradiation, the forward voltage drop of the PIN diode was measured by a Studsvik Type 3809A reader at a constant current of 25 mA. The voltage drop difference between before and after irradiation is proportional to the neutron fluence.

The results of the PIN diode measurement are shown in Table A.2.1. The value is in unit of Volt·cm²/source neutron. The response function of the PIN diode was experimentally determined; it will be published elsewhere.⁽³⁰⁾

Table A.2.1 Measured response rate of PIN diodes
in the Li₂O assembly.

Position ^{*1} [cm]	PIN-diode response ^{*2} [V·cm ² /source neutron]	Error [± %]
22.4	2.68 -15 ^{*3}	5.2
25.0	2.07 -15	5.3
27.5	1.67 ₀ -15	5.4
30.1	1.36 ₆ -15	5.1
53.1	7.74 ₉ -16	5.5
40.2	4.63 -16	5.4
45.3	2.83 -16	5.3
50.4	1.68 ₉ -16	5.3
55.5	1.12 ₀ -16	5.3
60.6	6.96 -17	5.4
65.6	4.58 -17	5.6
80.7	1.02 -17	4.9

*1 Distance from the target.

*2 The PIN diodes were measured at one day after the irradiation.

*3 Read as 2.68×10^{-15} .

** D-T neutron yield during the irradiation was $1.17\text{e} \times 10^{15}$ at the target.

A.3 Response Distribution of Thermoluminescence Dosimeters

In preparation for the experimental study of nuclear heating in a simulated fusion blanket assembly, response distributions of thermoluminescence dosimeters (TLD) were measured in the Li₂O slab assembly. Types of TLDs are summarized in Table A.3.1. The TLD powder was sealed in an Pyrex glass ampoule of 2 mm dia. × 12 mm length.

Five or seven TLDs of each type were placed in the spaces between the special-sized Li₂O blocks. These blocks were loaded in the drawer and inserted in the experimental channel. Some TLDs were also placed on the front and the back surfaces. Ten or fifteen TLDs of each type were used for the determination of background. Deuteron beam current, Irradiation time and total neutron yield at the target were 150 μA, 1300 sec and 1.99₀ × 10¹³, respectively.

A TLD reader of type UD-502B (Matsushita Electric Industrial Co., Ltd.) was used for measurement of the absorbed dose. The observed data are summarized in Table A.3.2. The errors in the table were estimated from the standard deviation of the observation and the uncertainty in the neutron yield (2.2 %). Measured response-rate distributions are shown in Fig. A.3.1.

Table A.3.1 Thermoluminescence dosimeters (TLD) used in the experiment.

Type*	TLD material
UD-110S	$\text{CaSO}_4 : \text{Tm}$
UD-136N	$\text{CaSO}_4 : \text{Tm} + {}^6\text{LiF}$ (95.6 atom%)
UD-137N	$\text{CaSO}_4 : \text{Tm} + {}^7\text{LiF}$ (99.99 atom%)

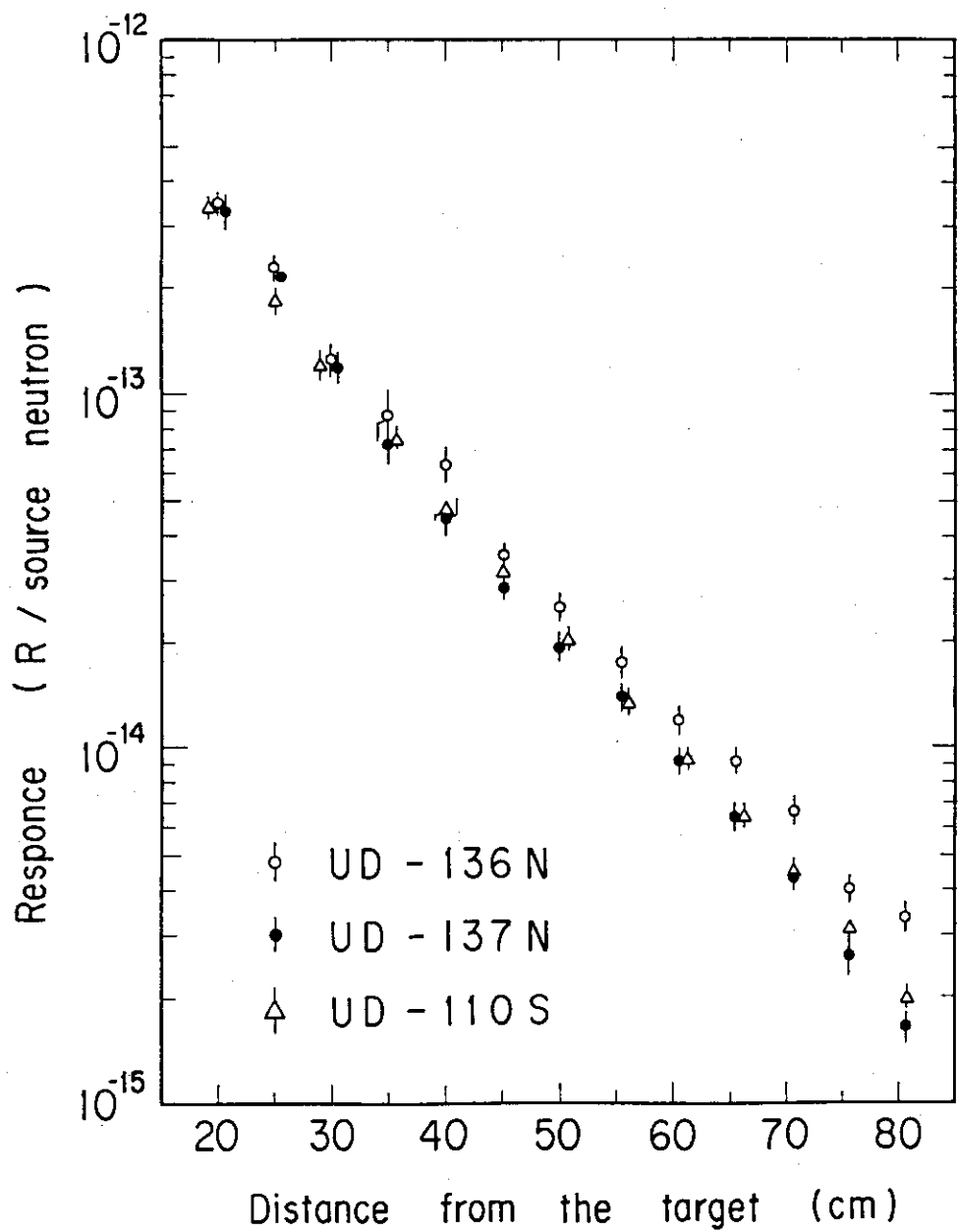
* All TLDs were manufactured by Matsushita Electric Industrial Co.

Table A.3.2 Response-rate distributions of TLDs in the Li_2O assembly.

Position* ¹ [cm]	Response [R/source neutron]		
	UD-136N	UD-137N	UD-110S
19.9	3.48 -13 (5.9 %) ^{*2}	3.32 -13 (12.0 %)	3.38 -13 (5.5 %)
24.9	2.25 -13 (8.7 %)	2.15 -13 (6.7 %)	1.82 ₅ -13 (6.4 %)
30.0	1.25 ₂ -13 (10.8 %)	1.17 ₁ -13 (11.3 %)	1.21 ₂ -13 (9.0 %)
35.1	8.73 -14 (16.7 %)	7.17 -14 (11.3 %)	7.33 -14 (3.9 %)
40.2	6.33 -14 (8.9 %)	4.47 -14 (13.5 %)	4.72 -14 (5.5 %)
45.3	3.53 -14 (7.6 %)	2.86 -14 (4.1 %)	3.15 -14 (4.7 %)
50.3	2.49 -14 (6.1 %)	1.95 ₅ -14 (9.6 %)	2.00 -14 (4.5 %)
55.4	1.75 ₆ -14 (8.7 %)	1.40 ₆ -14 (8.9 %)	1.35 ₄ -14 (5.7 %)
60.5	1.20 ₄ -14 (6.3 %)	9.24 -15 (6.7 %)	9.25 -15 (3.3 %)
65.6	9.12 -15 (5.3 %)	6.37 -15 (8.3 %)	6.36 -15 (5.8 %)
70.7	6.61 -15 (9.2 %)	4.35 -15 (8.0 %)	4.42 -15 (5.1 %)
75.7	4.00 -15 (8.1 %)	2.65 -15 (12.2 %)	3.03 -15 (4.1 %)
80.8	3.32 -15 (12.3 %)	1.64 ₇ -15 (8.9 %)	1.96 ₄ -15 (6.7 %)

*1 Distance from the target

*2 Read as 3.48×10^{-13}

Fig. A.3.1 TLD response-rate distributions in Li_2O slab assembly.

A.4 Sample Calculation

In order to make clear how the calculational model is used for analysis, a sample calculation using the DOT3.5 is described in this Appendix.

A two-dimensional R-Z model was adopted in this calculation. The equivalent radius was 31.5 cm. The experimental channel was modeled as two regions : a lithium-oxide region and a thin stainless steel layer. The calculational model is shown in Fig. A.4.1.

The zero-degree source neutron spectrum, calculated by a Monte Carlo program⁽¹⁵⁾, was used as a isotropic input spectrum. All experimental data were normalized to one source neutron generated at the target. It is noticeable that the integrated flux of input source neutron spectrum is not unity but 1.173 because of its anisotropy.

The GRTUNCL code was used to calculate the first collision source in order to eliminate the "ray effect". The number of Legendre polynomials was 5 ; the number of angular quadratures was 16. The mesh width was 9 cm in air and about 1 cm in the lithium-oxide region except near the front surface of assembly. A sample of input data for the GRTUNCL and the DOT3.5⁽¹⁶⁾ is shown in Fig. A.4.2. The cross section set JACKAS⁽³¹⁾ is taken from the JENDL-3PR1 using the PROF-GROUCH-G/B⁽³²⁾ process code. The group structure is just the same as used in MORSE-DD.⁽¹³⁾ The source neutron spectrum data of 3* in Fig. A.4.2 (a) were interpolated from the result of a Monte Carlo calculation.⁽¹⁵⁾ In this sample calculation, air was assumed to be made of Oxygen and Mn in SS304 was included in Fe. After calculation of the neutron flux distribution in the assembly, the APPLE-2 code⁽³³⁾ was used for calculating the reaction-rate distributions. As a typical example, the calculated-to-experimental ratios (C/E) for the ^6Li tritium production rate were shown in Fig. A.4.3.

Additional points of information are as follows:

1) Aluminum support

homogenized nuclide density : 1.234×10^{22}

effective outer radius : 56.7 cm

* A pre-analysis showed that the effect of the aluminum support was very small.

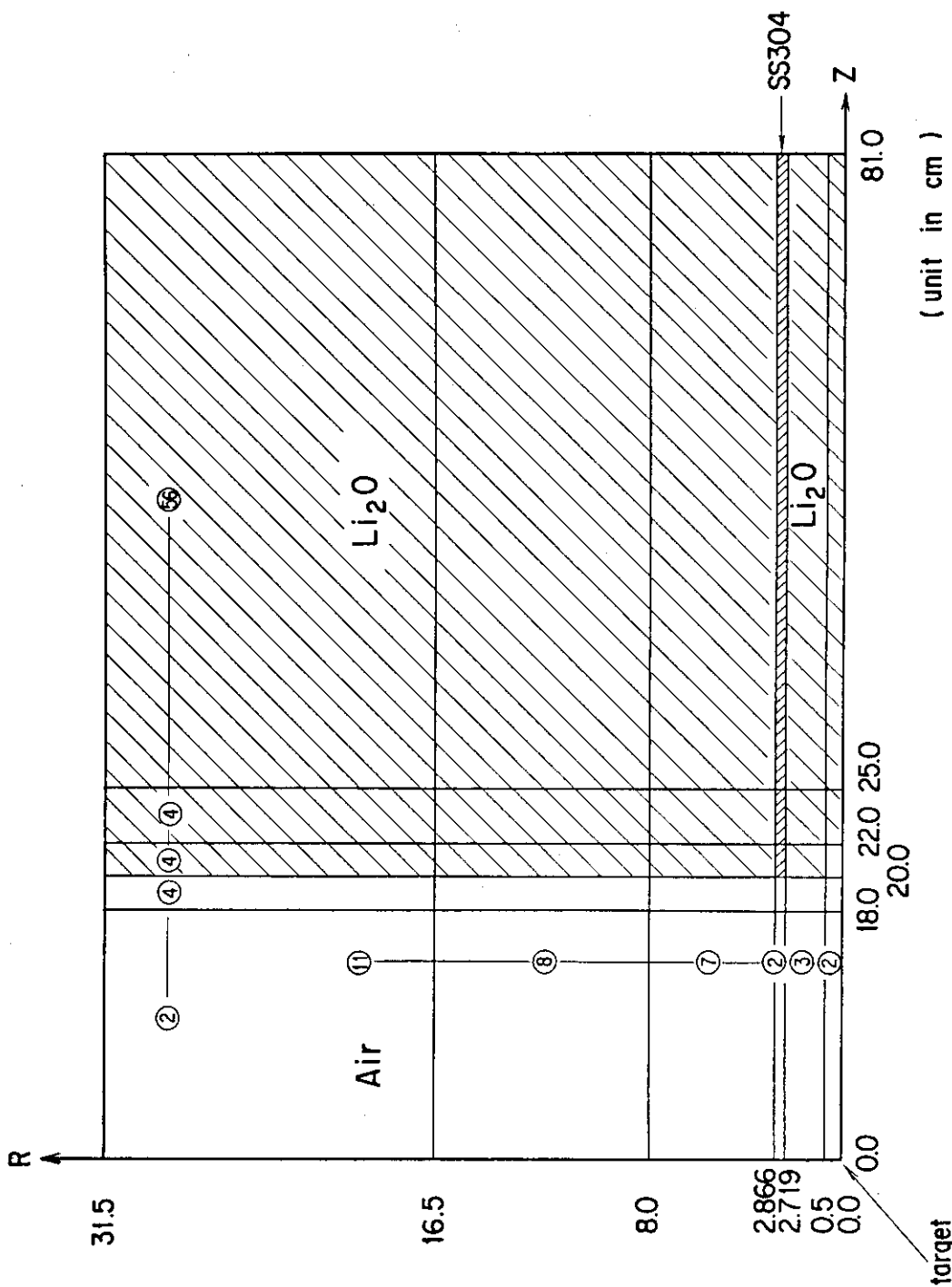
2) Anisotropy of source neutrons

The effect of this anisotropy may be small but we will consider it in further analysis.

3) Room return effect

A layout of the target vicinity is shown in Fig. A.4.4.

Room-return effect was calculated by the MORSE-DD code.⁽¹³⁾ The results showed that the room-return neutrons had some effect on the reaction rates that were sensitive to low energy neutrons⁽²¹⁾.



* Digit in a circle means mesh number for each region.

Fig. A.4.1 Computational model for the two-dimensional transport code DOT3.5.

JAERI-M 86-182

THH-GRTUNCL L120 SLAB ASSEMBLY #4 AIR(20)-L120(61.0) OPTIONS JEFGIX
 0
 1¥¥
 0 5 4 33 70 1250044002 LOS4GU
 4 5 129 156 0 1560050001 LOS4GU
 156 2 1 30000 10 000060001 LOS4GU
 1 0 18 0 0 1600070002 LOS4GU
 2**
 1.1767+00 0.0 0.0 00080002 LOS4GU
 T 00090002 LOS4GU
 1**
 F0.0 00100002 LOS4GU
 2**
 110.0 3118.0 3120.0 3122.0 55125.0 81.0 00110002 LOS4GU
 110.0 3118.0 3120.0 3122.0 55125.0 81.0 00120000 LOS4GU
 3**
 0.0 0.0 2.7828-03 1.7363-02 7.1310-02 2.3566-0100160002 LOS4GU
 2.8044-01 1.9088-01 8.8741-02 1.9619-02 4.7824-03 3.6889-0300170002 LOS4GU
 4.0824-03 3.0739-03 2.0627-03 1.5353-03 1.3058-03 1.0510-0300180002 LOS4GU
 9.1815-04 6.6341-04 4.9328-04 4.3340-04 3.5410-04 3.3956-0400190002 LOS4GU
 3.3951-04 4.7551-04 5.2166-04 5.4544-04 6.0839-04 5.8562-0400200002 LOS4GU
 5.9851-04 5.9892-04 2.3220-03 2.1711-03 1.9259-03 2.0821-0300210002 LOS4GU
 2.4699-03 2.3331-03 2.1203-03 2.3830-03 2.7193-03 2.5754-0300220002 LOS4GU
 2.5194-03 2.9628-03 3.5164-03 3.9704-03 4.3379-03 4.2412-0300230002 LOS4GU
 3.6099-03 3.3610-03 3.4485-03 3.7938-03 4.3795-03 4.7354-0300240002 LOS4GU
 5.0664-03 5.2928-03 5.3299-03 5.3383-03 5.3194-03 5.3179-0300250002 LOS4GU
 1.0130-02 9.9677-03 9.7640-03 9.6236-03 9.7275-03 9.9713-0300260002 LOS4GU
 9.7540-03 9.3421-03 8.6681-03 7.7929-03 6.8688-03 5.9791-0300270002 LOS4GU
 4.9397-03 3.8479-03 3.2890-03 2.8136-03 2.4317-03 2.1040-0300280002 LOS4GU
 1.8527-03 1.6141-03 1.4051-03 1.2219-03 9.1106-04 7.9663-0400290002 LOS4GU
 6.9762-04 6.1088-04 5.3606-04 4.7077-04 4.1340-04 3.6436-0400300002 LOS4GU
 3.2144-04 2.8444-04 2.5200-04 2.2407-04 2.0045-04 1.7891-0400310002 LOS4GU
 3.0516-04 2.4812-04 2.1369-04 1.9164-04 1.6038-04 1.3521-0400320002 LOS4GU
 1.1447-04 9.7598-05 8.3682-05 7.2417-05 6.3421-05 5.5907-0500330002 LOS4GU
 4.3479-05 00340002 LOS4GU
 F0.0 00350002 LOS4GU
 4**
 110.0 210.5 112.719 612.866 718.0 10116.5 00360000 LOS4GU
 31.5 00370002 LOS4GU
 5**
 F1.0 00380002 LOS4GU
 6**
 1.0 00390002 LOS4GU
 7**
 1.0 00400002 LOS4GU
 8¥¥
 33R1 5R2 2R3 26R4 5Q33 63Q33 00440002 LOS4GU
 9¥¥
 -97 -103 -109 -115 00450002 LOS4GU
 10¥¥
 4197 102 1Q6 00460002 LOS4GU
 41103 108 6Q6 00470002 LOS4GU
 41109 114 3Q6 00480000 LOS4GU
 41115 120 6Q6 00490001 LOS4GU
 341121 156 00500000 LOS4GU
 00510001 LOS4GU
 11¥¥
 6Z 4131 36 00520001 LOS4GU
 6Z 411 6 00530001 LOS4GU
 4161 66 4167 72 4173 78 00540001 LOS4GU
 6Z 4161 66 4167 72 4173 78 00550001 LOS4GU
 6Z 411 6 417 12 4131 36 00560000 LOS4GU
 4161 66 4167 72 4173 78 00570002 LOS4GU
 36Z 00580002 LOS4GU
 12**
 6R0.0 6R4.9210-5 00590002 LOS4GU
 6R0.0 6R4.2211-3 6R5.2774-2 6R2.8498-2 6R1.4333-4 6R5.2773-6400660002 LOS4GU
 6R6.2963-5 00670002 LOS4GU
 6R0.0 6R6.3975-3 6R2.3574-2 6R2.8121-3 00680002 LOS4GU
 6R0.0 6R4.1915-3 6R5.2404-2 6R2.8298-2 6R3.0675-4 6R1.1307-3 00690002 LOS4GU
 6R1.3516-4 00700002 LOS4GU
 00710001 LOS4GU
 36R0.0 00720002 LOS4GU
 13**
 -0.97753 -0.90676 -0.82999 -0.74536 -0.64979 -0.53748 00730002 LOS4GU
 -0.39441 -0.14907 1M8 00740002 LOS4GU
 00750002 LOS4GU
 14**
 F1.0 00760002 LOS4GU
 T 00770002 LOS4GU

Fig. A.4.2 Input data for a sample calculation.

(a) Input data for GRTUNCL code

THH-DOT35 LI20 SLAB ASSEMBLY #4 AIR(20)-LI20(61.0) OPTION JEFGIX 00010000 LOS4DT
 00020000 LOS4DT
 00030001 LOS4DT
 61**
 0 5 4 33 70 12500040001 LOS4DT
 4 5 129 156 0 000050001 LOS4DT
 156 1 160 1 1 000060001 LOS4DT
 0 0 1 10 15 400070001 LOS4DT
 6 2 0 0 0 000080001 LOS4DT
 0 0 0 0 0 000090001 LOS4DT
 0 0 0 0 3 000100001 LOS4DT
 0 0 0 0 0 000110001 LOS4DT
 0 0 0 2 1 000120001 LOS4DT
 0 0 0 0 0 800130001 LOS4DT
 0 0 0 0 0 00140001 LOS4DT
 0 0 0 0 0 00150001 LOS4DT
 62**
 2 3 4 14 15 900160001 LOS4DT
 10 11 12 13 8 6000170001 LOS4DT
 0 0 0 0 0 00180001 LOS4DT
 00190001 LOS4DT
 63**
 0.0 1.000E-02 0.0 0.0 0.0 0.0 00200001 LOS4DT
 0.0 0.0 0.0 0.0 0.0 0.0 00210001 LOS4DT
 0.0 0.0 0.0 0.0 0.0 0.0 00220001 LOS4DT
 T
 7**
 -0.21082 -0.14907 1M1 00230000 LOS4DT
 -0.42164 -0.39441 -0.14907 1M2 00240001 LOS4DT
 -0.55777 -0.53748 -0.39441 -0.14907 1M3 00250001 LOS4DT
 -0.66667 -0.64979 -0.53748 -0.39441 -0.14907 1M4 00260001 LOS4DT
 -0.76012 -0.74536 -0.64979 -0.53748 -0.39441 -0.14907 00270001 LOS4DT
 1MS 00280001 LOS4DT
 -0.84327 -0.82999 -0.74536 -0.64979 -0.53748 -0.39441 00290001 LOS4DT
 -0.14907 1M6 00300001 LOS4DT
 -0.91894 -0.90676 -0.82999 -0.74536 -0.64979 -0.53748 00310001 LOS4DT
 -0.39441 -0.14907 1M7 00320001 LOS4DT
 -0.98883 -0.97753 -0.90676 -0.82999 -0.74536 -0.64979 00330001 LOS4DT
 -0.53748 -0.39441 -0.14907 1M8 00340001 LOS4DT
 1Q80 00350001 LOS4DT
 3R-0.97753 5R-0.90676 7R-0.82999 9R-0.74536 11R-0.64979 13R-0.53748 00360001 LOS4DT
 15R-0.39441 17R-0.14907 3R0.97753 5R0.90676 7R0.82999 9R0.74536 00390001 LOS4DT
 11R0.64979 13R0.53748 15R0.39441 17R0.14907 00400001 LOS4DT
 T 00410001 LOS4DT
 6**
 0.0 2R0.13586-1 0.0 4R0.97681-2 00420001 LOS4DT
 0.0 0.64738-2 0.50390-2 0.64738-2 1N3 00430001 LOS4DT
 0.0 0.64634-2 2R0.71124-2 0.64634-2 1N4 00440001 LOS4DT
 0.0 0.64634-2 0.14381-2 0.36342-2 0.14381-2 0.64634-200460001 LOS4DT
 1N5 00450001 LOS4DT
 0.0 0.64738-2 0.71124-2 0.36342-2 1N3 1Q6 00460001 LOS4DT
 0.0 0.97681-2 0.50390-2 0.71124-2 0.14381-2 0.71124-200490001 LOS4DT
 0.0 0.50390-2 0.97681-2 1N7 00470001 LOS4DT
 0.0 0.13586-1 0.97681-2 2R0.64738-2 1N4 1Q8 00480001 LOS4DT
 1Q80 00490001 LOS4DT
 T 00500001 LOS4DT
 3**
 F0.0 00510001 LOS4DT
 T 00520001 LOS4DT
 1**
 F0.0 00530001 LOS4DT
 2**
 110.0 3I18.0 3I20.0 3I22.0 55125.0 81.0 00540001 LOS4DT
 4**
 110.0 2I0.5 1I2.719 6I2.866 718.0 10I16.5 00550001 LOS4DT
 31.5 00560001 LOS4DT
 5**
 F0.0 00570001 LOS4DT
 8**
 33R1 5Q33 00580000 LOS4DT
 9**
 5R2 2R3 26R4 63Q33 00590000 LOS4DT
 -97 -103 -109 -115 00600001 LOS4DT
 10**
 4I97 102 1Q6 00610000 LOS4DT
 4I103 108 6Q6 00620001 LOS4DT
 4I109 114 3Q6 00630001 LOS4DT
 4I115 120 6Q6 00640001 LOS4DT
 34I121 156 00650001 LOS4DT
 11**
 6Z 4I31 36 00660001 LOS4DT
 6Z 4I1 6 4I7 12 4I31 36 00670001 LOS4DT
 4I61 66 4I67 72 4I73 78 00680001 LOS4DT
 6Z 4I61 66 4I67 72 4I73 78 00690001 LOS4DT
 6Z 4I1 6 4I7 12 4I31 36 00700001 LOS4DT
 4I61 66 4I67 72 4I73 78 00710001 LOS4DT
 36Z 00720001 LOS4DT
 12**
 6R0.0 6R4.9210-5 00730001 LOS4DT
 6R0.0 6R4.2211-3 6R5.2774-2 6R2.8498-2 6R1.4333-4 6R5.2773-4 00740001 LOS4DT
 6R6.2963-5 00750001 LOS4DT
 6R0.0 6R6.3975-3 6R2.3574-2 6R2.8121-3 00760001 LOS4DT
 6R0.0 6R4.1915-3 6R5.2404-2 6R2.8298-2 6R3.0675-4 6R1.1307-3 00770001 LOS4DT
 6R1.3516-4 00780001 LOS4DT
 36R0.0 00790001 LOS4DT
 T T 00800001 LOS4DT
 00810001 LOS4DT
 00820001 LOS4DT
 00830001 LOS4DT
 00840001 LOS4DT
 00850001 LOS4DT
 00860001 LOS4DT
 00870001 LOS4DT
 00880001 LOS4DT
 00890001 LOS4DT
 00900001 LOS4DT
 00910001 LOS4DT
 00920001 LOS4DT
 00930001 LOS4DT

Fig. A.4.2 Input data for a sample calculation.

(b) Input data for DOT3.5

Comparison of tritium production rate

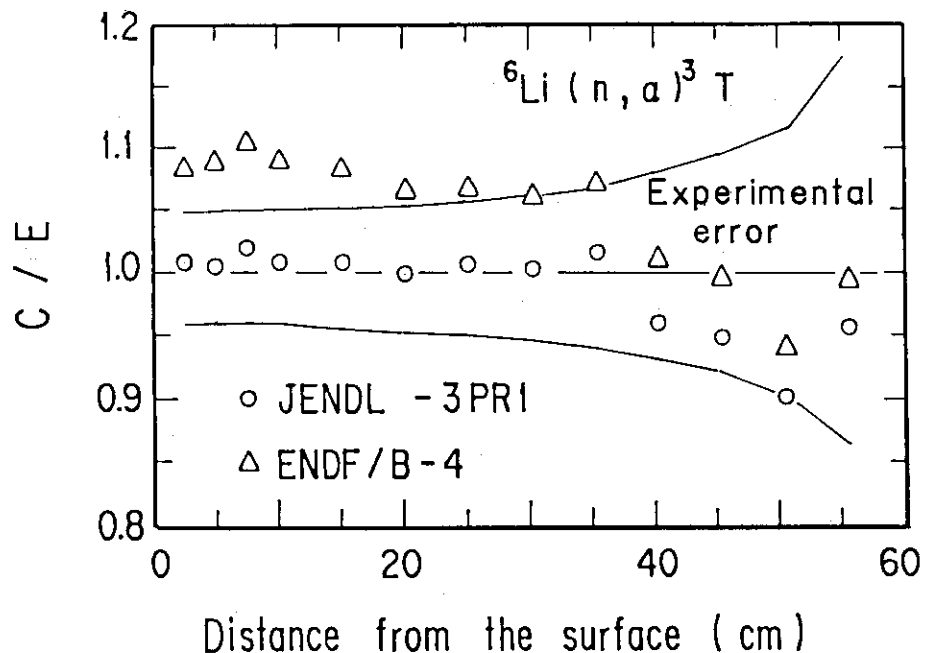


Fig. A.4.3 Comparison of C/E values for the ${}^6\text{Li}$ tritium production rate.

Experimental data are corrected for self-shielding and room-return effects.

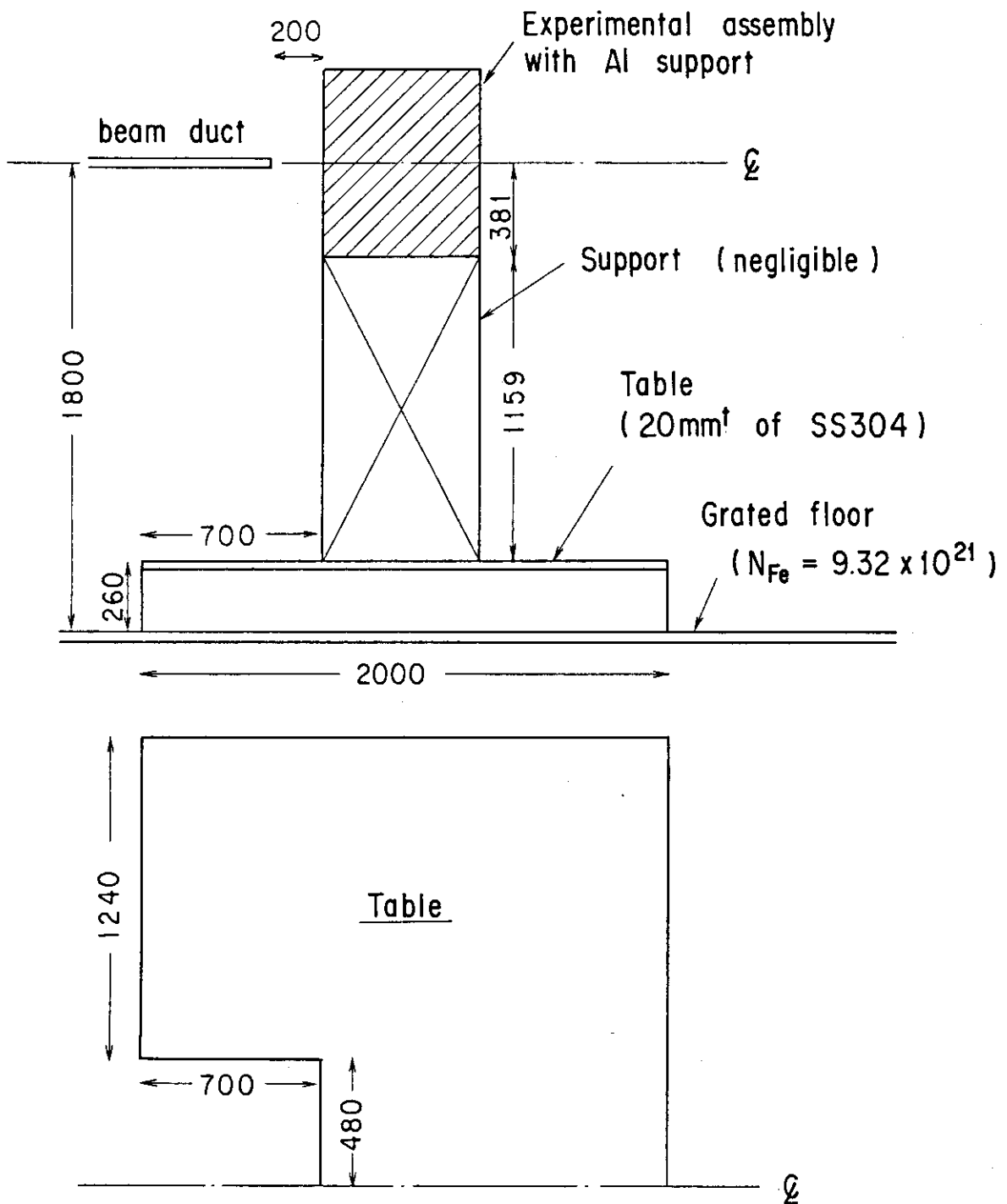


Fig. A.4.4 Configuration around the experimental assembly.